Examining TRPA1 channel expression and functionality in human peripheral blood basophil granulocytes

Von der Fakultät für Medizin und Gesundheitswissenschaften der Carl von Ossietzky Universität Oldenburg zur Erlangung des Grades und Titels einer

Doktorin der Naturwissenschaften (Dr. rer. nat.)

angenommene Dissertation

von Frau Daniela Wiebe

geboren am 29.05.1992 in Detmold

Gutachterin Univ.-Prof. Dr. med. Ulrike Raap

Weitere Gutachter*in

Prof. Dr. Anja U. Bräuer

Prof. Dr. rer. nat. David Vöhringer

Tag der Disputation: 17.11.2025

Abstract

Basophil granulocytes are involved in allergic inflammation and neuro-immune interactions. In pruritic skin diseases, such as atopic dermatitis (AD), basophil granulocytes infiltrate into inflamed skin, where they drive inflammation and pruritus. AD is an inflammatory skin disease characterized by the presence of itchy skin lesions, which affect the quality of life of patients. The acute phase of AD is associated with T helper 2 (Th2) cytokines, especially interleukin (IL)-31, which is increased in the serum of AD patients and correlates with disease severity. In AD, the transient receptor potential ankyrin 1 (TRPA1) channel is increased and a known part of disease pathogenesis. The expression of TRPA1 in basophil granulocytes has not yet been analyzed, despite the involvement of both in AD pathogenesis. In this doctoral thesis, human peripheral blood basophil granulocytes were isolated from nonatopic (NA) donors and AD patients by negative immunomagnetic bead selection. TRPA1 is expressed in basophil granulocytes of NA donors and patients with AD, while being significantly increased in the latter group. Calcium flux assay analysis demonstrated the functionality of the TRPA1 channel when stimulated with its selective agonist JT010. However, activation of the channel did not result in upregulation or externalization of the basophil granulocyte markers CD203c and CD63, respectively. Modulation of TRPA1 was observed after stimulation with the inflammatory mediators IL-3, IL-31, and nerve growth factor-beta (NGFβ). Furthermore, an inflammatory environment simulated by acidic pH also increased TRPA1, while elevated temperature did not affect expression. Activation of the TRPA1 channel did not affect basophil granulocyte viability. Immunofluorescence staining of lesional skin from AD patients confirmed TRPA1 expression in basophil granulocytes. As TRPA1 expression is often observed in TRP vanilloid 1 (TRPV1)-positive neurons, TRPA1/TRPV1 co-expression was investigated and confirmed in basophil granulocytes of NA donors and AD patients. Co-expression was modulated by IL-3, IL-33, and NGFβ. An acidic milieu also significantly increased TRPA1/TRPV1 co-expression, while changes in temperature had no effect. These results indicate the importance of basophil granulocytes and TRP channels in AD.

Zusammenfassung

Basophile Granulozyten sind an allergischen Entzündungen und neuro-immunen Interaktionen beteiligt. Bei juckenden Hauterkrankungen wie der atopischen Dermatitis (AD) infiltrieren basophile Granulozyten in die entzündete Haut, wo sie Entzündungen und Juckreiz auslösen. Die AD ist eine entzündliche Hauterkrankung, die durch juckende Hautläsionen gekennzeichnet ist und die Lebensqualität der Patienten beeinträchtigt. Die akute Phase der AD ist durch T-Helfer-2 (Th2)-Zytokine geprägt, insbesondere mit Interleukin (IL)-31, das im Serum von AD-Patienten erhöht ist und mit der Schwere der Erkrankung korreliert. Bei der AD ist der transient receptor potential ankyrin 1-Kanal (TRPA1) erhöht und ein bekannter Bestandteil der Pathogenese. Die Expression von TRPA1 in basophilen Granulozyten wurde bisher noch nicht untersucht, obwohl beide an der AD-Pathogenese beteiligt sind. In dieser Doktorarbeit wurden humane basophile Granulozyten aus peripherem Blut von nicht-atopischen (NA)-Spendern und AD-Patienten durch negative immunomagnetische Bead-Selektion isoliert. TRPA1 wurde in basophilen Granulozyten von NA-Spendern und Patienten mit AD analysiert, wobei es in der letzteren Gruppe signifikant erhöht war. Ein Kalziumfluss-Assay zeigte die Funktionalität des TRPA1-Kanals bei Stimulation mit dem spezifischen Agonisten JT010. Die Aktivierung des Kanals führte jedoch nicht zu einer Hochregulierung oder Externalisierung der basophilen Granulozytenmarker CD203c bzw. CD63. Die Modulation von TRPA1 durch Entzündungsmediatoren erfolgte durch Stimulation mit IL-3, IL-31 und Nervenwachstumsfaktor-beta (NGFβ). Eine entzündliche Umgebung, die durch einen sauren pH-Wert simuliert wurde, steigerte ebenfalls die TRPA1-Expression auf Basophilen, während eine erhöhte Temperatur die Expression nicht beeinflusste. Die Aktivierung des TRPA1-Kanals hatte keinen Effekt auf die Lebensfähigkeit der basophilen Granulozyten. Die Immunfluoreszenzfärbung von Hautläsionen von AD-Patienten bestätigte die TRPA1-Expression in basophilen Granulozyten. Da die TRPA1-Expression häufig in TRP Vanilloid 1 (TRPV1)-positiven Neuronen beobachtet wird, wurde die TRPA1/TRPV1-Koexpression in basophilen Granulozyten von NA-Spendern und AD-Patienten untersucht und bestätigt. Die Koexpression der Kanäle wurde durch IL-3, IL-33 und NGFβ moduliert. Ein saures

Milieu erhöhte ebenfalls signifikant die TRPA1/TRPV1-Expression auf Basophilen, während die Temperatur keine Auswirkungen hatte. Diese Ergebnisse verdeutlichen die Bedeutung von basophilen Granulozyten und TRP-Kanälen bei der AD.

Table of contents

List of figures

List of tables

List of abbreviations

Abbreviation	Explanation
AD	atopic dermatitis
a-IgE	anti-IgE
AITC	allyl isothiocyanate
APC	allophycocyanin
aqua dest.	aqua destillata
BAT	basophil activation test
BDNF	brain-derived neurotrophic factor
cDNA	complementary DNA
DNA	deoxyribonucleic acid
DRG	dorsal root ganglion
EDTA	ethylenediamine tetraacetic acid
FITC	fluorescein isothiocyanate
fMLP	N-formyl-L-methionyl-L-leucyl-L-phenylalanine
g	gram
GAPDH	glyceraldehyde 3-phosphate dehydrogenase
GM-CSF	granulocyte-macrophage colony-stimulating factor
IL	interleukin
IL-4Rα	IL-4 receptor alpha
IL-13Rα1	IL-13 receptor subunit alpha 1
IL-31RA	IL-31 receptor A
JAK	Janus kinase
MFI	mean fluorescence intensity
min	minute
mL	milliliter
NA	nonatopic
NaCl	sodium chloride

Abbreviation	Explanation
NGFβ	nerve growth factor-beta
nM	nanomolar
N-terminal	NH_2-terminal
PBS	phosphate-buffered saline
PBS-EDTA	phosphate-buffered saline-ethylenediamine tetraacetic acid buffer
PBS-T	phosphate-buffered saline-Tween
PE	phycoerythrin
PI	propidium iodide
qPCR	quantitative real-time PCR
rcf	relative centrifugal force
RNA	ribonucleic acid
RT	room temperature
s	second
SEM	standard error of the mean
Th1	T helper 1
Th2	T helper 2
TNF-α	tumor necrosis factor alpha
TRP	transient receptor potential
TRPA1	transient receptor potential ankyrin 1
TRPC	transient receptor potential canonical
TRPM	transient receptor potential melastatin
TRPML	transient receptor potential mucolipin
TRPP	transient receptor potential polycystin
TRPV1	transient receptor potential vanilloid 1
TSLP	thymic stromal lymphopoietin
U	unit
µl	microliter

1 Introduction

1.1 Basophil granulocytes

Basophil granulocytes were first described in 1879 by Paul Ehrlich due to their affinity to basic dyes, which stain the cytoplasmic basophilic granules [1]. Originating from the bone marrow [2], basophil granulocytes differentiate into mature cells when exposed to their most prominent differentiation factor, interleukin (IL)-3 [3, 4]. Hematopoietic stem cells differentiate into granulocyte-monocyte precursors [2]. These precursors then give rise to eosinophil, basophil-mast cell, mast cell, and basophil precursors [2]. The basophil-mast cell precursor is suggested to migrate to the spleen for maturation, while the other precursors remain in the bone marrow [2, 5]. Upon maturation, basophil granulocytes enter the bloodstream [2], circulating until they migrate into inflamed tissues, e.g., during asthma or atopic dermatitis (AD) [6]. The fate of basophil granulocytes after migration is not fully understood, with possibilities including their return to the bloodstream or migration to draining lymph nodes [7, 8].

Originally, basophil granulocytes were thought to be phenotypically and functionally similar to mast cells since both express the high-affinity IgE receptor FcεRI and contain basophilic granules [9]. However, basophil granulocytes were later discovered to differ in their location and their lifespan. While mast cells are found primarily in peripheral tissues, basophil granulocytes enter the bloodstream and infiltrate into the skin during inflammation [6]. Additionally, mast cells have a lifespan of 2–3 weeks, whereas murine and human basophil granulocytes only live for approximately 60 hours and are unable to proliferate [2, 6, 10, 11].

Basophil granulocytes are spherical cells measuring approximately 10-14 μM in diameter [12], which possess a polylobed nucleus [13]. The cytoplasm contains numerous round or oval, purple, dark granules when stained, of variable size that partially cover the nucleus (Figure 1) [12]. Accounting for less than 1% of all leukocytes, basophil granulocytes are the rarest type of granulocytes in peripheral blood [1].

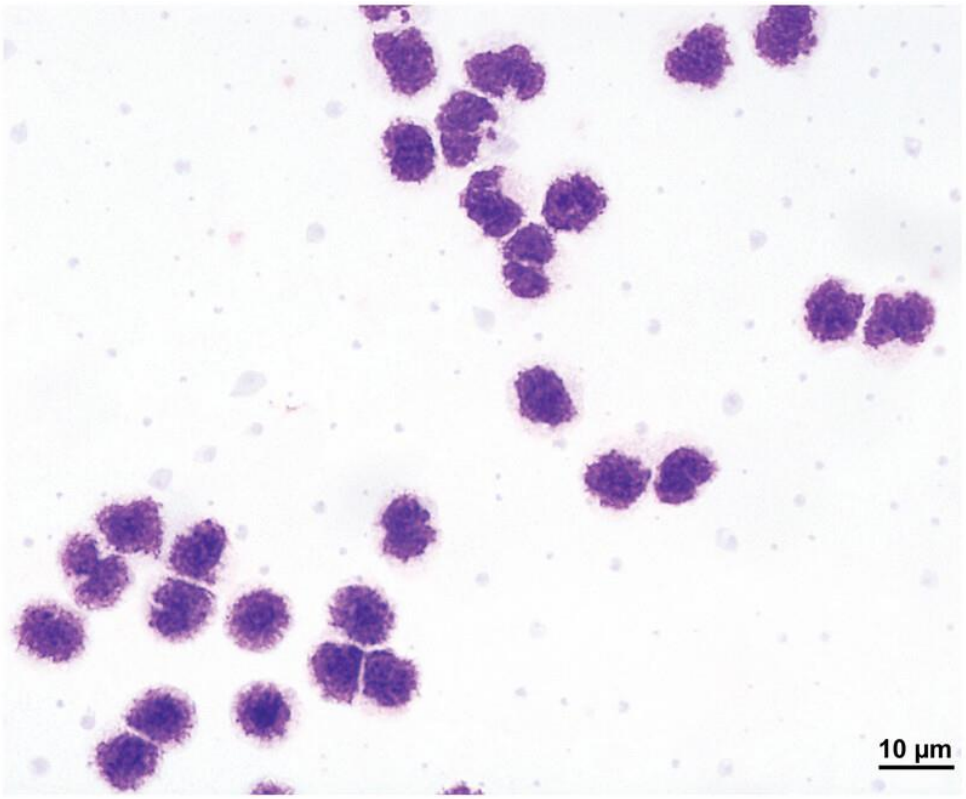

Figure 1: Basophil granulocytes. Giemsa staining of isolated human peripheral blood basophil granulocytes showing the granulocytes in purple and the polylobed nuclei in violet [14].

Basophil granulocytes play important roles in immunity, including protection against helminths [10, 15], mediation of allergic inflammation [6], and involvement in neuro-immune interactions with sensory neurons in the skin [16]. As early infiltrators of inflamed skin in pruritic diseases, basophil granulocytes act as drivers of inflammation and itch in conditions such as AD, bullous pemphigoid, and chronic spontaneous urticaria [16]. Upon activation, basophil granulocytes release an armory of cytokines, such as tumor necrosis factor alpha (TNF-α), IL-3, granulocyte-macrophage colony-stimulating factor (GM-CSF), T helper 2 (Th2) cytokines IL-4, IL-5, IL-6, IL-13, the pruritogenic cytokine IL-31, and thymic stromal lymphopoietin (TSLP). Furthermore, basophil granulocytes also release the lipid mediators sphingosine-1-phosphate (S1P) and leukotriene C4 (LTC4), the neurotrophin nerve growth factor (NGF), the neuropeptide substance P, and the biogenic amine histamine (Figure 2) [16–20]. IL-31 induces chemotaxis in basophil granulocytes and facilitates neuro-immune interaction with sensory neurons [16, 18]. Basophil granulocytes express receptors

for IL-4 and IL-13, more specifically the IL-4 receptor alpha subunit (IL-4Rα) and IL-13 receptor subunit alpha 1 (IL-13Rα1) [21], along with the IL-31 receptor complex consisting of IL-31 receptor A (IL-31RA) and oncostatin M receptor β (OSMRβ) [18].

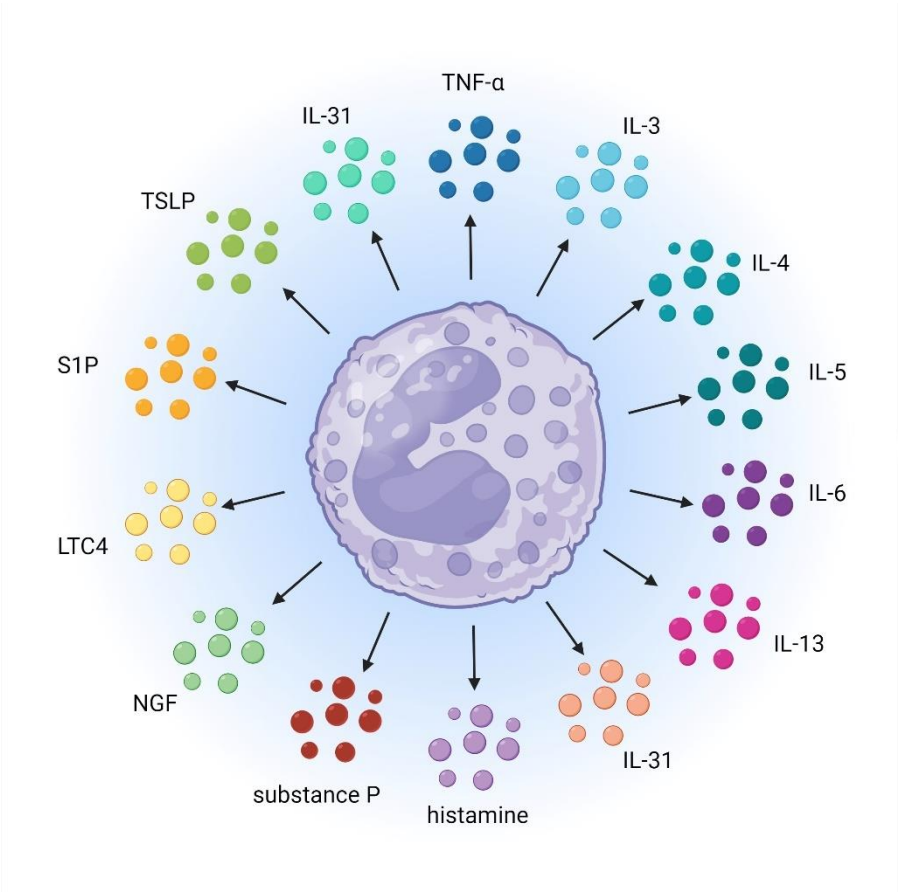

Figure 2: Release of basophil granulocyte mediators. Basophil granulocytes release various mediators upon stimulation. GM-CSF: Granulocyte-Macrophage Colony-Stimulating Factor; IL: Interleukin; LTC4: Leukotriene C4; NGF: Nerve Growth Factor; TNF-α: Tumor Necrosis Factor Alpha; TSLP: Thymic Stromal Lymphopoietin; S1P: Sphingosine-1-Phosphate. Figure created with BioRender.

Basophil granulocytes can be activated via IgE-dependent pathways, as they express the high-affinity IgE receptor FcεRI [9] and its ligand [22], leading to histamine release upon stimulation [9]. However, IgE-independent activation occurs via cytokines, e.g., IL-3 and IL-33, antibodies, such as IgG, Toll-like receptor ligands, including lipopolysaccharides, proteases, and complement factors [2, 23]. IgE-independent activation, however, causes less histamine release than the IgE-dependent activation [23]. IL-3 is the most potent activator

and priming factor of basophil granulocytes, enhancing the release of mediators [24, 25]. It additionally promotes basophil granulocyte differentiation [4], and its receptor α-chain CD123 is expressed on the basophil granulocyte surface [24, 26]. IL-5, NGFß [27], and GM-CSF, the latter of which is also secreted by basophil granulocytes [17], further prime basophil granulocytes for activation [28].

The basophil granulocyte activation test (BAT), which was developed in the 1950s, assesses IgE-mediated allergic responses by measuring the upregulation of activation markers such as CD13, CD45, CD63, CD69, and CD203c [29, 30] after contact with IgE [31]. CD63 and CD203c are the most prominent members of basophil granulocyte activation markers [29]. CD203c, a basophil-specific ecto-nucleotide pyrophosphatase/phosphodiesterase, is constitutively expressed on the surface of basophil granulocytes and upregulated following allergen-induced cross-linking of IgE on FcεRI [32]. This reaction precedes the externalization of CD63 [32]. CD63 is a membrane component of histamine-containing granules. Upon activation, the granules fuse with the membrane, causing the externalization of CD63 and histamine release during anaphylactic degranulation [33]. Within 1–6 hours of activation, basophil granulocytes release leukotrienes, prostaglandins, proteases, and cytokines, such as IL-4, IL-6, and IL-13 [23]. While anaphylactic degranulation is a rapid, IgE-dependent process, basophil granulocytes can also undergo piecemeal degranulation, a slower, IgE-independent process. During piecemeal degranulation, small vesicles form from granules and release their content without fusing with the cell membrane [34]. This process occurs during chronic diseases, such as bullous pemphigoid, ulcerative colitis, and Crohn's disease [34]. After IgE-independent stimulation, basophil granulocytes release IL-4 and IL-13. Taken together, these findings show the importance of basophil granulocytes in inflammation and itch.

1.2 Atopic dermatitis

AD is an inflammatory skin disease which is associated with dry skin and eczematous skin lesions (Figure 3) [35]. The main symptom, however, is pruritus [35] severely affecting the

quality of life in 5–20% of children [36] and 1–3% of adults [37]. Worldwide, AD is the most common skin disease in children. AD severely impairs the quality of life of all patients, affecting sleep, social life, their mental well-being, and that of their families [38]. As the first step in the atopic march, AD often precedes the development of asthma or allergic rhinitis [39] in approximately 80% of children [40].

Figure 3: Eczematous skin lesions in atopic dermatitis. Image provided by Ulrike Raap.

The pathogenesis of AD remains incompletely understood, with two competing hypotheses having been proposed: the "outside-in" and the "inside-out" hypotheses [41]. "Outside-in" describes a dysfunction of the epidermal barrier, which then triggers immune activation. This may occur due to a mutation in the skin barrier protein filaggrin; however, only approximately 20% of mild-to-moderate AD patients present with filaggrin mutations [42, 43], and >50% of mutation carriers never develop AD [42]. Even if they do, some adults outgrow the disease [43]. The "inside-out" hypothesis postulates that the development of AD is caused by immune dysregulation, which then leads to skin barrier dysfunction [41], enabling pathogens to enter the skin and cause inflammation [44]. The most recently

proposed model is called "outside-inside-outside," where environmental factors and the skin microbiome affect the skin from the outside through skin barrier defects, causing immune dysregulation that subsequently affects the skin barrier [44].

Injury of the epidermis causes the release of IL-25, IL-33, and TSLP, resulting in the activation of innate type II lymphoid cells [45]. This leads to a type II immune response, which is induced by IL-5 and IL-13 [45]. While IL-5 activates eosinophils [46], it is also one priming factor of basophil granulocytes [28]. During acute phases in AD, the cytokine profile is reported to be mainly Th2, which is characterized by cytokines such as IL-4, IL-13, and IL-31, while in chronic phases, T helper 1 (Th1) cytokines, such as IL-1 and IL-17, are predominantly present [40, 47]. Basophil granulocytes play an important role in the pathogenesis of AD, where they infiltrate into the lesional skin and perpetuate inflammation and itch [48–50] via IgE-independent pathways [6]. The production of IL-4, an important cytokine in AD pathogenesis, is induced by IL-18, IL-33, IL-3 by itself, and IL-3 in combination with Toll-like receptor ligands [6].

The exact mechanisms for the development of itch in AD are still not fully understood. However, it is known that IL-31, a key pruritogen in AD, activates sensory neurons and immune cells, creating an itch-scratch cycle [51]. *Staphylococcus aureus*, a Gram-positive bacterium, colonizes skin during AD flares due to changes in microflora [52]. It has been detected in 39% of non-lesional skin and 70% of lesional skin [53], correlating with disease severity [54]. Treatment for AD has been shown to increase microbial skin diversity [54]. The pathogen can activate basophil granulocytes through the release of protein A, causing histamine release [55], which suggests an interaction between *Staphylococcus aureus* and basophil granulocytes in AD.

In AD, peripheral nerve density is significantly increased at different stages of the disease in comparison to healthy subjects [56]. The enhanced presence of infiltrated basophil granulocytes close to neurons suggests a neuro-immune interaction [16]. Furthermore, basophil granulocytes are often located in close proximity to $CD4^+$ T cells and innate lymphoid type II cells in the skin of AD patients [57, 58]. Additionally, basophil granulocytes recruit eosinophils into the skin in AD [59], intensifying inflammation [60].

Pruritus in AD is difficult to treat. Antihistamines, which are used due to their mild side effects, often do not have any effect on pruritus treatment [61, 62]. However, novel therapies, including biologics and Janus kinase (JAK) inhibitors, have been proven to be very effective in treating both inflammation and pruritus in AD. These biologic therapies include dupilumab [63], tralokinumab [64], lebrikizumab [65], and nemolizumab [66]. The monoclonal antibody dupilumab targets IL-4Rα, the shared receptor for IL-4 and IL-13 [63], while tralokinumab and lebrikizumab bind directly to IL-13 [64, 65]. Nemolizumab, an anti-IL-31RA monoclonal antibody, relieves itch in AD patients and has been found to improve sleep, inflammation, and quality of life of patients [66], underscoring the pruritic effect of IL-31 in this disease. Further, JAK inhibitors have been proven to significantly inhibit pruritus and inflammation in AD [67]. Licensed JAK inhibitors include upadacitinib, abrocitinib, and baricitinib, targeting either JAK1, 2, or both signaling pathways [67].

There are two pathways of itch in AD. One is driven by IgE and histamine release [68]; the other is mediated by inflammatory mediators such as cytokines, neurotransmitters, neurotrophins, and neuropeptides, to name only a few [69, 70]. Itch in general has a broad spectrum of mediators that includes not only cytokines and neurotrophins but also ion channels [69], which are further discussed in Chapter 1.3.

1.3 Transient receptor potential channels

Transient receptor potential (TRP) channels were first discovered in 1969 by Cosens and Manning in a mutant of *Drosophila melanogaster* [71]. Instead of the usual constant response to a bright light stimulus, the mutant reacted in a transient manner [71]. This was caused by a mutation in the *trp* gene [72]. So far, 28 TRP channels have been identified in mammals, which are divided into six subfamilies based on their genetic composition: TRP ankyrin (TRPA, with 1 member), TRP canonical (TRPC comprising 7 members), TRP melastatin (TRPM containing 8 members), TRP mucolipin (TRPML with 3 members), TRP polycystin (TRPP comprising 3 members), and TRP vanilloid (TRPV containing 6 members) [73, 74].

TRP channels are widely expressed in the body, e.g., in sensory neurons [75, 76], epithelial cells [77], and immune cells [77], where they regulate processes such as leukocyte migration [78] and cytokine release [78]. When activated, cation influx occurs, leading to the depolarization of the membrane potential in neurons [79]. In the context of itch, pruritic signals are then transmitted [80]. The general structure of a TRP subunit consists of six transmembrane α-helices, with a pore-forming loop being located between transmembrane domains 5 and 6 (Figure 4A) [81]. Intracellularly, each subunit contains an N-terminal (NH_2) and C-terminal (COOH) domain (Figure 4A) [82]. These termini vary among subfamilies, with TRPA, TRPC, and TRPV possessing ankyrin repeats in their N-terminus [81]. A functional TRP channel is formed by four TRP subunits, either as a homo- or heterotetramer with other members of the same or different subfamilies (Figure 4B, C, respectively) [81, 82]. Once assembled, these channels enable the transport of cations across cellular membranes [81].

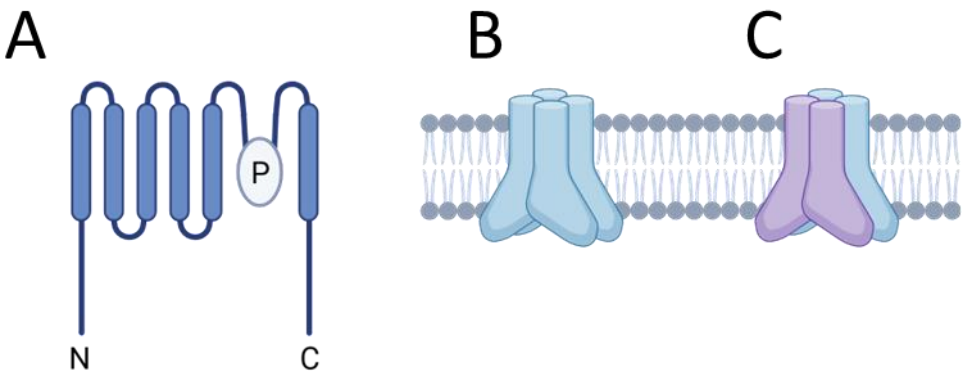

Figure 4: General structure of a transient receptor potential (TRP) channel. A: Structure of a single TRP subunit showing six transmembrane domains with a pore-forming loop (P) between segments 5 and 6. Intracellular NH_2-terminus (N) and COOH-terminus (C). **B:** Four homologous subunits forming a functional homotetrameric channel. **C:** Example of a heterologous channel containing subunits from the same or different TRP subfamilies. Figure created with BioRender.

TRP channels are involved in mediating diverse physiological functions, including thermosensation (TRPV1-4, TRPA1, TRPM8) [83], nociception (TRPA1, TRPV1) [83], chemosensation (TRPV1, TRPA1, TRPM5) [84], mechanosensation (TRPA1, TRPV4, TRPC1,

TRPC6) [85], neurogenic inflammation (TRPA1, TRPV1) [86–88], pain modulation (TRPV1) [89], and respiratory diseases (TRPA1, TRPM8, TRPV1) [90].

TRPA1 is of particular interest in dermatology due to its role in itch signaling [91] and neurogenic inflammation [86]. Interestingly, TRPA1 mRNA was also shown to be upregulated in the epidermis of AD patients [92]. Thus, this makes the TRPA1 an interesting target for investigation in AD.

1.3.1 TRPA1

The TRPA1 channel represents the most recently discovered member of the TRP superfamily in mammals. TRPA1 was first identified in human fibroblasts [93, 94]. Initially termed ankyrin-like with transmembrane domains protein 1 (ANKTM1) due to its N-terminal ankyrin repeats [94], subsequent studies revealed 14–18 ankyrin repeats across species, with 16 repeats being present in humans [94, 95]. It is expressed in sensory neurons [94], keratinocytes [96], melanocytes [97], and dorsal root ganglia (DRGs) [75]. Its presence has been confirmed in cells of the innate immune system, e.g., mast cells [98, 99] and macrophages [99], as well as in the adaptive immune system, such as B cells [100] and T cells [99, 101, 102].

TRPA1 is activated by diverse stimuli, with the most prominent compounds including allicin [103], carvacrol [104], cinnamaldehyde [101], and mustard oil [101], also known as allyl isothiocyanate (AITC) (Figure 5). Other activators of TRPA1 include the electrophilic compound JT010 [105], heat [106], and cold, with temperatures less than 18°C activating the channel in mice and rats [94, 107]; however, this effect in humans remains controversial [108, 109].

Modulation of TRPA1 channel expression occurs through intracellular Ca^{2+} [95], changes in pH [95], and antagonists, such as A-967079 [110], AP-18 [111], and HC-030031 [112]. Upon activation, TRPA1 mediates cation influx, causing membrane depolarization and elevated intracellular Ca^{2+} [99, 113]. Agonist-dependent trafficking occurs, as AITC increases membrane expression via translocation [114, 115], while carvacrol does not [104].

TRPA1 contributes to diseases such as asthma [116], diabetes mellitus [116], and AD [92, 98, 117]. Its activation evokes neuropathic and inflammatory pain and heat hypersensitivity [118]. While HC-030031 suppresses TRPA1 activation by AITC or cinnamaldehyde in humans and attenuates pain in mice [112], its inhibitory mechanism remains unclear [83].

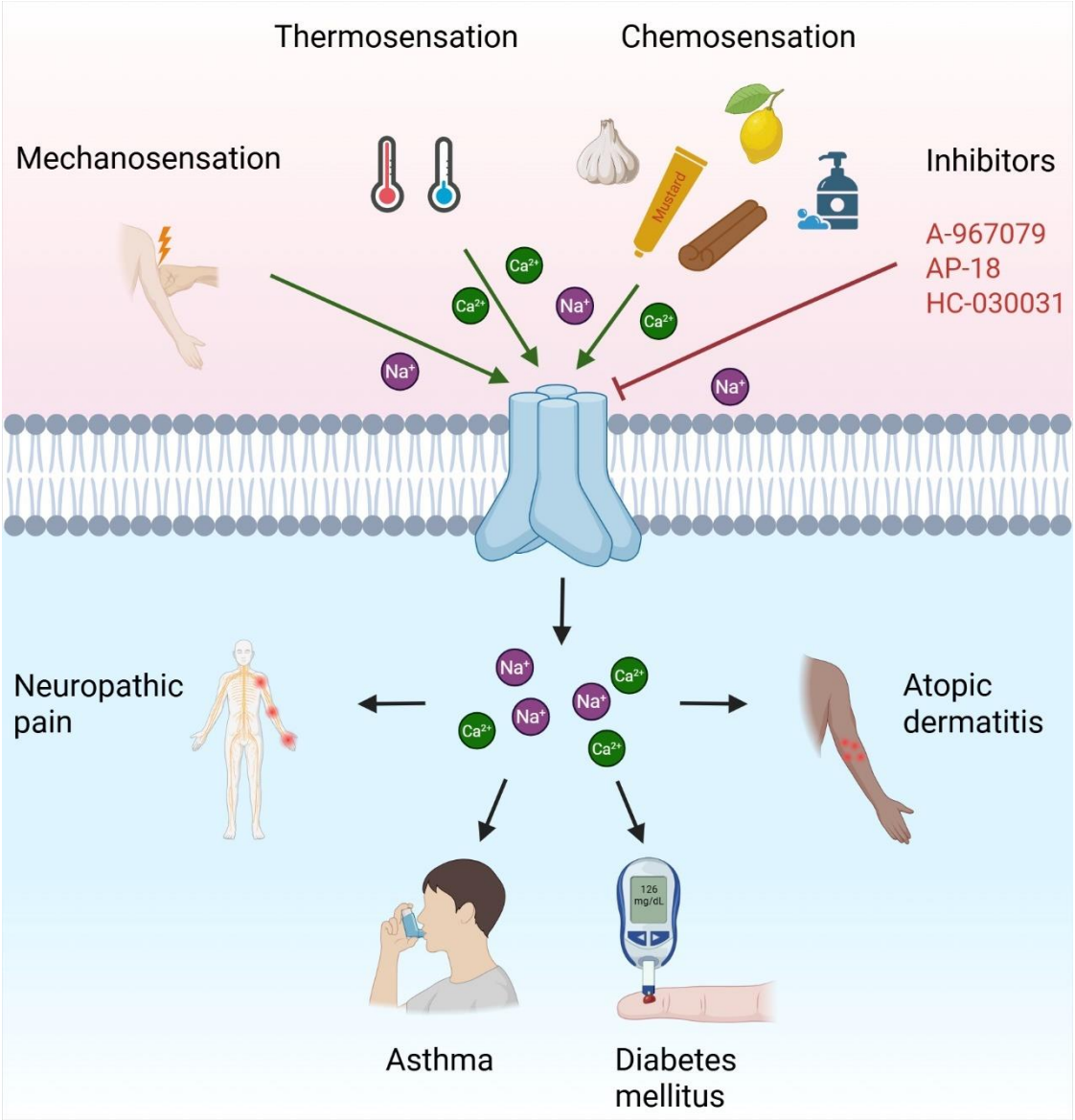

Figure 5: TRPA1 agonists and antagonists. The TRPA1 channel can be activated by a variety of agonists and actions and can also be inhibited. When activated, it is involved in multiple diseases. Figure adapted from Talavera *et al.* [95] and created with BioRender.

TRPA1 is primarily known for its role in itch, as it mediates histamine-independent pruritus via direct activation or through downstream G protein-coupled receptors signaling [119]. TRPA1 is also an important factor in AD, as was shown in a mouse model, where knockout of TRPA1 improved the scratching behavior [117]. Expression of the channel is increased in sensory neurons, DRGs, and mast cells in mice [98]. Similar results were discovered in humans, where TRPA1 was overexpressed in dermal afferent nerves, mast cells, and the skin of AD patients [92, 98]. Interestingly, TRPA1 was not only elevated in the lesional pruritic skin of AD patients but also in the non-lesional, non-pruritic tissue [92]. Given basophil granulocytes' role in allergic inflammation and their infiltration into AD lesions [49], understanding TRPA1 regulation in these cells could provide new insights into AD-associated itch. Aberrant serotonin signaling has been suspected to be part of the development of AD in humans [120]. The serotonin receptor HTR7 is expressed on sensory neurons responsible for itch and functionally coupled to TRPA1, as the receptor activates the channel via adenylate cyclase signaling [121]. The study by Morita *et al.* also indicated that HTR7 and TRPA1 were required to elicit an increase in the intracellular calcium level in humans, and both were necessary for the development of AD in mice [121].

Cevikbas *et al.* [51] successfully showed that DRGs express TRPA1 and TRPV1 channels. Co-expression of both channels has been documented before, as 97% of sensory neurons expressing TRPA1 also expressed TRPV1 [94]. In mice, the co-expression of TRPA1, TRPV1, and IL-31RA in DRGs is required to cause IL-31-induced scratching [51], highlighting the importance of TRPV1 in itch, which is further explained in the following chapter.

1.3.2 TRPV1

TRPV1 is primarily known for being activated by its agonist capsaicin, the spicy component in chili, which evokes a painful burning sensation [122]. The channel was first discovered in 1997 and has since been extensively studied for its role in pain pathways. Its importance has been demonstrated in mice, where TRPV1 knockout leads to reduced pain responses to TRPV1 agonists [123].

Similar to the TRPA1 channel, TRPV1 is expressed in neurons and immune cells. It has been found on human and murine nociceptive DRG neurons [51], the human trigeminal ganglion [124], and immune cells such as neutrophils [125], eosinophils [126], and basophil granulocytes [127]. While TRPV1 expression has been confirmed in basophil granulocytes, its specific function and regulation, particularly in the context of AD, remain to be fully elucidated.

TRPV1 plays a role in pain perception, as it is expressed on C- and Aδ nociceptive nerves [128]. When activated, the channel allows for Ca^{2+} and Na^{2+} ions to enter into nociceptive afferent neurons, which then release glutamate and peptides, such as substance P, neurokinin A, and calcitonin gene-related peptide [128, 129]. These neurotransmitters transmit pain signals to the dorsal horn of the spinal cord, which subsequently travel to the brain [128, 129]. Intradermal injection of capsaicin induces pain, confirming TRPV1's involvement in pain signaling [129].

The role of TRPV1 in inflammation was initially focused on neurogenic inflammation because it was thought to be expressed only in neurons [87, 88]. However, the discovery of TRPV1 in other cell types has led to investigations into its involvement in inflammatory diseases, such as asthma, rheumatoid arthritis, or inflammatory bowel diseases [88]. The application of TRPV1 antagonists, such as capsazepine, A-889425, and JNJ-17203212, has shown potential for improving these conditions [88, 130, 131].

The TRPV1 channel is also involved in itch signaling pathways. It is through this receptor that capsaicin can induce itch [132]. However, long-term activation of TRPV1 with capsaicin has analgesic and antipruritic effects as the TRPV1 channel on afferent neurons becomes desensitized [89]. TRPV1 signaling is part of the histaminergic itch pathway, as the channel is present on histamine-sensitive C-fibers and is activated by phospholipase A2 and 12-lipoxygenase [133]. It also contributes to non-histaminergic pruritus, as the activation of protease-activated receptors by their ligands causes the sensitization of TRPV1, leading to itch responses [80].

TRPV1 plays a significant role in pruritus signaling associated with AD. The pruritogenic cytokine IL-31 activates TRPV1 and TRPA1 on cutaneous sensory neurons and DRGs that express receptors for both TRP channels and IL-31RA [51], as mentioned in Chapter 1.3.1. A similar result was demonstrated by Lee *et al.* [134], where an AD disease model in mice evoked increased IL-31RA and TRPV1 overexpression in peripheral nerve fibers.

Clinical trials have further highlighted the therapeutic potential of targeting TRPV1. A Phase III clinical trial which investigated the TRPV1 antagonist Asivatrep provided promising results by significantly decreasing eczema along with attenuating pruritus [135]. Treatment with another TRPV1 antagonist, PAC-14028, improved skin barrier function in mice by suppressing AD-like symptoms such as increased serum IgE and scratching behavior [136]. TRPV1 mRNA is significantly increased in the pruritic skin of AD patients in comparison to healthy controls [92]. The channel was found to be expressed in eosinophilic and basophilic granulocytes in close proximity to neurons [126, 127]. Furthermore, TRPV1 expression is significantly increased in peripheral blood basophil granulocytes from AD patients [127].

1.4 Thesis aim

Atopic dermatitis, a chronic inflammatory and itchy skin condition, severely impairs the quality of life in patients [38]. Basophil granulocytes, which have been shown to infiltrate the skin of AD patients, do play a role in the inflammatory response [48–50]. However, the mechanisms of itch and inflammation in AD remain incompletely understood. While TRPV1 has been identified in human basophil granulocytes [127], the expression and functional relevance of TRPA1 in basophil granulocytes has not been investigated. Thus, this doctoral thesis aims to investigate the role of basophil granulocytes and the TRPA1 channel, along with its co-expression with TRPV1, in human peripheral blood basophil granulocytes of AD patients in addition to those of nonatopic (NA) controls. This research will help to understand the mechanism of itch and inflammation in AD, possibly revealing novel therapeutic targets for itch and inflammation.

The aim of the thesis was to examine the TRPA1 channel expression and functionality in human peripheral blood basophils of NA donors and AD patients.

Therefore, four main aspects were investigated:

1. TRPA1 expression in human peripheral basophil granulocytes from NA donors and AD patients were characterized. Basophil granulocytes were isolated and analyzed for their TRPA1 expression on both the mRNA and protein level. Further, TRPA1 expression on peripheral human blood basophils was analyzed in the context of Th2 inflammation of AD patients in comparison to NA donors. Moreover, skin samples from NA donors and AD patients were analyzed for basophil granulocyte infiltration with immunofluorescence staining.
2. TRPA1 functionality in human peripheral blood basophil granulocytes and its modulation by Th2 AD-associated cytokines and neurotrophins were assessed. The functionality of the TRPA1 channel was tested through a calcium flux assay. Afterwards, the effect of cytokines and neurotrophins, which are increased during AD [137–142], was analyzed to determine whether basophil granulocytes expressed more TRPA1 when stimulated with these inflammatory mediators.
3. Human peripheral blood basophil granulocyte viability was assessed to evaluate the effect of TRPA1 activation on basophil granulocytes.
4. The co-expression of TRPA1 and TRPV1 was analyzed in human peripheral blood basophils using flow cytometry.

Investigating these aims will give novel insights into the role of TRPA1 in basophil granulocytes during AD.

2 Materials and methods

2.1 Materials

2.1.1 Laboratory equipment

Equipment name	Manufacturer
Analytical scale	Sartorius, Göttingen
Arium® Pro Ultrapure Water Systems	Sartorius, Göttingen
BioSpectrometer® basic	Eppendorf, Hamburg
BSH200 Myblock Mini Dry Bath	Benchmark Scientific, Sayreville, NJ, USA
Centrifuge 5418	Eppendorf, Hamburg
Centrifuge 5424 R	Eppendorf, Hamburg
Centrifuge 5810 R	Eppendorf, Hamburg
Color Sprout® Plus Mini-Centrifuge	Biozym Scientific, Hessisch Oldendorf
Cryostat CM1950	Leica Biosystems, Nussloch
Cytoflex S Flow Cytometer	Beckman Coulter, Brea, CA, USA
FiveEasy Plus pH meter FP20-TRIS-Kit	METTLER TOLEDO, Columbus, OH, USA
Galaxy® 170 S CO2 Incubator	Eppendorf, Hamburg
LightCycler® 96	Roche Diagnostics, Basel, Switzerland
Olympus BX63F microscope with Olympus DP80 camera	EVIDENT Europe, Hamburg
PCR Workstation	VWR International, Radnor, PA, USA
Pipetus®	Hirschmann® Laborgeräte, Eberstadt
Precision scale	Sartorius, Göttingen
RH basic 2 magnetic stirrer	IKA, Staufen
ROCKER 3D digital	IKA, Staufen
Safety cabinet class II claire® pure	Berner International, Elmshorn
Scanning stage with ultrasonic BX3-SSU	EVIDENT Europe, Hamburg
Sola light engine	Lumencor, Beaverton, OR, USA
Specimen disc 20, assy.	Leica Biosystems, Nussloch

Equipment name	Manufacturer
Staining chamber StainTray™	Carl Roth, Karlsruhe
Staining trough acc. to Hellendahl with expansion	Carl Roth, Karlsruhe
Staining trough ROTILABO®	Carl Roth, Karlsruhe
SureCycler 8800	Agilent Technologies, Santa Clara, CA, USA
„The Big Easy“ EasySep™ Magnet	STEMCELL Technologies, Vancouver, Canada
Vornado™ Mini Vortex Mixer	Benchmark Scientific, Sayreville, NJ, USA
Water Bath 1002	GFL, Burgwedel

2.1.2 Disposables

Name	Manufacturer
Cap strips, PP, BIO-CERT® PCR QUALITY	Brand, Wertheim
Cover Slips, Rectangular	VWR International, Radnor, PA, USA
Finntip™ Filtered Pipette Tips	Thermo Fisher Scientific, Waltham, MA, USA
Gel-Loading Pipette Tips	VWR International, Radnor, PA, USA
LightCycler® 480 Multiwell Plate 96, white	Roche Diagnostics, Basel, Switzerland
LightCycler® 480 Sealing Foil	Roche Diagnostics, Basel, Switzerland
Nunc™ Serological Pipettes	Thermo Fisher Scientific, Waltham, MA, USA
Pasteur-Plast Makro Pipets, 3 mL	Ratiolab, Dreieich
PCR strips, PP, BIO-CERT® PCR QUALITY	Brand, Wertheim
Reaction tube, 1.5 ml, PP	SARSTEDT, Nümbrecht
Safe-Lock reaction tube, 1.5 mL, PCR clean	Eppendorf, Hamburg
SafeSeal reaction tube, 0.5 ml	SARSTEDT, Nümbrecht

Name	Manufacturer
SafeSeal SurPhob filter	Biozym Scientific, Hessisch Oldendorf
SafeSeal Tips Professional, steril	Biozym Scientific, Hessisch Oldendorf
Screw cap tube, 50 ml, (LxØ): 114 x 28 mm, PP, with print	SARSTEDT, Nümbrecht
S-Monovette® EDTA K3E, 9-ml	SARSTEDT, Nümbrecht
Superior™ HistoBond™ Adhesive Microscope Slides	Fisher Scientific, Leicestershire, UK
13 mL, 95 x 16.8 mm tube, round base tube, polystyrene	SARSTEDT, Nümbrecht

2.1.3 Chemicals and kits

Name	Manufacturer
Annexin V-FITC	Beckman Coulter, Brea, CA, USA
Anti-Human IgE (ε-chain specific) antibody produced in goat	Merck, Darmstadt
Bovine serum albumin (BSA)	VWR International, Radnor, PA, USA
Calcium chloride dihydrate	VWR International, Radnor, PA, USA
Cryo-Gel® embedding medium	Leica Biosystems, Nussloch
Cyto-Fast™ Fix/Perm Buffer Set	BioLegend, San Diego, CA, USA
Dako Pen	Agilent Technologies, Santa Clara, CA, USA
Decontamination solution, RNase AWAY®	VWR International, Radnor, PA, USA
Dimethylsulfoxid for cell culture	VWR International, Radnor, PA, USA
EasySep™ Direct Human Basophil Isolation Kit	STEMCELL Technologies, Vancouver, Canada
Ethylenediamine tetraacetic acid	Carl Roth, Karlsruhe
FastStart Essential DNA Green Master	Roche Diagnostics, Basel, Switzerland
Fetal bovine serum	Bio-Techne, Minneapolis, MN, USA

Name	Manufacturer
Fluo-4, AM, cell permeant	Thermo Fisher Scientific, Waltham, MA, USA
Gel sealant	got2be, Düsseldorf
HEPES	Carl Roth, Karlsruhe
High Pure RNA Isolation Kit	Roche Diagnostics, Basel, Switzerland
Ionomycin, Calcium Salt	Fisher Scientific, Leicestershire, UK
JT010	Merck, Darmstadt
Methanol	Merck, Darmstadt
N-Formyl-L-methionyl-L-leucyl-L-phenylalanin	Merck, Darmstadt
Penicillin : Streptomycin solution 6.0/10.0 g/L 100X	VWR International, Radnor, PA, USA
Recombinant Human IL-3	PeproTech, Cranbury, NJ, USA
Recombinant Human IL-13	PeproTech, Cranbury, NJ, USA
Recombinant Human IL-31	PeproTech, Cranbury, NJ, USA
Recombinant Human IL-33	PeproTech, Cranbury, NJ, USA
Recombinant Human TNF-α	PeproTech, Cranbury, NJ, USA
Recombinant Human TSLP	PeproTech, Cranbury, NJ, USA
Recombinant Human β-NGF	PeproTech, Cranbury, NJ, USA
Recombinant Human/Murine/Rat BDNF	PeproTech, Cranbury, NJ, USA
RNA*later*™ Solution	Thermo Fisher Scientific, Waltham, MA, USA
ROTI®Cell PBS	Carl Roth, Karlsruhe
ROTI®Mount FluorCare DAPI	Carl Roth, Karlsruhe
ROTI®PreMix PBS	Carl Roth, Karlsruhe
RPMI 1640, Cell culture medium	VWR International, Radnor, PA, USA
RPMI 1640 medium, w/o glutamine, phenol red	Thermo Fisher Scientific, Waltham, MA, USA

Name	Manufacturer
Sodium chloride	Merck, Darmstadt
Staurosporine	Fisher Scientific, Leicestershire, UK
Transcriptor First Strand cDNA Synthesis Kit	Roche Diagnostics, Basel, Switzerland
Tween® 20	AppliChem, Darmstadt
Water, Ultrapure for molecular biology nuclease-free	VWR International, Radnor, PA, USA

2.1.4 Media and buffers

Name	Composition
Binding buffer	*phosphate-buffered saline (PBS) (pH 7.4)* *10 mM HEPES* *150 nM NaCl* *2.5 mM $CaCl_2$ * $2H_2O$*
Blocking buffer	*PBS-Tween (PBS-T)* *1% bovine serum albumin*
PBS buffer	*1 L distilled water (aqua dest.)* *9.55 g PBS*
PBS-EDTA buffer	*1 L PBS* *1 mM ethylenediamine tetraacetic acid (EDTA)*
PBS-T buffer	*1 L aqua dest.* *9.55 g PBS* *0.1% Tween 20*
RPMI complete medium	*500 mL RPMI 1640* *10% fetal bovine serum* *1% Penicillin:Streptomycin solution*

2.1.5 Primary antibodies

Antigen	Conjugate	Species	Clone	Manufacturer	Dilution
CD123	PB	mouse	6H6	BioLegend	1:50
CD203c	PE	mouse	NP4D6	BioLegend	1:100
CD63	FITC	mouse	H5C6	BioLegend	1:100
FcεRIα	APC	mouse	AER-37 (CRA-1)	BioLegend	1:50
TRPA1	FITC	rabbit	polyclonal	LSBio	1:20
TRPA1	unconjugated	rabbit	polyclonal	abcam	1:400
TRPV1	PE	rabbit	polyclonal	LSBio	1:20
2D7	AF647	mouse	Basophil/2D7	BioLegend	1:100

2.1.6 Secondary antibodies

Antigen	Conjugate	Species	Clone	Manufacturer	Dilution
anti-rabbit IgG	AF488	goat	polyclonal	Invitrogen	1:2000

2.1.7 Primers

Gene	Sequence
GAPDH	for: AGCCACATCGCTCAGACAC
	rev: GCCCAATACGACCAAATCC
TRPA1	for: ACGATCATCAGGAGCAAAAGA
	rev: TCATGCATTCAGGGAGGTATT

2.1.8 Software

Software	Manufacturer/Provider
BioRender Software	Science Suite Inc., Toronto, Canada
cellSense Dimension Desktop 3.2	EVIDENT Europe, Hamburg
GraphPad Prism 9	GraphPad Software, San Diego, CA, USA
Kaluza Analysis 2.1	Beckman Coulter, Brea, CA, USA
LightCycler® 96 SW 1.1.0.1320	Roche Diagnostics, Basel, Switzerland
Microsoft Office 2016	Microsoft Cooperation, Redmond, WA, USA

2.2 Methods

2.2.1 Patient materials

Informed written consent was obtained from all patients and donors prior to sample collection. Human peripheral blood samples and skin biopsies were collected with the approval of the ethics committee of the Carl von Ossietzky University Oldenburg, under the reference numbers 2021-025 and 2017-106, respectively, within the Department of Dermatology and Allergology at the University Clinic Oldenburg. The experiments were conducted in accordance with the principles outlined in the Declaration of Helsinki. All blood donors were required to be at least 18 years old and not pregnant. Participants were categorized into two groups: nonatopic (NA) donors and AD patients. NA donors did not have any atopic diseases, such as allergic rhinitis, allergic asthma, or chronic inflammatory skin diseases. AD patients had not received systemic immunosuppressive therapy, biological therapy, or other systemic therapies, including JAK-inhibitors or light therapy, in the two weeks prior to blood donation. Blood samples were collected in 9 mL S-Monovette® EDTA K3E tubes. Skin samples were obtained from NA donors and AD patients, specifically from lesional sites in the latter group.

2.2.2 Isolation of human basophil granulocytes

Human peripheral basophil granulocytes were isolated from whole blood by negative selection according to Gray *et al.* [14] using the EasySep™ Direct Human Basophil Isolation Kit. In brief, whole blood was transferred to a polystyrene round base tube, and per mL of blood, 25 µL of EasySep™ antibody cocktail and 25 µL of EasySep™ RapidSpheres were added. The antibodies bind to every present cell except basophil granulocytes, while the magnetic RapidSpheres adhere to the aforementioned antibodies. During the isolation, the tube containing blood is placed in a magnet, which pulls the magnetically labeled cells to the tube wall, while unlabeled basophil granulocytes are transferred into a new tube. After the addition of the RapidSpheres, the volume was adjusted to 12 mL with phosphate-buffered saline-ethylenediamine tetraacetic acid buffer (PBS-EDTA, see Chapter 2.1.4). The

tube was placed in „The Big Easy“ EasySep™ Magnet, and the unlabeled basophil granulocytes were decanted into a new tube. This process was repeated three times to ensure the purity of basophil granulocytes and removal of all other cells. During each purification step, 12.5 µL/mL of EasySep™ RapidSpheres™ were added, while 20 µL of EasySep™ antibody cocktail were added only during the final step. Purified basophil granulocytes were pooled in a screw cap tube. 50 µL of isolated basophil granulocytes were stained with 1 µL of the basophil granulocyte markers APC anti-human FcεRI*α* Antibody and Pacific Blue™ anti-human CD123 Antibody (see Chapter 2.1.5), respectively. The purity of basophil granulocytes was confirmed by flow cytometry using the CytoFLEX S Flow Cytometer, with a required median purity of 97.2% to ensure reliable results. Afterwards, the sample was centrifuged using the 5810 R centrifuge for 7 min at 350 relative centrifugal force (rcf) at room temperature (RT), and the supernatant was removed with a 3 mL Pasteur-Plast Makro Pipet. Flow cytometry data were analyzed using Kaluza Analysis 2.1.

2.2.3 RNA analysis

2.2.3.1 Basophil granulocyte pellets

After basophil granulocyte isolation (see Chapter 2.2.2), a pellet of ≥ 3×10^5 basophil granulocytes from each donor was resuspended in 500 µL of PBS and transferred to a 1.5 mL reaction tube. The median purity of basophil granulocytes across all donors was 97.2%. The suspension was centrifuged using the 5424 R centrifuge for 8 min at 350 rcf at RT, followed by removal of the supernatant. To preserve the RNA for the subsequent isolation, basophil granulocytes were resuspended in 200 µL of RNA*later*™. The resuspended basophil granulocyte pellet was stored at -80°C.

2.2.3.2 RNA isolation

Total RNA was isolated using the High Pure RNA Isolation Kit according to the manufacturer’s instructions, except for the centrifugation step, which was performed for

varying amounts of time, ranging from 30 s up to 2 min, in order to ensure that the filter was completely dry. Since the thawed basophil granulocytes were suspended in 200 µL of RNA*later*™ Solution (see Chapter 2.2.3.1), resuspension with PBS was not necessary. In short, basophil granulocytes were lysed with 400 µL of Lysis/Binding Buffer while being shaken on the Vornado™ Mini Vortex Mixer for 15 s. A High Pure Filter Tube was placed into a Collection Tube and basophil granulocytes were transferred onto the filter. First, the supernatant was removed by centrifugation for 30 s at 8,000 rcf and at RT. Then, DNA was degraded by the addition of 90 µL of DNase I Incubation Buffer combined with 10 µL of DNase I for 15 min at RT. Afterwards, the sample was washed a total of three times: once with Wash Buffer I and once with Wash Buffer II for 30 s at 8,000 rcf at RT. The final wash step was performed with 200 µL of Wash Buffer II for 2 min at 13,000 rcf at RT. Thereafter, the High Pure Filter Tube was transferred into a PCR clean 1.5 mL reaction tube, and 50 µL of Elution Buffer were used to elute the RNA into the reaction tube by centrifugation for 1 min at 8,000 rcf and at RT. 1.5 µL of RNA were used to determine the concentration using the BioSpectrometer® basic, and the remaining RNA was stored at -80°C.

2.2.3.3 Reverse transcription

To generate complementary DNA (cDNA), reverse transcription was performed with the Transcriptor First Strand cDNA Synthesis Kit according to the manufacturer's instructions. The highest possible volume of RNA (11 µL) was added, as the isolated RNA was low in concentration. In essence, RNA, OR Random Hexamer Primer, Transcriptor Reverse Transcriptase Reaction Buffer, Protector RNase Inhibitor, Deoxynucleotide Mix, and Transcriptor Reverse Transcriptase were added to a PCR strip reaction tube according to Table 1. The reagents were mixed, the tube was closed with a cap strip, and placed in the SureCycler 8800 for reverse transcription according to the program outlined in Table 2. Following this process, the cDNA was transferred to a 1.5 mL reaction tube and stored at -20°C.

Table 1: Master mix for reverse transcription per sample

Reagent	Volume [µL]	Final concentration
RNA	variable	Up to 1 µg
OR Random Hexamer Primer	2	60 µM
Transcriptor Reverse Transcriptase Reaction Buffer	4	8 mM $MgCl_2$
Protector RNase Inhibitor	0.5	20 U
Deoxynucleotide Mix	2	1 mM
Transcriptor Reverse Transcriptase	0.5	10 U
Total	20	

Table 2: Reverse transcription program

Stage	Time	Temperature
Primer annealing	10 min	25°C
DNA polymerization	30 min	55°C
Enzyme deactivation	5 min	85°C
Cooling	∞	4°C

2.2.3.4 Quantitative real-time PCR

TRPA1 mRNA expression was analyzed by quantitative real-time PCR (qPCR) using the FastStart Essential Green Master reagent and the LightCycler® 96 platform. Forward and reverse intron-spanning primers for human TRPA1 and glyceraldehyde 3-phosphate dehydrogenase (GAPDH) (see Chapter 2.1.7) were utilized. The components for one reaction are listed in Table 3. Prior to analysis, the cDNA was diluted 1:10 with nuclease-free PCR-grade H_2O. Each sample was analyzed in duplicate to assess the expression of the TRPA1 channel. The expression was calculated in relation to the well-established housekeeping gene GAPDH [143]. Therefore, the sample was analyzed for both genes. 15 µL of the master mix for each target (TRPA1 and GAPDH, respectively), including all

components except the sample cDNA, were pipetted into a 480 Multiwell Plate 96. Then, 5 µL of the diluted sample were added to each well, to a total of 20 µL. The negative control consisted of 5 µL of PCR-grade H_2O. Additionally, to confirm that all genomic DNA was denatured, a no-RT control was performed: RNA that was not reverse transcribed was added to the master mix in the well, applying the same dilution factor. The 96-well plate was sealed with 480 Sealing Foil and centrifuged briefly at up to 1200 rcf to spin potential droplets to the bottom of the well. Afterwards, the plate was placed in the LightCycler® 96, and the qPCR program (Table 4) was started. The TRPA1 expression relative to GAPDH was calculated using the LightCycler® 96 SW 1.1.0.1320 program.

Table 3: Master mix for qPCR. Components and amounts for a single reaction. The cDNA sample was diluted with PCR-grade H_2O 1:10.

Component	**Amount**
FastStart Essential DNA Green Master (2x)	10 µL
Forward primer	300 nM
Reverse primer	300 nM
PCR-grade H_2O	5 µL – x µL forward and reverse primer
Diluted cDNA sample	5 µL
Total volume	**20 µL**

Table 4: qPCR program

Stage	Temperature [°C]	Ramp [°C/s]	Duration [s]	Acquisition mode
Pre-incubation	95	4.4	600	None
3-step	95	4.4	10	None
amplification	56	2.2	10	None
(45 cycles)	72	4.4	10	Single
Melting	95	4.4	10	None
	65	2.2	60	None
	97	0.1	1	5 Readings/°C

2.2.4 Flow cytometry analysis of TRP surface expression and total TRPA1 expression

To stain for TRP surface expression, 50 µL of freshly isolated basophil granulocytes (see Chapter 2.2.2) were stained with 1 µL each of antibodies against the basophil granulocyte markers FcεRIα and CD123. Additionally, 2.5 µL of Polyclonal Rabbit anti-Human TRPA1 Antibody (FITC) were added. When staining for the co-expression of TRPA1 and TRPV1 was performed, 2.5 µL of Polyclonal Rabbit anti-Human TRPV1 Antibody (PE) were also used. Staining was performed for 10 min at RT in the dark. Afterwards, 200 µL of PBS were added, and the stained basophil granulocytes were analyzed for TRPA1 and TRPV1 surface expression using the CytoFLEX S flow cytometer.

Total TRPA1 expression was analyzed by both intracellular and extracellular staining of basophil granulocytes. First, the extracellular staining for basophil granulocyte markers was performed. 5×10^4 basophil granulocytes were resuspended in 50 µL of PBS per condition and transferred into 1.5 mL reaction tubes. Staining was performed with 1 µL each of FcεRIα and CD123 by incubating for 10 min at RT in the dark, followed by centrifugation at 350 rcf for 5 min at RT to remove the supernatant. Next, the staining for total intracellular and extracellular expression of TRPA1 was performed. For this, basophil granulocytes were fixated and permeated with the Cyto-Fast™ Fix/Perm Buffer Set according to the manufacturer's instructions. In brief, basophil granulocytes were resuspended in 100 µL of

PBS and mixed with 150 µL of Fix/Perm Buffer, followed by incubation for 20 min at RT in the dark. 10X Perm Wash solution was diluted with aqua dest. 1:10, resulting in a 1X Perm Wash solution. 1 mL of the diluted Perm Wash solution was added to the reaction tubes, which were then centrifuged at 350 rcf for 5 min at RT. The supernatant was removed, and the wash step was repeated. Afterwards, basophil granulocytes were stained with 2.5 µL of anti-TRPA1 (see Chapter 2.1.5) per tube in 97.5 µL of Perm Wash solution for 20 min at RT in the dark. Basophil granulocytes were washed with 1 mL of 1X Perm Wash solution, followed by 1 mL PBS. Finally, basophil granulocytes were resuspended in 200 µL of PBS and analyzed by flow cytometry using the CytoFLEX S.

2.2.5 Calcium flux assay

The calcium flux assay was performed as previously described by Gray *et al.* [14]. In brief, isolated basophil granulocytes were resuspended in 500 µL of RPMI which does not contain phenol red per condition, pre-warmed to 37°C, and transferred to 1.5 mL reaction tubes. 1.5 µL of Fluo-4 AM, a cell membrane-permeable fluorescent Ca^{2+}-dye [144], were added to each reaction and incubated for 20 min at 37°C and 5% CO_2. Afterwards, the supernatant and excess dye were removed by centrifugation for 3 min at 350 rcf at RT. Basophil granulocytes were resuspended in 450 µL of pre-warmed RPMI without phenol red. The stimulants were diluted in RPMI without phenol red to a total volume of 50 µL. For the negative control, 50 µL of RPMI without phenol red were added, while for the positive control, 500 nM of ionomycin were used. Ionomycin is an ionophore that preferentially binds calcium in a 1:1 ratio [145]. It transports cations across the cell membrane, thereby increasing the calcium concentration [145]. The TRPA1 agonist JT010 [105], which was dissolved in dimethyl sulfoxide (DMSO), was diluted in RPMI without phenol red in various concentrations (10, 100, 1000 nM). The reaction tube containing basophil granulocytes was placed in the CytoFLEX S for analysis. For one minute, calcium-induced fluorescence was measured until the baseline stabilized. At the 1 min mark, the stimulant was added to the reaction tube with a Gel-Loading Pipette Tip; the uptake of the flow

cytometer was increased to maximum for 2 s and then decreased back to medium. The measurement was continued for 4 min.

2.2.6 Basophil granulocyte activation test

To evaluate the ability of a stimulant to activate basophil granulocytes, a basophil granulocyte activation test (BAT) was conducted according to the method described by Gray *et al*. [14]. In short, at least 5 x 10^4 isolated basophil granulocytes per condition were resuspended in 90 µL of pre-warmed RPMI complete medium (see Chapter 2.1.4) and transferred to separate 1.5 mL reaction tubes. Basophil granulocytes were incubated for 2 min at 37°C. Subsequently, 10 µL of the stimulants were added to the reaction tubes. As a negative control, 10 µL of RPMI complete medium were used. N-formyl-L-methionyl-L-leucyl-L-phenylalanine (fMLP) and anti-human IgE (ε-chain specific) antibody (a-IgE) served as positive controls. Following concentrations of the TRPA1 agonist JT010 were tested: 10, 100, and 1000 nM. Basophil granulocytes were incubated for 30 min at 37°C and 5% CO_2 with the lid of each reaction tube tilted to ensure gas exchange. Afterwards, the tubes were placed on ice for 2 min to stop the reaction, followed by centrifugation for 7 min at 350 rcf at 4°C and removal of the supernatant. Basophil granulocytes were then resuspended in 46 µL of PBS and stained with 1 µL each of antibodies against FcεRIα, CD123, CD203c (PE), and CD63 (FITC) for 10 min at RT in the dark. Finally, 100 µL PBS were added, and basophil granulocytes were analyzed by flow cytometry.

2.2.7 Stimulation of basophil granulocytes under inflammatory conditions

Isolated human peripheral blood basophil granulocytes were stimulated with cytokines, neurotrophins, at different temperatures or in distinct pH media, respectively, to analyze the effects of these conditions on TRPA surface expression. For each condition, 5 x 10^4 basophil granulocytes were used.

For stimulation, isolated and purified human peripheral blood basophil granulocytes were resuspended in 475 µL of RPMI complete medium pre-warmed to 37°C and transferred into 1.5 mL reaction tubes. 10 ng/mL of IL-3, IL-31, IL-33, TSLP, NGFβ, TNF-α, and 50 ng/mL of IL-13 or brain-derived neurotrophic factor (BDNF) were added to the respective reaction tubes. If necessary, RPMI complete medium was added to achieve a total volume of 500 µL.

To assess the effect of pH on TRPA1 expression, basophil granulocytes were incubated with pH-neutral (7.0) RPMI complete medium as a control and acidified media with pH levels of 6.5 and 5.0, also in total volumes of 500 µL.

The impact of temperature on the upregulation of surface TRPA1 expression was evaluated by incubating basophil granulocytes at 37°C as a control and at 40°C to simulate the increase in temperature during inflammation.

The stimulations were performed for 4 h at 37°C, if not mentioned otherwise, and 5% CO_2. Afterwards, basophil granulocytes were centrifuged at 350 rcf for 7 min at RT. The supernatant was discarded, and basophil granulocytes were resuspended in 50 µL of PBS with antibodies. Basophil granulocytes were stained with 1 µL each of anti-FcεRIα and anti-CD123, along with 2.5 µL of anti-TRPA1 and anti-TRPV1, respectively, for 10 min at RT in the dark. Then, 200 µL of PBS were added, and 8,000 events per sample were analyzed by flow cytometry using the CytoFLEX S.

2.2.8 Apoptosis assay

An apoptosis assay was performed to analyze whether the activation of the TRPA1 channel influences basophil granulocyte viability, as well as to test if JT010 has a cytotoxic effect. During the assay, basophil granulocytes are stained with annexin V and propidium iodide (PI) to differentiate viable from apoptotic and necrotic basophil granulocytes. Under normal conditions, phosphatidylserine residues are located on the inside of the cell membrane but are exposed during early apoptosis, enabling binding of annexin V [146]. PI binds to nucleic acids, which become accessible during cell death due to disrupted cell membrane integrity [147]. This allows for the differentiation of cell populations: viable cells are characterized as

annexin V^-/PI^-, apoptotic cells as annexin V^+/PI^-, late apoptotic cells as annexin V^+/PI^+, and necrotic cells as annexin V^-/PI^+ [148]. Isolated basophil granulocytes were resuspended in 90 µL of RPMI complete medium, pre-warmed to 37°C, for each reaction, with approximately 1×10^5 basophil granulocytes per condition, and transferred to 1.5 mL reaction tubes for the apoptosis assay with the Annexin V-FITC Kit. 10 µL of the respective stimulants were added to the reaction. RPMI complete medium was used as a negative control, while staurosporine acted as a positive control. The TRPA1 agonist JT010 was added at concentrations of 10, 100, or 1,000 nM. Basophil granulocytes were incubated for 4 or 24 h at 37°C and 5% CO_2. To ensure gas exchange, the lids of the reaction tubes were tilted. Afterwards, the tubes were placed on ice for 2 min to halt the reaction, followed by centrifugation at 350 rcf for 7 min at 4°C. The supernatant was removed, and basophil granulocytes were resuspended in 500 µL of cold PBS. Centrifugation was repeated, and the supernatant was discarded again. Basophil granulocytes were stained with 0.5 µL of annexin V and 2.5 µL of PI in 47 µL of PBS per reaction for 15 min on ice in the dark. Afterwards, 200 µL of ice-cold binding buffer (see Chapter 2.1.4) were added, and basophil granulocytes were analyzed by flow cytometry using the CytoFLEX S within 30 min.

2.2.9 Immunofluorescence analysis

2.2.9.1 Embedding skin biopsies

Skin samples were collected from NA donors and patients with AD at the Department of Dermatology and Allergology at the University Clinic Oldenburg. For AD patients, samples were taken from lesional sites. In general, each skin sample of NA or AD measured 2-4 mm in size, was wrapped in a sterile swab soaked in saline, and then placed in a container. To prevent autolysis, samples were embedded within 30 min of collection. A specimen disc was positioned on the -20°C cooled Peltier element of the Cryostat CM1950, oriented with its groove at 12 o'clock. The skin tissue was placed onto the specimen disc and covered with Cryo-Gel® embedding medium, ensuring that the gel filled every groove of the disc. The sample was oriented with the epidermis facing either 3 or 9 o'clock on the disc. Additional

embedding medium was applied to the tissue and smoothed with a finger to ensure complete coverage. Once the gel solidified, indicated by the change to a white color, the embedded skin samples were stored at -80°C.

2.2.9.2 Cryo-sectioning skin biopsies

To preserve the tissue structure, cryo-sectioning was used. The specimen disc containing the frozen tissue was secured in the cryostat. Excess embedding medium on top was removed using the razor blade of the cryostat until the tissue became visible. Then, a cut of 6 µm thickness was made, and a Superior™ HistoBond™ Adhesive Microscope Slide at RT was placed onto it. Due to the temperature difference, the sliced tissue transfers onto the slide [149]. The slides were subsequently frozen at -80°C.

2.2.9.3 Immunofluorescence staining

Frozen skin sections from patients with AD or NA donors (see Chapter 2.2.9.2) were placed in the fume hood to thaw. Afterwards, they were transferred to a staining trough acc. to Hellendahl, which was filled with -20°C cold methanol and incubated for 10 min at -20°C. The slides were then air-dried in the fume hood. Subsequently, the tissue areas were circled with a hydrophobic Dako Pen. To wash the slides, they were placed in a ROTILABO® staining trough filled with PBS-Tween (PBS-T, see Chapter 2.1.4) and agitated on the 3D-Rocker for 5 min at 40 revolutions per minute at RT. Afterwards, the samples were patted dry on paper tissue, and the hydrophobic borders were renewed if necessary. The slides were positioned in the StainTray™ staining chamber, the floor of which was covered with aqua dest. 50 µL of blocking buffer (see Chapter 2.1.4) were pipetted onto each circled sample, followed by incubation for 30 min at RT in the dark. The slides were then patted dry on paper tissue, and the washing steps with PBS-T were repeated. Staining was performed in the chamber using the appropriate dilutions (see Chapters 2.1.5 and 2.1.6). The samples were incubated overnight at 4°C in the dark with 25 µL of the primary antibody against TRPA1 (unconjugated). Afterwards, the slides were washed four times with PBS-T

in the dark. The samples were then stained with 25 µL of the secondary antibody anti-rabbit Alexa Fluor 488 for 1 h at RT in the dark, followed by washing with PBS-T four times. 25 µL of anti-2D7 Alexa Fluor 647 were added, and incubation was repeated. Subsequently, the slides were washed four times with PBS-T and twice with PBS (see Chapter 2.1.4). Afterwards, 20 µL of ROTI®Mount FluorCare DAPI were pipetted onto the samples, ensuring that no bubbles were present, and a cover slip was placed on top. To prevent the mounting medium from drying out, a gel sealant was applied to seal the edges of the cover slip. Once dried, the slides were stored at 4°C. The negative control was treated similarly, but blocking buffer was added instead of antibody solution. For the secondary antibody control, blocking buffer replaced both the primary antibody and basophil granulocyte marker antibody. Analysis was performed with the Olympus BX63F microscope equipped with the Olympus DP80 camera, and images were edited using the cellSense Dimension Desktop 3.2 software.

2.2.10 Statistical analysis

All data were presented as mean ± standard error of the mean (SEM). If data were normally distributed, a Student's t-test was performed to compare two groups. Results among three or more groups were assessed with one-way ANOVA followed by Dunnett's post-hoc test. For analyzing two factors, a two-way ANOVA mixed-effects analysis followed by Šídák's post-hoc test was performed. The calculated p-values are listed in the Supplementary Tables S1-S26. Flow cytometry analysis was reported as mean fluorescence intensity (MFI) or as a percentage of positive cells. Kaluza Analysis 2.1 was used for fluorescence analysis. All statistical significance levels were evaluated and illustrated using GraphPad Prism 9, with the alpha level set at $p < 0.05$.

3 Results

3.1 TRPA1 expression in basophil granulocytes

3.1.1 TRPA1 is expressed in human peripheral blood basophil granulocytes

To see if human peripheral blood basophil granulocytes express the TRPA1 channel, different approaches were utilized, including flow cytometry and RNA analysis. For this, human basophil granulocytes of NA donors were isolated from peripheral blood by negative selection, as described by Gray *et al.* [14]. Isolated basophil granulocytes had a median purity of 97.2% (Figure 6A), confirmed by flow cytometry with the use of antibodies against the basophil granulocyte markers CD123 and FcεRIα. Next, the specificity of the TRPA1 antibody was validated using an isotype control (Figure 6B), since both antibodies have distinct peaks, making it well-suited for continued use. TRPA1 expression was first analyzed on the mRNA level. Total RNA was isolated from the purified basophil granulocytes, reverse-transcribed into cDNA, and analyzed for TRPA1 mRNA expression as outlined in Chapter 2.2.3. The results showed that basophil granulocytes of NA donors contained TRPA1 mRNA (Figure 6C). As mRNA expression was confirmed, the question arose whether basophil granulocytes produced the TRPA1 protein as well. Therefore, the surface expression was analyzed. The flow cytometry analysis was evaluated as MFI (Figure 6D) and percentage of positive basophil granulocytes (Figure 6E). The analysis confirmed the surface expression of TRPA1 protein on 69.37 ± 5.56% of basophil granulocytes. This finding demonstrates that basophil granulocytes express TRPA1 on both the mRNA and protein level.

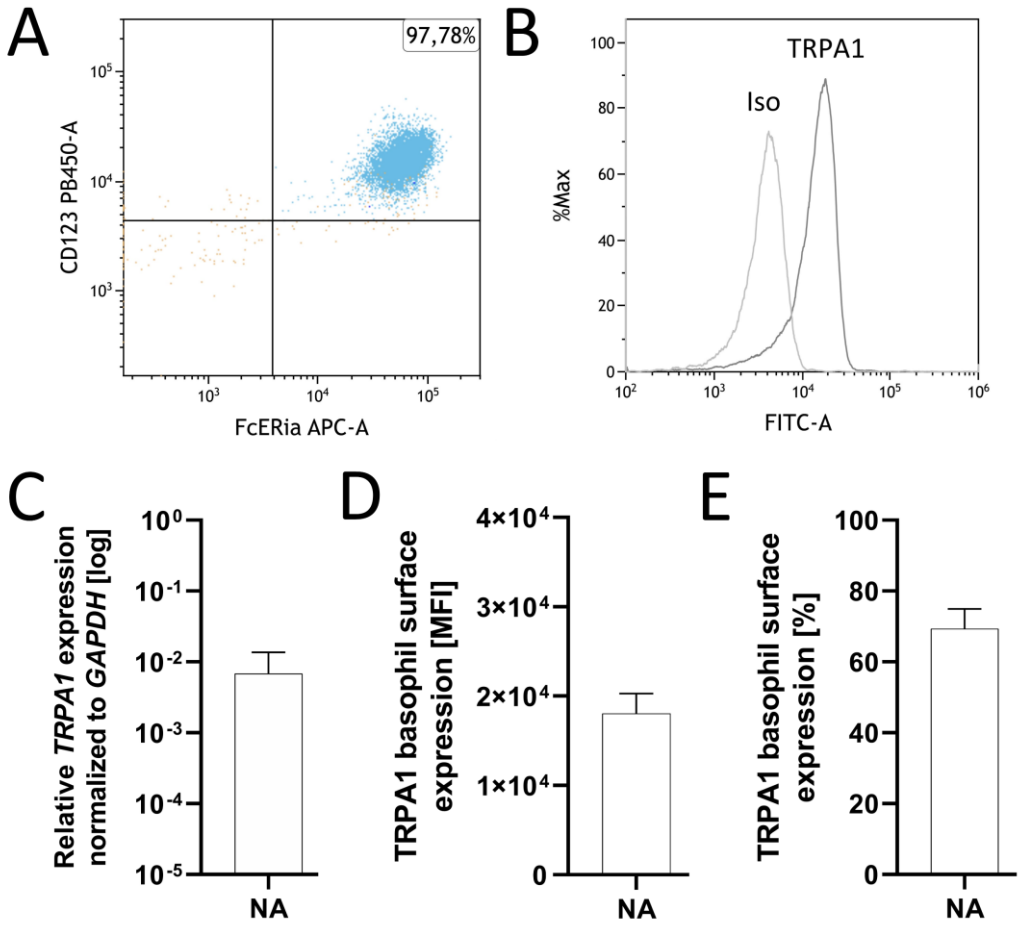

Figure 6: TRPA1 expression in human basophil granulocytes. Human basophil granulocytes of nonatopic donors (NA) were isolated and analyzed for TRPA1 expression by flow cytometry and quantitative real-time PCR (qPCR). **A:** Percentage of purified basophil granulocytes. **B:** One representative histogram out of n=3 of isotype control and TRPA1 stained basophil granulocytes. **C:** TRPA1 mRNA expression analyzed by qPCR (n=4). **D:** TRPA1 surface protein expression (n=8) illustrated as mean fluorescence intensity (MFI). **E:** Percentage of basophil granulocytes from NA donors (n=8) expressing TRPA1. Data are presented as mean ± SEM.

3.1.2 TRPA1 expression is increased in basophil granulocytes of AD patients

After analyzing TRPA1 in NA donors, the channel's expression in AD patients was investigated, as TRPA1 is known to be present and upregulated in the neurons and skin of patients with AD [92, 98]. For this, analysis of mRNA with qPCR and detection of protein expression with flow cytometry analysis were performed on isolated peripheral blood basophil granulocytes. The mRNA analysis revealed that TRPA1 mRNA was significantly increased in basophil granulocytes of patients with AD compared to NA donors (p=0.0347)

(Figure 7A, Supplementary Table 1). This finding is in accordance with the results of Nattkemper *et al.* [92], where TRPA1 was significantly overexpressed in the skin of AD patients compared to the healthy controls. Subsequently, the surface protein expression was determined, which showed two distinct peaks in the MFI (Figure 7B), indicating a higher expression in peripheral blood basophil granulocytes of AD patients compared to NA controls. The difference in surface protein expression was significantly increased in basophil

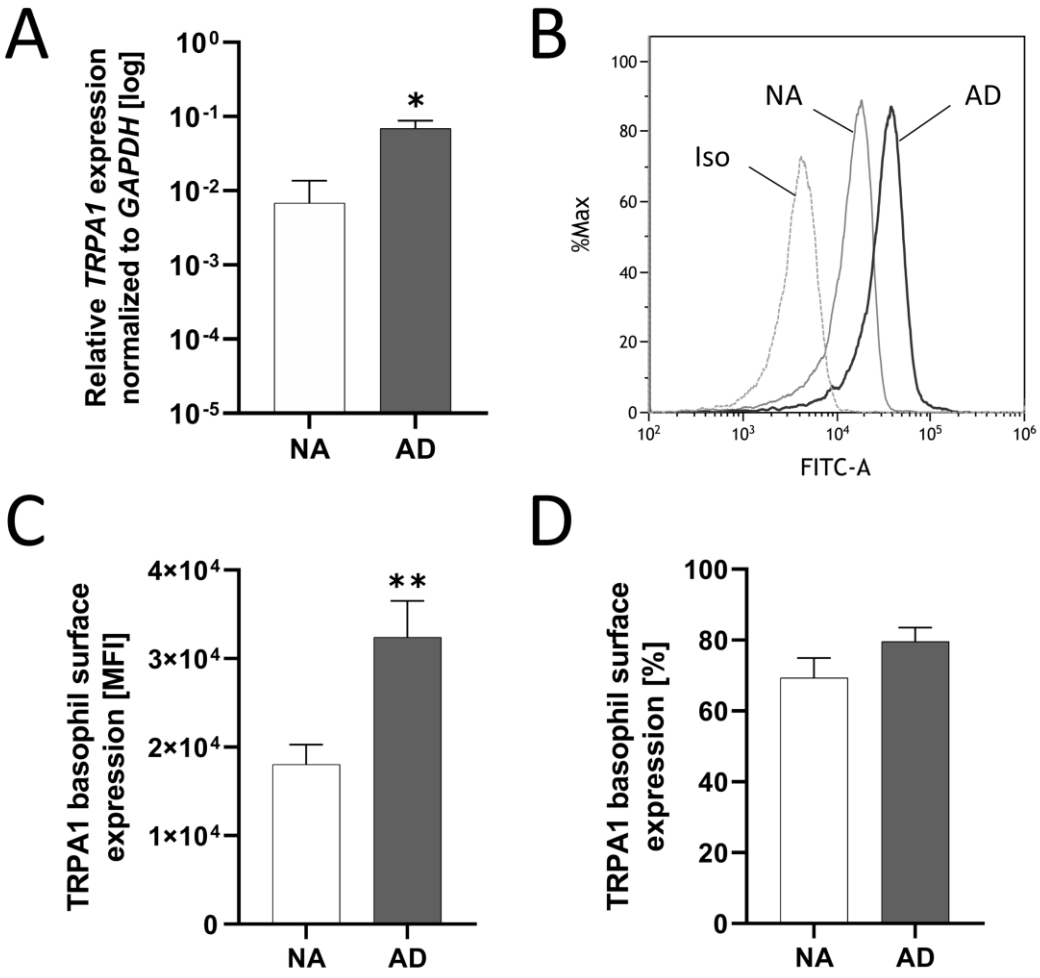

Figure 7: Basophil granulocyte TRPA1 mRNA and surface protein expression in nonatopic (NA) donors and patients with atopic dermatitis (AD). A: qPCR analysis for the detection of TRPA1 mRNA of basophil granulocytes from NA donors (n=4) and AD patients (n=6). **B:** One representative histogram out of n=3 showing the mean fluorescence intensity (MFI) of isotype control (Iso) and TRPA1 stained basophil granulocytes of NA donors and AD patients. **C:** TRPA1 surface expression in NA donors (n=8) and patients with AD (n=7) illustrated in MFI. **D:** Percentage of basophil granulocytes expressing TRPA1 on the surface in NA donors (n=8) and patients with AD (n=7). Statistical analysis was performed using an unpaired Student's t-test. A p-value < 0.05 was considered significant. * < 0.05, ** < 0.01. Data are presented as mean ± SEM.

granulocytes of AD patients compared to basophil granulocytes of NA controls as determined by the MFI (p=0.0073) (Figure 7C, Supplementary Table 2). However, the percentage of TRPA1-positive basophil granulocytes was not significantly altered (Figure 7D, Supplementary Table 3). Together, these data demonstrate that TRPA1 is expressed in basophil granulocytes of AD patients at significantly higher levels compared to NA donors.

3.1.3 Functionally active TRPA1 channel in human basophil granulocytes

After confirming the presence of the TRPA1 channel on human basophil granulocytes, the next step was to analyze the functionality of the channel through measurement of intracellular calcium flux. Isolated human peripheral blood basophil granulocytes of NA donors were stimulated with ionomycin (500 nM), an ionophore serving as a positive control due to its ability to facilitate ion transport across membranes [150], and the TRPA1 agonist JT010 (10, 100, 1000 nM) [105] (Figure 8). The relative cytosolic calcium level [F] was normalized to the baseline calcium level at 40 s [F_0]. To quantify the increase in intracellular calcium, the relative cytosolic calcium level at 50 to 60 s was subtracted from the calcium level at 240 to 250 s, indicated by the grey dotted rectangles in Figure 8B and D. The addition of ionomycin induced a rapid increase in intracellular calcium levels of human basophil granulocytes (Figure 8A, B, and C), confirming the effectiveness of the assay. To assess the functionality of the TRPA1 channel, various concentrations of JT010 were applied, resulting in a gradual increase in calcium levels over time (Figure 8A, D, and E). The response to the agonist occurred in a dose-dependent manner, with statistically significant effects observed at the middle (p=0.0128) and highest concentrations (p=0.0003) (Supplementary Table 4). These results demonstrate that the TRPA1 channel on human peripheral blood basophil granulocytes is functional and responds to stimulation in a dose-dependent manner.

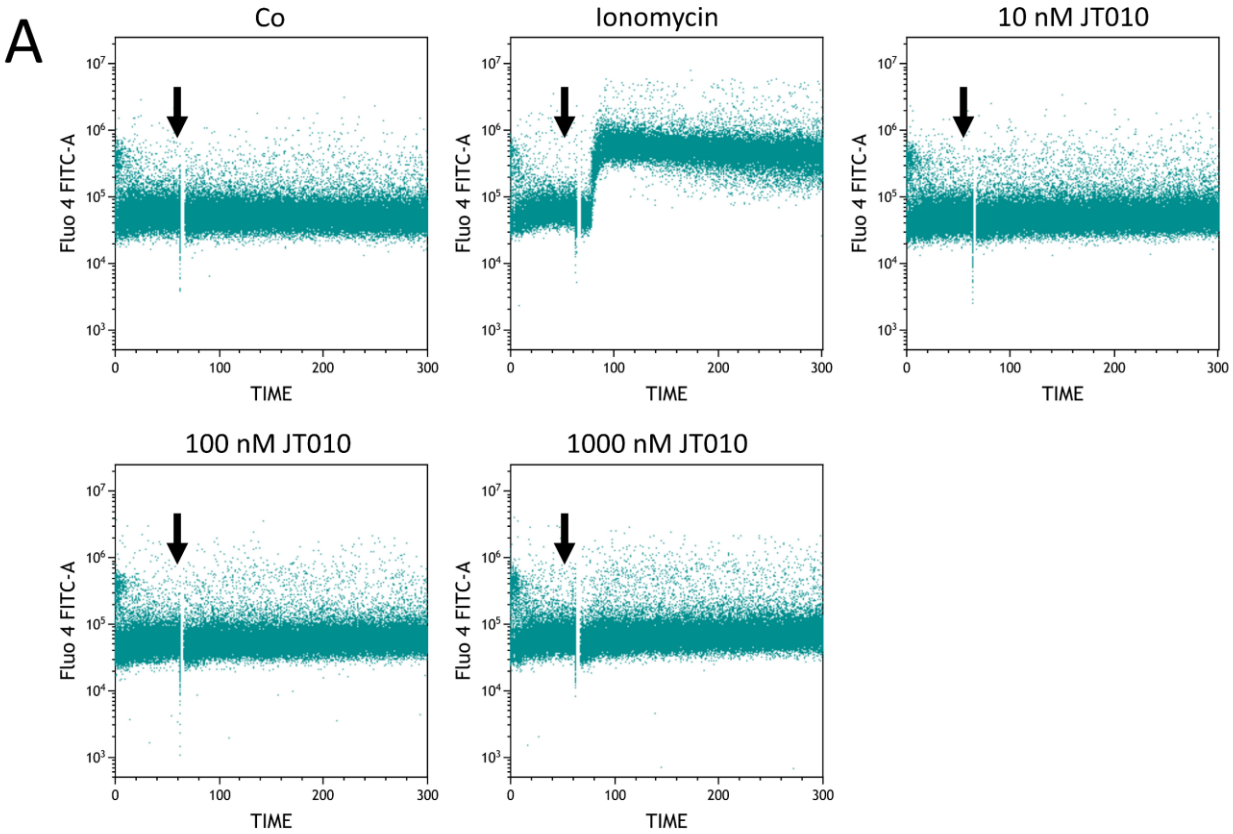
A
Co
Ionomycin
10 nM JT010
100 nM JT010
1000 nM JT010
Fluo 4 FITC-A
TIME

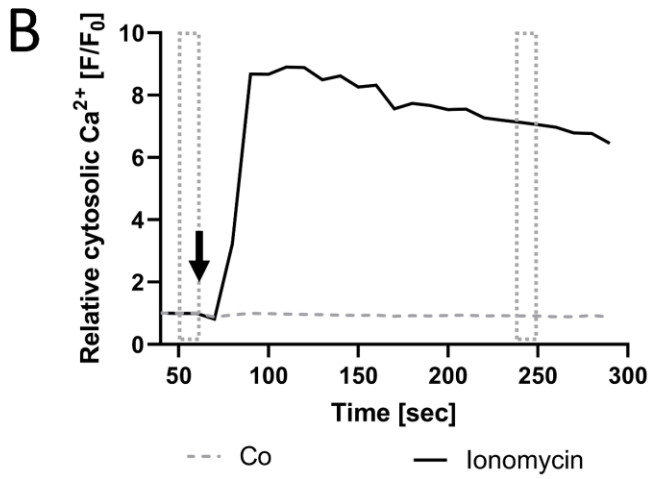
B
Relative cytosolic Ca2+ [F/F0]
Time [sec]
Co
Ionomycin

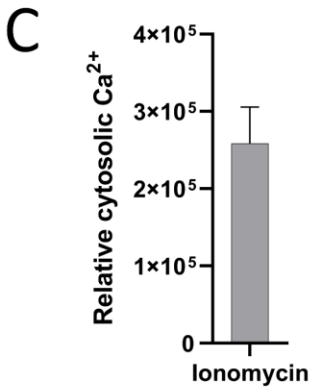
C
Relative cytosolic Ca2+
Ionomycin

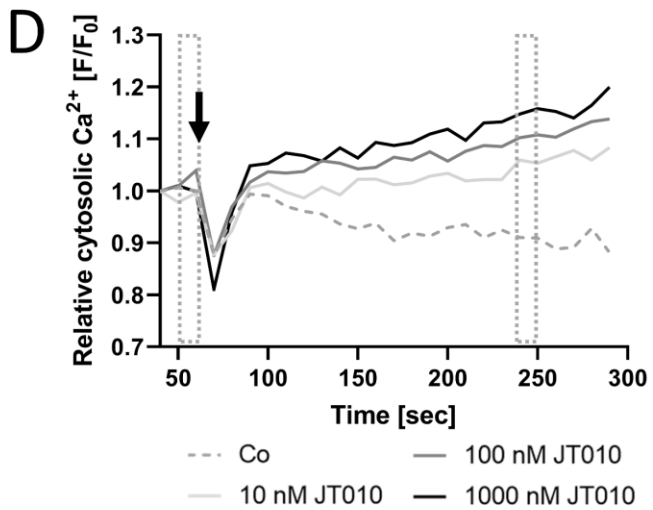
D
Relative cytosolic Ca2+ [F/F0]
Time [sec]
Co
10 nM JT010
100 nM JT010
1000 nM JT010

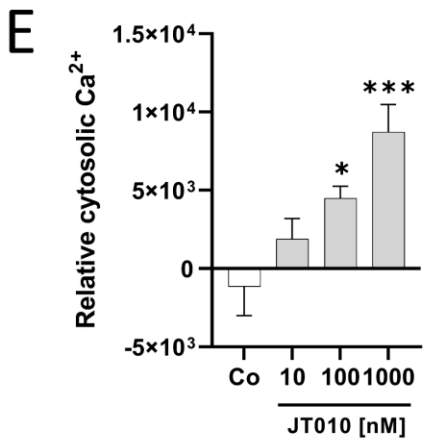
E
Relative cytosolic Ca2+
Co
10
100
1000
JT010 [nM]

Figure 8: Calcium flux analysis after TRPA1 activation. Isolated basophil granulocytes from NA donors were labeled with Fluo-4 AM (3 μM). After baseline stabilization, RPMI complete medium (Co), ionomycin (500 nM), or TRPA1 agonist JT010 (10, 100, or 1,000 nM) was added at 60 s (arrow). Relative cytosolic calcium levels were analyzed for 5 min by flow cytometry (n=4 different experiments). To account for baseline variations, the relative cytosolic calcium level [F] was normalized to the baseline calcium level at 40 s [F_0] and expressed as the ratio [F/F_0]. **A:** One representative dot plot out of n=4 different experiments of intracellular calcium levels after basophil granulocyte stimulation. **B:** One representative graph out of n=4 of the normalized changes in cytosolic calcium levels of human NA basophil granulocytes [F/F_0] after ionomycin application, which served as a positive control. **C:** The relative cytosolic calcium increase was calculated as the difference between calcium levels after (250 s, right dotted rectangle in B) and before (60 s, left dotted rectangle in B) the application of ionomycin. **D:** One representative graph out of n=4 of normalized intracellular calcium concentration [F/F_0] after TRPA1 activation with JT010. **E:** Changes in relative cytosolic calcium after TRPA1 activation with different concentrations of JT010. The relative cytosolic calcium increase was calculated as the difference between calcium levels after (250 s, right dotted rectangle in D) and before (60 s, left dotted rectangle in D) the application of the stimulant. Statistical analysis was performed using one-way ANOVA followed by Dunnett's post-hoc test. A p-value < 0.05 was considered significant. * < 0.05, *** < 0.001. Data are presented as mean ± SEM.

3.1.4 TRPA1 activation did not modulate CD63 and CD203c surface expression

After confirming the functionality of the TRPA1 channel with calcium flux, the next step was to determine the effect of its activation on basophil granulocyte degranulation and activation. To this end, a BAT was performed, which assesses the externalization of CD63, a marker associated with histamine release, and upregulation of CD203c upon activation of basophil granulocytes [16]. In this process, basophil granulocytes were stimulated for 30 min using fMLP or a-IgE, which served as positive controls for basophil granulocyte activation. To activate the TRPA1 channel, its agonist JT010 was added in various concentrations (10, 100, 1,000 nM) to the culture medium with isolated human peripheral blood basophil granulocytes. The results showed that the addition of anti-IgE resulted in significantly increased CD63 externalization and CD203c upregulation (p=<0.001 in both cases), while fMLP only caused a significant change in CD203c upregulation (p=<0.001) (Figure 9, Supplementary Table 5, Supplementary Table 6). Stimulation with JT010 had no impact on the presence of the basophil granulocyte activation markers CD63 and CD203c compared to the control. These results suggest that the activation of the TRPA1 channel does not directly affect the surface externalization of CD63 and CD203c, assuming that TRPA1

does not drive the release of histamine since CD63 surface expression has been shown to correlate with histamine release [151].

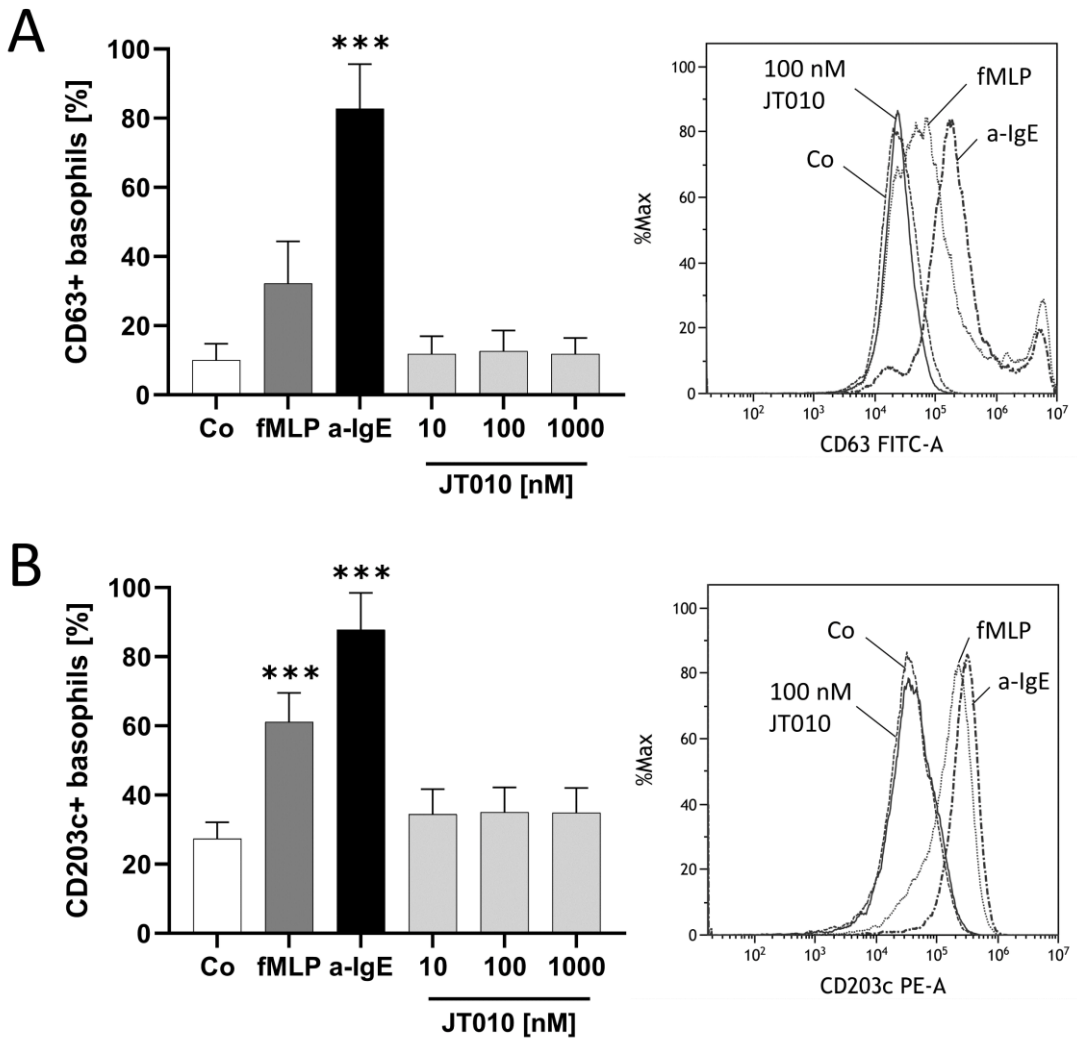

Figure 9: Effect of TRPA1 activation on CD63 externalization and CD203c upregulation in human peripheral blood basophil granulocytes. Basophil granulocytes from NA donors were stimulated with N-formyl-methionyl-leucyl-phenylalanine (fMLP, 1 μM), anti-IgE (a-IgE, 1 μg/mL), or TRPA1-specific agonist JT010 (10, 100, 1000 nM) for 30 min at 37°C and 5% CO_2. RPMI complete medium (Co) was used as a control. **A:** CD63 externalization after stimulation. One representative histogram out of n=4 of CD63 externalization (right). **B:** Upregulation of CD203c after incubation. One representative histogram out of n=4 of CD203c upregulation (right). One-way ANOVA followed by Dunnett's post-hoc test was performed to assess statistical significance. A p-value < 0.05 was considered significant. *** < 0.001. Data are presented as mean ± SEM.

3.1.5 TRPA1 protein expression on basophil granulocytes is modulated by cytokines and growth factors

In the next step, specific cytokines of itch were investigated for their potential to modify TRPA1 regulation. As AD is characterized by itch and IL-31, a well-known pruritogen, which is increased in the peripheral blood of AD patients and has been observed to correlate with disease severity [139], the effect of IL-31 on TRPA1 expression in basophil granulocytes was assessed (Figure 10). For this, human peripheral blood basophil granulocytes from NA donors were stimulated with IL-31 as described in Chapter 2.2.7. Total RNA was isolated and analyzed by qPCR, which revealed significantly increased TRPA1 mRNA expression in basophil granulocytes treated with IL-31 ($p=0.0147$) (Figure 10A, Supplementary Table 7). The total protein expression of TRPA1 assessing both the surface and intracellular levels in basophil granulocytes was then evaluated, which also revealed a significant increase of TRPA1 expression in basophil granulocytes stimulated with IL-31 compared to those stimulated with RPMI complete medium, which was used as the control ($p=0.0329$) (Figure 10B, D, Supplementary Table 8). All intra- and extracellularly stained basophil granulocytes expressed TRPA1 (Figure 10C, Supplementary Table 9), while only 69.37 ± 5.56% of basophil granulocytes expressed TRPA1 when stained on the surface (Figure 7D). A similar effect was discovered by Limberg *et al.* [127] regarding TRPV1 expression in basophil granulocytes. One possible explanation for this difference might be the different time points of analysis. While basophil granulocytes in Figure 7 were analyzed directly after isolation, basophil granulocytes in Figure 10 were first stimulated for 4 hours, resulting in a difference in TRPA1 expression. Alternatively, TRP channels may be expressed intracellularly, which are then detectable due to the permeation process. The intracellular expression of TRPA1 has already been confirmed in murine endolysosomes of DRG neurons [113], but still needs further investigation in humans. Moreover, extracellular staining of basophil granulocytes stimulated with RPMI complete medium and IL-31 should be performed in the future to directly compare the surface staining to the intra- and extracellular TRPA1 staining. These findings collectively indicate that IL-31 can modulate TRPA1 expression in basophil granulocytes.

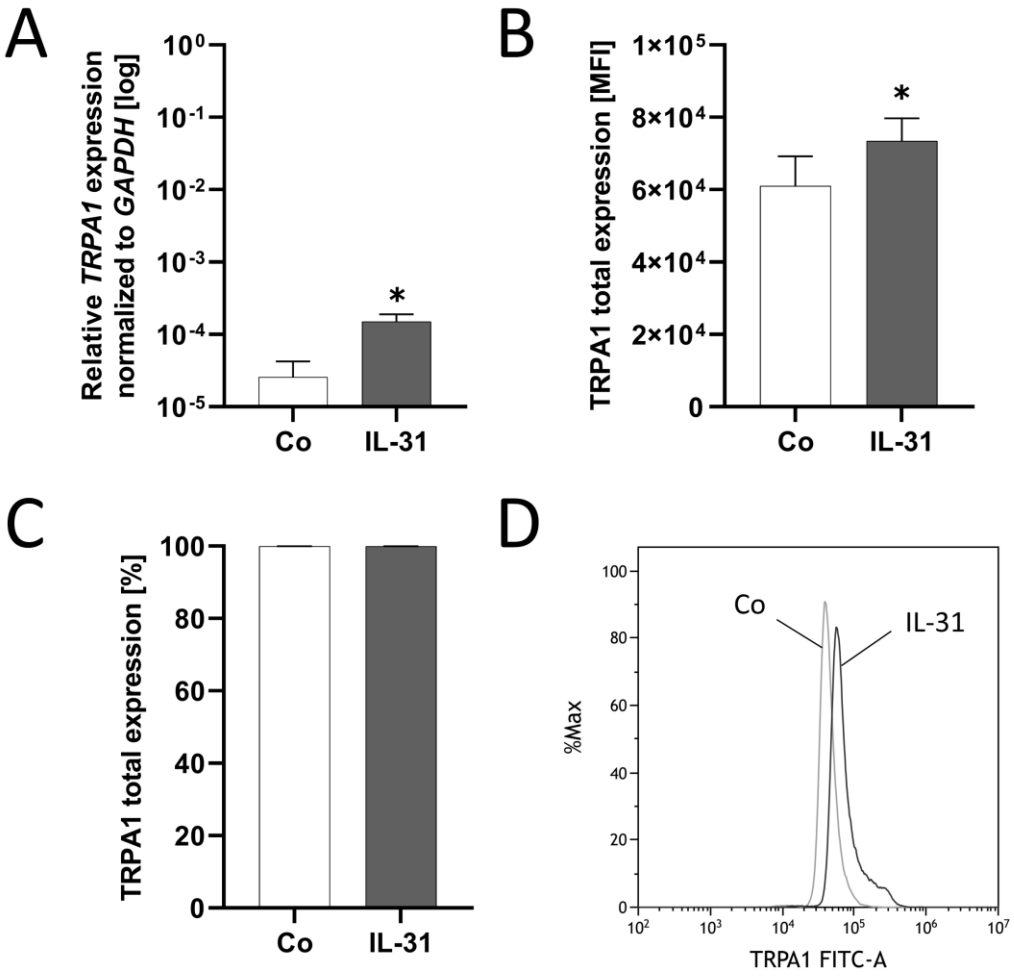

Figure 10: TRPA1 protein expression after stimulation with IL-31. Isolated human peripheral blood basophil granulocytes from nonatopic (NA) donors were stimulated with RPMI complete medium (Co) and interleukin (IL)-31 (10 ng/mL) for 4 hours at 37°C and 5% CO_2. **A:** Quantitative real-time PCR analysis of TRPA1 mRNA expression (n=4). **B:** Analysis of total TRPA1 protein expression after IL-31 stimulation (n=5). The expression is shown as mean fluorescence intensity (MFI). **C:** Percentage of total expression including intra- and extracellular levels of TRPA1 in basophil granulocytes after stimulation (n=5). **D:** One representative histogram out of n=5 showing MFI of TRPA1 expression in basophil granulocyte populations treated with RPMI complete medium or IL-31. Statistical analysis was performed using a paired Student's t-test. A p-value < 0.05 was considered significant. * < 0.05. Data are presented as mean ± SEM.

Given that IL-31 influences TRPA1 surface expression and that AD is characterized by a Th2 cytokine profile, the effects of Th2 cytokines, neurotrophins, and the basophil-priming cytokine IL-3 on TRPA1 expression in basophil granulocytes were analyzed (Figure 11). Basophil granulocytes from NA donors were stimulated with IL-3, IL-13, IL-31, IL-33, TSLP, NGFβ, BDNF, and TNF-α as described in Chapter 2.2.7. The aim was to mimic the inflammatory microenvironment of AD to determine which cytokines or growth factors

induce TRPA1 upregulation. Incubation with IL-3 resulted in significantly increased TRPA1 surface expression in isolated blood basophil granulocytes (p=<0.0001 in both cases) (Figure 11A, Supplementary Table 10, Figure 11B, Supplementary Table 11). While the percentage of TRPA1-positive basophil granulocytes did not increase after stimulation with NGFβ, the MFI increased significantly (p=0.0061) (Figure 11A), indicating that the density of TRPA1 channels per basophil granulocyte was elevated. Expression after stimulation with IL-33

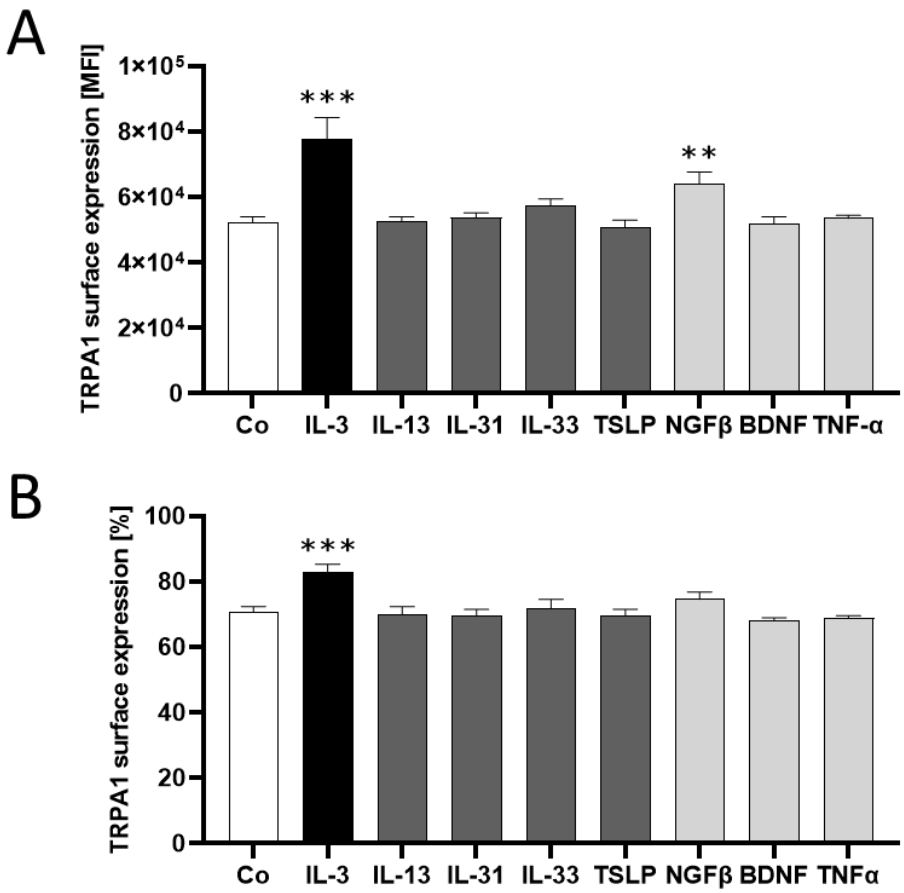

Figure 11: TRPA1 surface protein expression after stimulation with inflammatory mediators. TRPA1 surface expression on human basophil granulocytes from nonatopic donors was analyzed by flow cytometry after 4 hours stimulation at 37°C and 5% CO_2. Stimulation was performed with RPMI complete medium (Co), interleukin (IL)-3, IL-31, IL-33, thymic stromal lymphopoietin (TSLP), nerve growth factor-beta (NGFβ), tumor necrosis factor alpha (TNF-α) (10 ng/mL), IL-13, and brain-derived neurotrophic factor (BDNF) (50 ng/mL) (n=3). **A:** Surface expression of TRPA1 after stimulation is shown as mean fluorescence intensity (MFI). **B:** Percentage of positive basophil granulocytes expressing TRPA1 on the surface. Statistical analysis was performed using one-way ANOVA followed by Dunnett's post-hoc test. A p-value < 0.05 was considered significant. ** < 0.01, *** < 0.001. Data are presented as mean ± SEM.

was also enhanced, albeit not significantly. These results demonstrate that TRPA1 surface expression can be modulated by the priming factor IL-3 and the neurotrophin NGFβ.

3.1.6 TRPA1 expression of basophil granulocytes is modulated by pH

During inflammation, the pH is altered due to the production of lactate, creating an acidic environment [152], and the temperature is increased by 4-5°C [153]. As AD is an inflammatory disease, these aspects are important to consider. Although the pH of skin tissue during AD has not been directly investigated, it is plausible that the pH becomes acidified due to the inflammatory nature of the disease. Therefore, basophil granulocytes were incubated in media with lower pH (Figure 12A) and with increased temperature (Figure 12B) as described in Chapter 2.2.7. The lowered pH resulted in a significantly elevated TRPA1 expression at pH 5 (left panel: p=0.0011, right panel: p=0.0129) (Supplementary Table 12, Supplementary Table 13, respectively), which is consistent with the previous study by Wang *et al.* [154], showing that TRPA1 activation is dependent on pH, with pH in the range of 5.0 to 5.5 leading to activation. In contrast, increased temperature resulted in significantly less TRPA1 surface expression not in the MFI but when measured as a percentage of positive basophils (B: right panel p=0.0263) (Supplementary Table 14, Supplementary Table 15). While TRPA1 is known to be activated at temperatures less than 18°C in rats and mice, this does not apply to humans [108]. Nevertheless, it is possible that the expression of TRPA1 decreases with increasing temperature, as observed here. These findings suggest that the acidic microenvironment of AD may promote TRPA1 expression and, by extension, itch, while elevated temperature may decrease TRPA1 expression on basophil granulocytes.

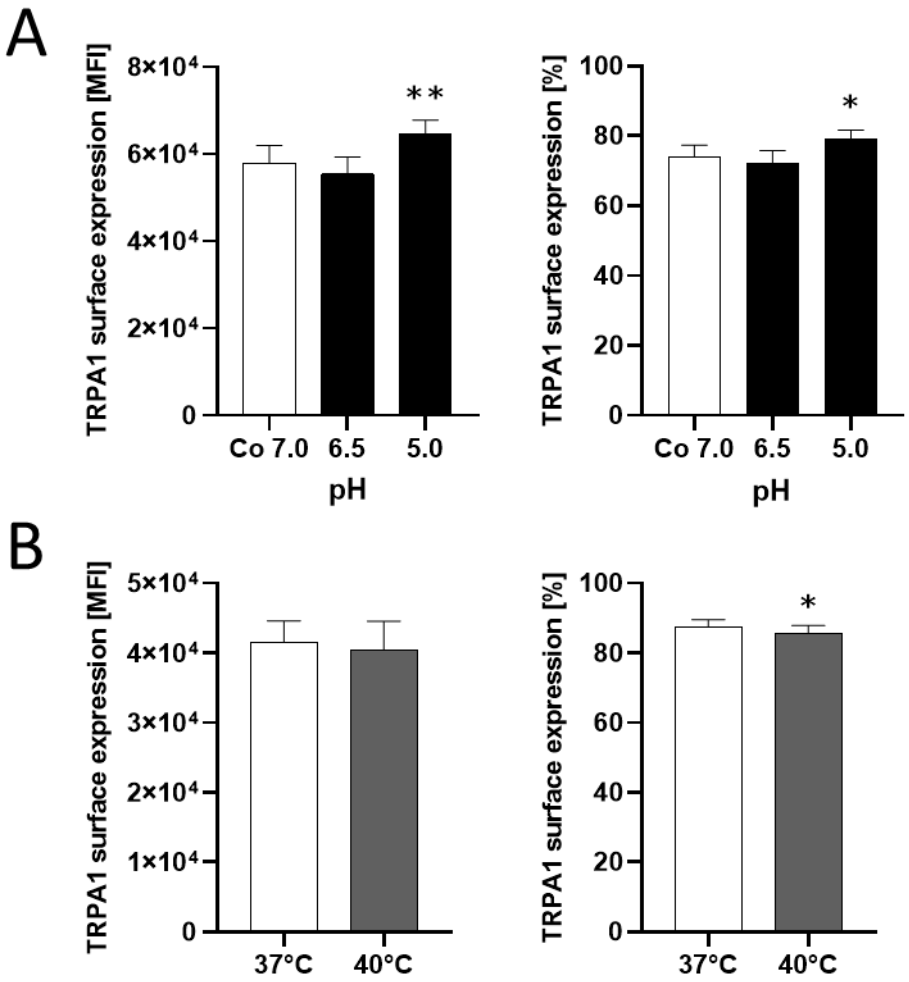

Figure 12: TRPA1 expression after incubation in acidic medium or at increased temperature. A: Expression of TRPA1 shown as mean fluorescence intensity (MFI) and the percentage of positive basophil granulocytes after stimulation with acidified RPMI complete medium (6.5, 5.0) for 4 hours at 37°C and 5% CO_2 (n=4) compared to neutral RPMI complete medium (Co, pH 7.0). **B:** TRPA1 expression after incubation at 37°C or 40°C for 4 hours at 5% CO_2 (n=3). The results are shown as MFI and the percentage of positive basophil granulocytes. Statistical analysis was performed using a one-way ANOVA followed by Dunnett's post-hoc test (A) or a paired Student's t-test (B). A p-value < 0.05 was considered significant. * < 0.05, ** < 0.01. Data are presented as mean ± SEM.

3.1.7 TRPA1 activation has no effect on basophil granulocyte viability

The next step was to investigate whether the activation of TRPA1 affects the viability of human peripheral blood basophil granulocytes. An apoptosis assay was performed according to Chapter 2.2.8. Basophil granulocytes were stained with annexin V and PI. Isolated human peripheral blood basophil granulocytes from NA donors and AD patients

were stimulated with 1 μM staurosporine or 10, 100, or 1000 nM JT010. Staurosporine, a strong inducer of apoptosis [155], was used as a positive control, while JT010 was used to activate the TRPA1 channel. Basophil granulocytes from NA donors were incubated for 4 hours (Figure 13) and 24 hours (Figure 14). Stimulation with staurosporine showed a significantly decreased percentage of viable basophil granulocytes at both time points (4 h: p=0.0203, 24 h: p=0.0006) (Supplementary Table 16, Supplementary Table 18, respectively). Correspondingly, the percentage of apoptotic basophil granulocytes increased in both cases (Figure 13C, Supplementary Table 17, Figure 14C, Supplementary Table 19). In contrast, the addition of JT010 did not significantly affect human basophil granulocyte viability, regardless of the stimulation duration (Figure 13 and Figure 14). Basophil granulocytes from AD patients were incubated for 24 h (Figure 15, Supplementary Table 21), showing similar results to basophil granulocytes from NA donors. Staurosporine caused a significant decrease in basophil granulocyte viability (p=0.0003) (Supplementary Table 20), demonstrating a stronger apoptotic effect than in basophil granulocytes from NA donors. JT010, however, did not affect basophil granulocyte viability (Figure 15B). Interestingly, human peripheral blood basophil granulocytes of AD patients had a lower rate of annexin V^+/PI^+ basophil granulocytes compared to NA donors after 24 hours stimulation, indicating a longer life span per se as already described for other granulocytes such as eosinophils in AD [156]. These findings suggest that the activation of TRPA1 neither promotes nor inhibits human peripheral blood basophil granulocyte viability and that the agonist itself has no cytotoxic effect.

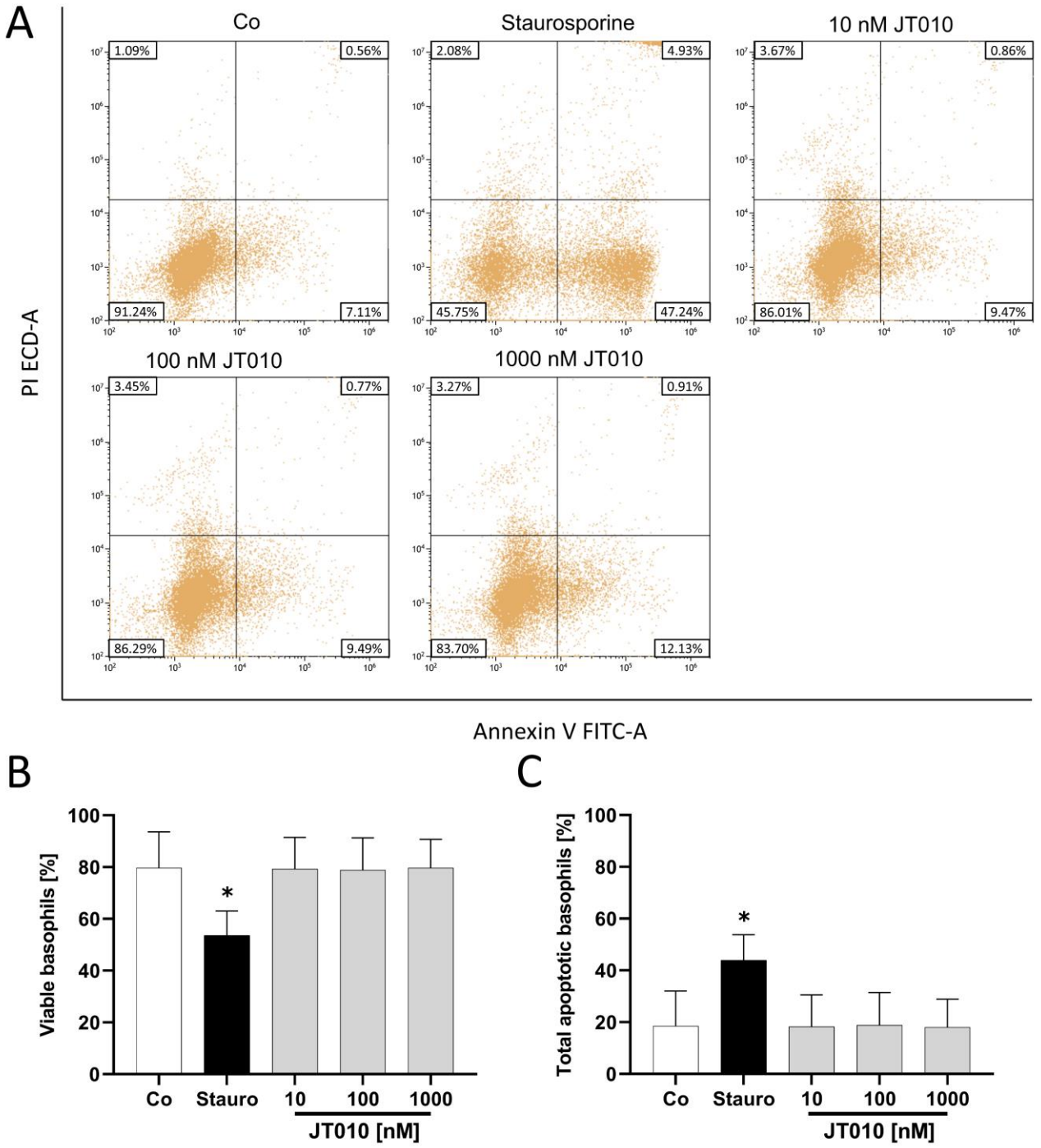

Figure 13: Viability assay of basophil granulocytes from nonatopic (NA) donors after 4 hours. Basophil granulocytes from NA donors were treated with RPMI complete medium (Co), staurosporine (Stauro, positive control, 1 μM), and JT010 (10, 100, 1000 μM) for 4 hours at 37°C and 5% CO_2. Afterwards, basophil granulocyte viability was analyzed by staining with annexin V and propidium iodide (PI). Flow cytometry was performed to determine the viability. **A:** Exemplary dot plots out of n=3 of basophil granulocytes after stimulation. Viable basophil granulocytes are shown in the bottom left quadrant, while apoptotic and late apoptotic basophil granulocytes are in the bottom right and top right quadrants, respectively. Necrotic basophil granulocytes are in the top left quadrant. **B:** Percentage of viable basophil granulocytes after apoptosis assay (n=3). **C:** Amount of apoptotic and late apoptotic basophil granulocytes combined (n=3). Statistical

analysis was performed using a one-way ANOVA followed by Dunnett's post-hoc test. A p-value < 0.05 was considered significant. * < 0.05. Data are presented as mean ± SEM.

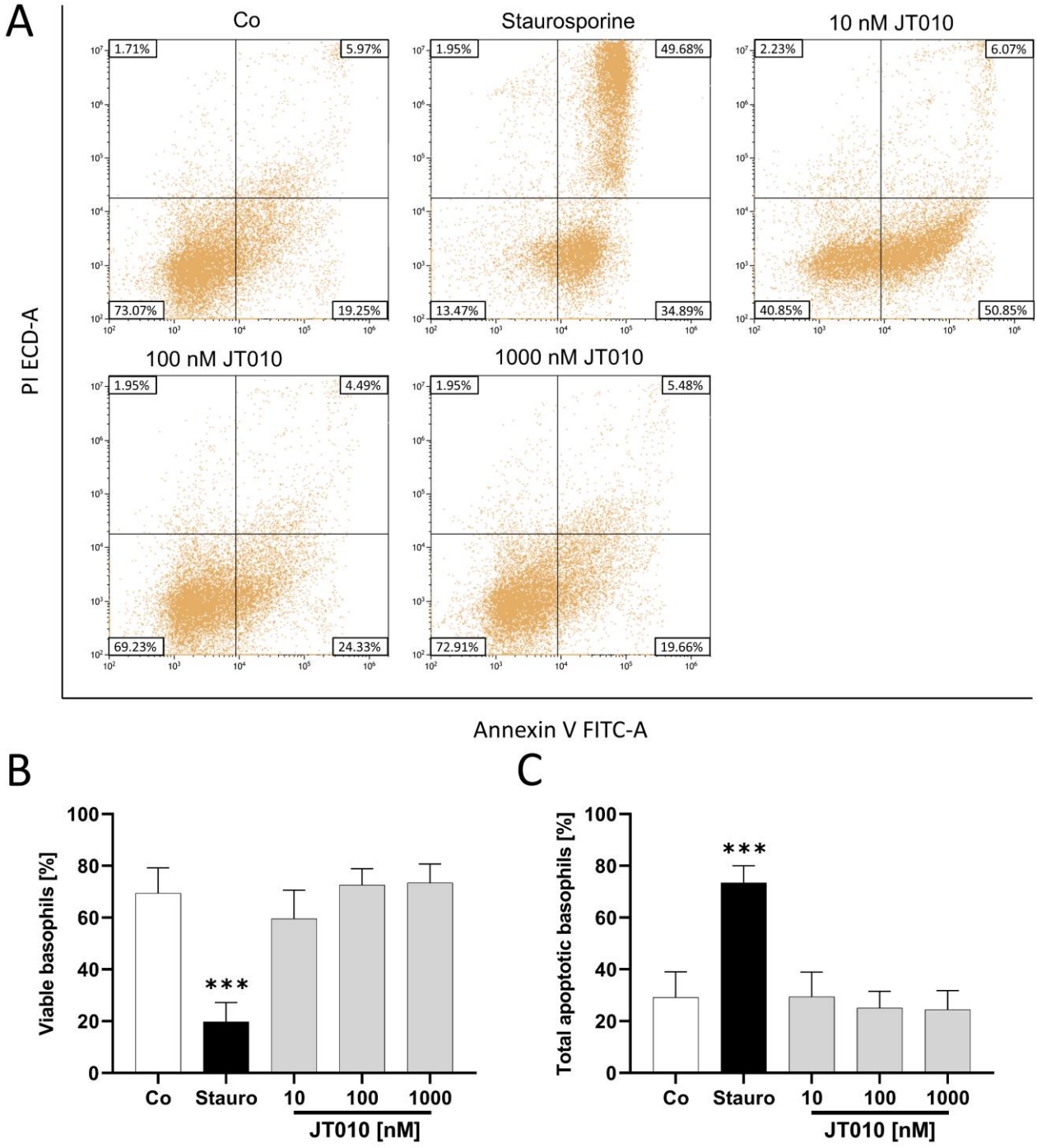

Figure 14: Viability assay of basophil granulocytes from nonatopic (NA) donors after 24 hours. Human basophil granulocytes of NA donors (n=4) were incubated for 24 hours at 37°C and 5% CO_2 with RPMI complete medium (Co), staurosporine (Stauro, positive control, 1 µM), or TRPA1 agonist JT010 (10, 100, 1000 nM). **A:** Representative dot plots out of 4 showing the various phases of apoptosis in basophil granulocytes after stimulation with RPMI complete medium, staurosporine, and increasing concentrations of JT010. Staining was performed with annexin V and propidium iodide (PI).

Viable basophil granulocytes are located in the bottom left quadrant, while apoptotic and late apoptotic basophil granulocytes are in the bottom right and top right quadrants, respectively. Necrotic basophil granulocytes are shown in the top left quadrant. **B:** Percentage of viable basophil granulocytes from NA donors. **C:** Percentage of apoptotic and late apoptotic basophil granulocytes combined. Statistical analysis was performed using a one-way ANOVA followed by Dunnett's post-hoc test. A p-value < 0.05 was considered significant. *** < 0.001. Data are presented as mean ± SEM.

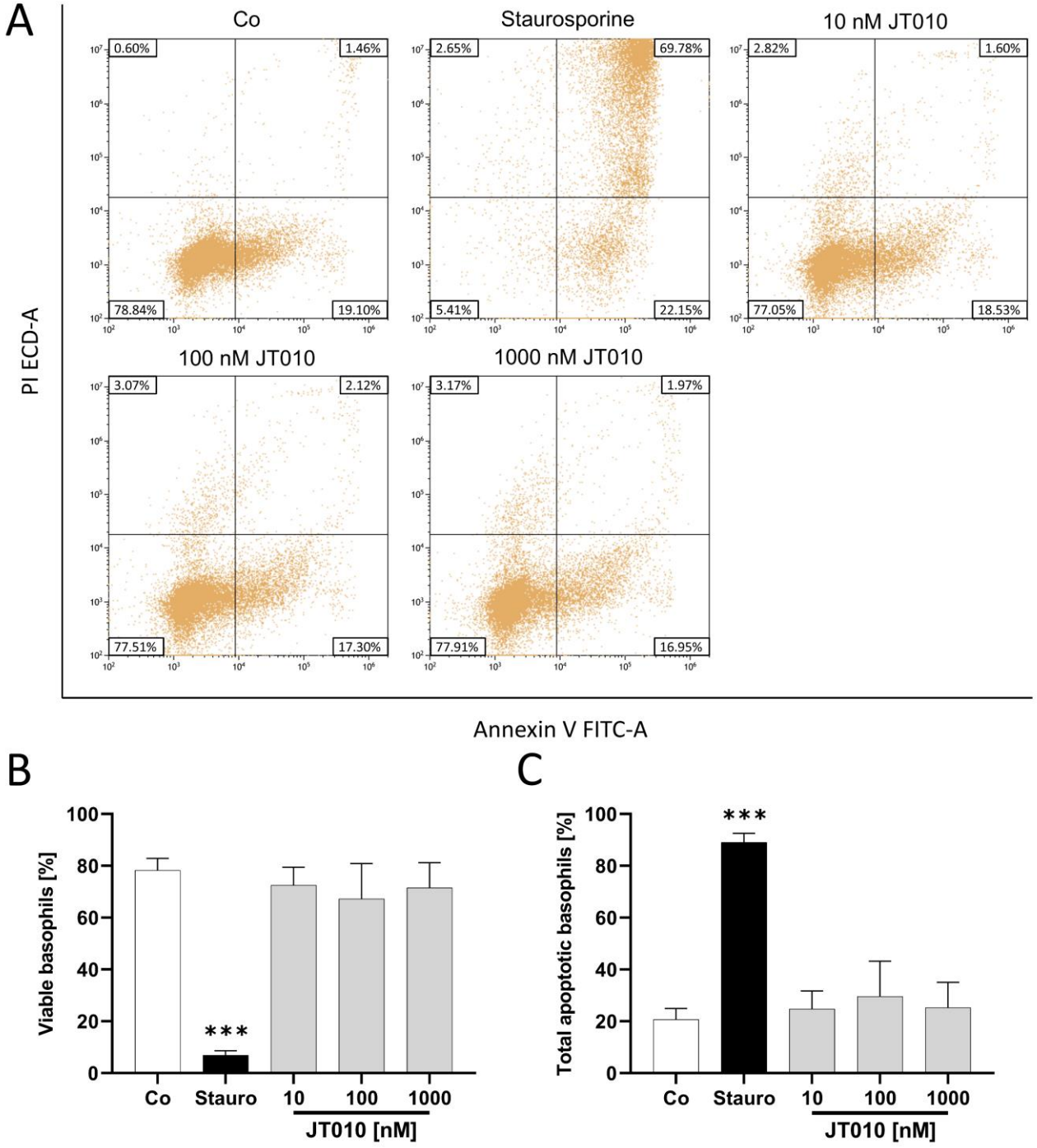

Figure 15: Apoptosis assay with basophil granulocytes of patients with atopic dermatitis (AD). An apoptosis assay was performed with basophil granulocytes isolated from AD patients (n=3) after 24 hours incubation at 37°C and 5% CO_2 with

RPMI complete medium (Co), staurosporine (Stauro, positive control, 1 µM), or TRPA1 agonist JT010 (10, 100, 1000 nM). **A:** Representative dot plots out of 3 of viable (bottom left quadrant), apoptotic (bottom right quadrant), late apoptotic (top right quadrant), and necrotic basophil granulocytes (top left quadrant) after incubation. Basophil granulocytes stained with annexin V and propidium iodide (PI) were used to assess basophil granulocyte viability. **B:** Percentage of basophil granulocyte viability from patients with AD. **C:** Combined percentage of apoptotic and late apoptotic basophil granulocytes. Statistical analysis was performed using a one-way ANOVA followed by Dunnett's post-hoc test. A p-value < 0.05 was considered significant. *** < 0.001. Data are presented as mean ± SEM.

3.1.8 TRPA1-positive basophil granulocytes in the skin of AD patients

After analyzing the TRPA1 channel's properties, the last step was to visualize the TRPA1-positive basophil granulocytes in the skin. Therefore, immunofluorescence imaging was performed on cryo-sectioned skin samples stained with DAPI to visualize the nucleus, anti-2D7 to identify basophil granulocytes, and anti-TRPA1 (see Chapter 2.2.9). In the skin of patients with AD, TRPA1-positive basophil granulocytes were detected in the dermis (Figure 16). Colocalization of 2D7 and TRPA1 was indicated by yellow fluorescence. As a control, the skin samples from nonatopic donors were treated equally. In these samples, no basophil granulocytes were visible (Figure 17), which is consistent with the known absence of basophil granulocytes in non-inflamed skin [7, 16].

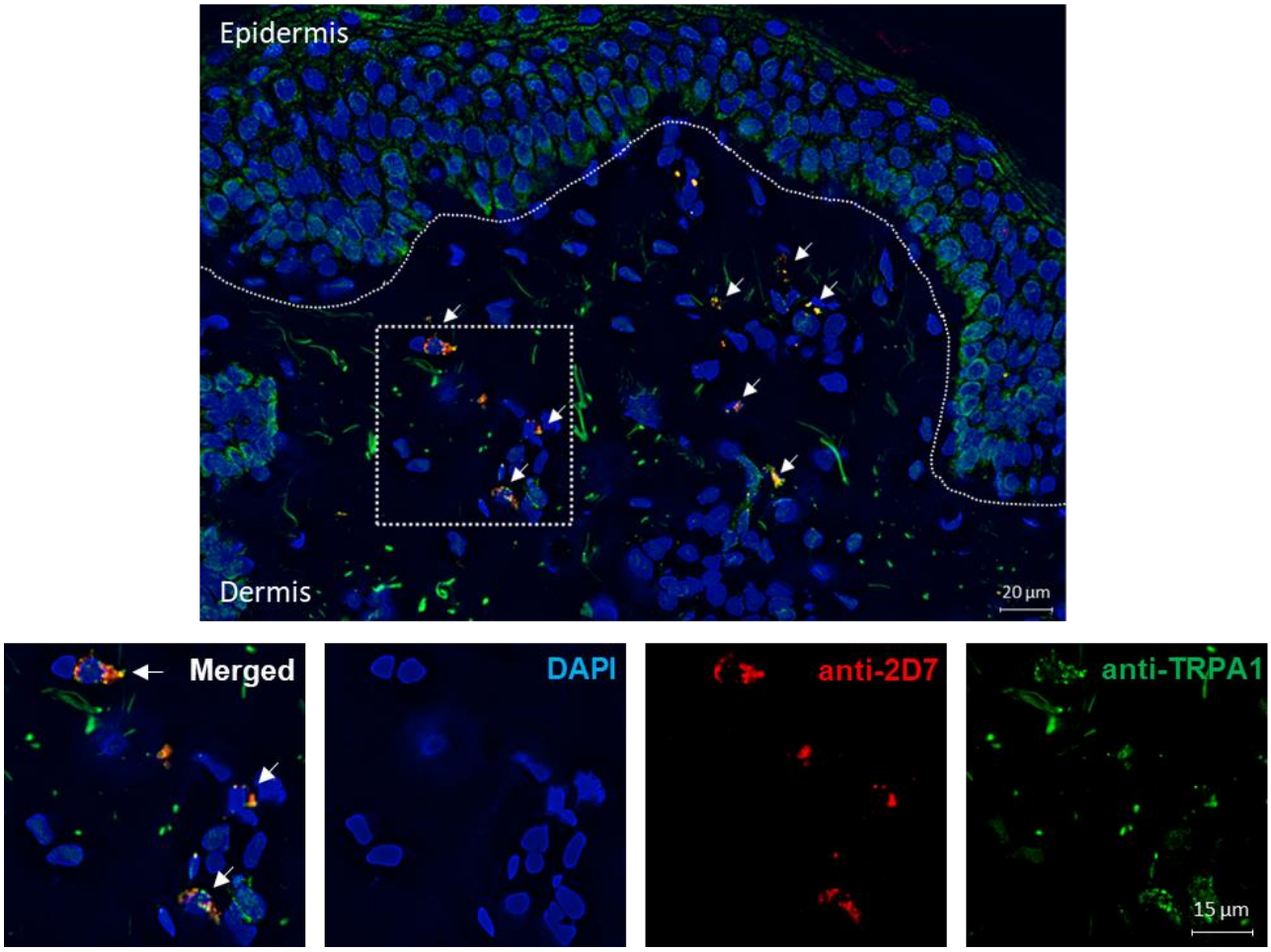

Figure 16: Expression of TRPA1 in human basophil granulocytes in atopic dermatitis (AD) skin. One representative example out of n=3 different stainings from skin samples of patients with AD. The samples were stained with DAPI (blue), anti-2D7 (basophil granulocyte marker, red), and anti-TRPA1 (green). Colocalization of TRPA1 and 2D7 is shown in yellow. The epidermis is located above the white dotted line. Basophil granulocytes expressing both 2D7 and TRPA1 are indicated with arrows. Images were acquired using fluorescence microscopy at 40x magnification. Top: Overview image of the stained skin section from AD. Magnification: View of the region containing TRPA1-positive basophil granulocytes (white dashed box at the top).

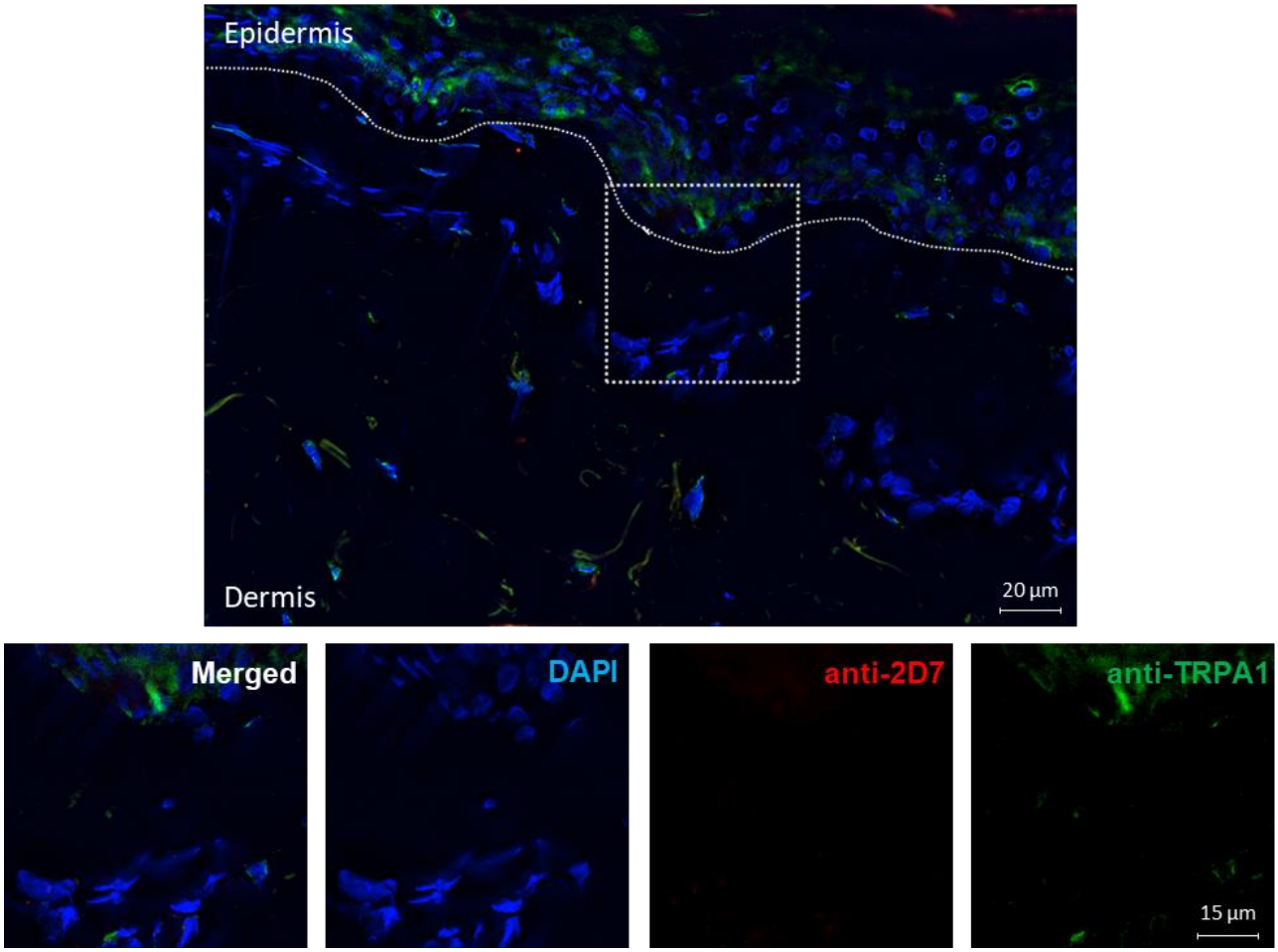

Figure 17: TRPA1 expression in basophil granulocytes in the skin of nonatopic (NA) donors. Representative skin section out of 3 different NA donors was stained with DAPI (blue), anti-2D7 (basophil granulocyte marker, red), and anti-TRPA1 (green). The epidermis and dermis are separated by the white dotted line. The skin sections were analyzed with fluorescence microscopy at 40x magnification. Top: Exemplary overview image of a stained skin section from an NA donor. Bottom: Magnification of the selected area (white dashed box in the top panel) shown in separate channels.

3.2 TRPA1/TRPV1 co-expression in basophil granulocytes

3.2.1 Human basophil granulocytes co-express TRPA1 and TRPV1

In sensory neurons, TRPA1 expression is often accompanied by TRPV1, with 97% of TRPA1-positive neurons also expressing TRPV1 [94]. Conversely, only 30% of TRPV1-positive neurons express TRPA1 [94]. Given that basophil granulocytes express TRPA1, as shown above, and TRPV1, as demonstrated in a previous study by Limberg *et al.* [127], the co-expression of both TRP channels is highly probable.

Therefore, the simultaneous expression of TRPA1 and TRPV1 was investigated in human peripheral basophil granulocytes of NA and AD patients, initially focusing on the presence of protein on the cell surface after isolation. First, the specificity of the TRPV1 antibody was confirmed using an isotype control (Figure 18A). Subsequently, the presence of TRPA1 and TRPV1 on the basophil granulocyte surface was analyzed. Approximately 50% of isolated basophil granulocytes expressed both TRP channels on the surface, while the majority of the remaining basophil granulocytes were only positive for TRPA1 in approximately 40% (Figure 18B). These results demonstrated the co-expression of TRPA1 and TRPV1 (TRPA1/TRPV1) on human basophil granulocytes for the first time. Thus, the expression patterns of TRPA1 and TRPV1 were compared in NA and AD patients (Figure 18C, Supplementary Table 22). The analysis revealed a slight increase in TRPA1/TRPV1 co-expression in patients with AD, which was not statistically significantly different. In conclusion, the co-expression of TRPA1/TRPV1 in human peripheral blood basophil granulocytes was confirmed.

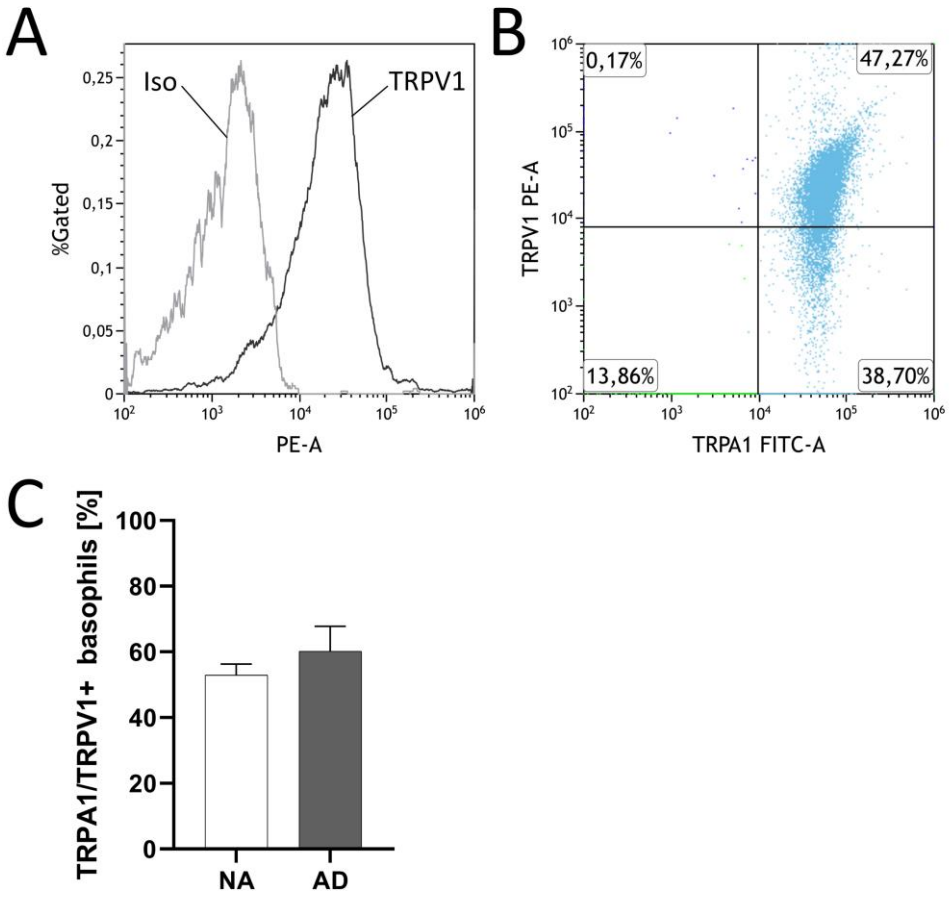

Figure 18: Co-expression of TRPA1 and TRPV1 (TRPA1/TRPV1) on basophil granulocytes. Human peripheral basophil granulocytes of nonatopic (NA) donors were purified, stained with anti-TRPA1 and anti-TRPV1 antibodies, and analyzed by flow cytometry. **A:** One representative histogram out of n=4 of isotype (Iso) control for anti-TRPV1 antibody. **B:** Flow cytometry analysis of TRPA1/TRPV1 surface co-expression. **C:** Percentage of basophil granulocytes co-expressing TRPA1/TRPV1 from atopic dermatitis (AD) patients (n=8) and NA donors (n=20). Statistical analysis was performed using an unpaired Student's t-test. Data are presented as mean ± SEM.

To further differentiate the exact composition of TRPA1 and TRPV1 channels on the surface of basophil granulocytes, the proportions of basophil granulocytes expressing one, both, or neither TRP channel were analyzed in NA donors (Figure 19A, B) and AD patients (Figure 19A, C). In NA donors, 22.1 ± 3.76% of basophil granulocytes expressed only TRPA1, while 4.94 ± 1.44% were positive for only TRPV1. Co-expression of both channels was observed in 52.99 ± 3.26% of all basophil granulocytes, and 19.97 ± 1.54% expressed neither channel (Figure 19A). In patients with AD, a similar trend was observed; the proportion of basophil granulocytes co-expressing both channels was 60.2 ± 7.62%, while the percentages of

basophil granulocytes expressing only TRPA1 (18.66 ± 7.47%) or neither channel (15.92 ± 2.67%) were decreased (Figure 19A, Supplementary Table 23). Taken together, the TRP channel expression patterns in NA donors and AD patients were similar.

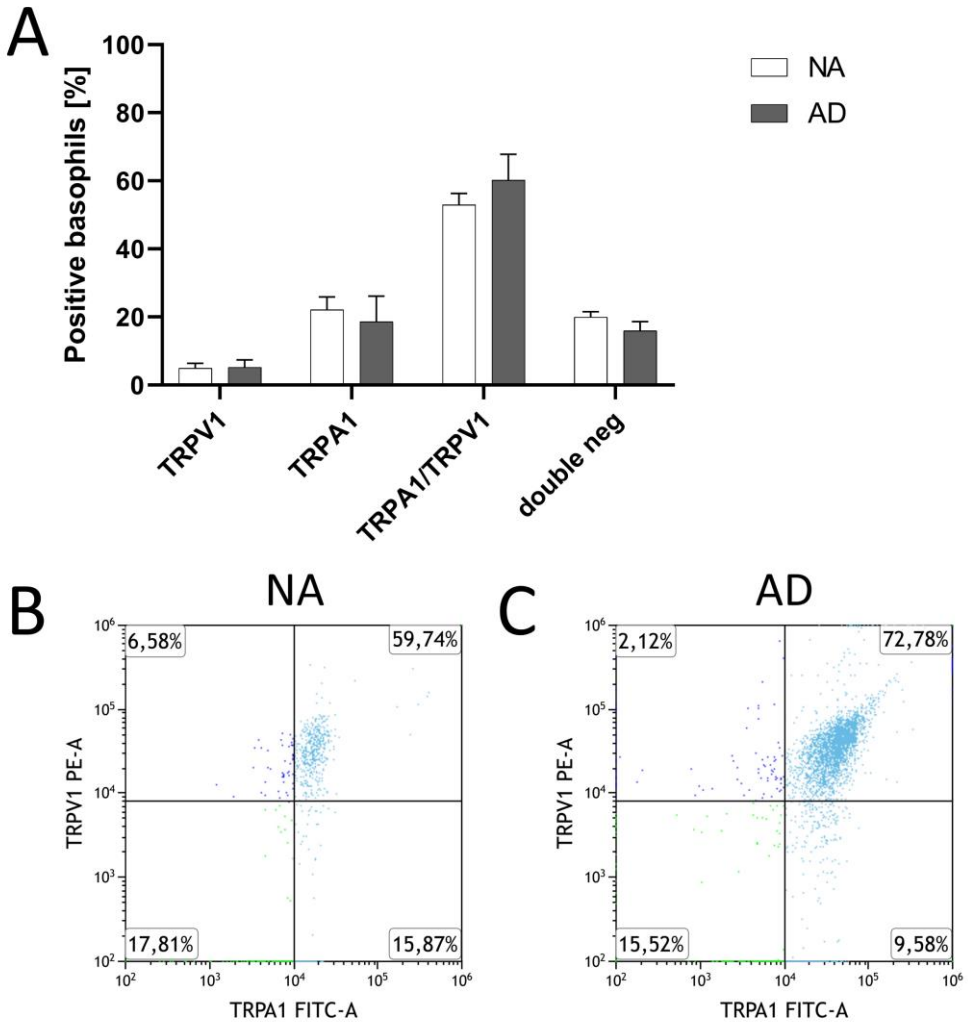

Figure 19: TRP channel distribution in basophil granulocytes of nonatopic (NA) donors and atopic dermatitis (AD) patients. Analysis of basophil granulocytes from NA donors (n=20) and patients with AD (n=8) expressing TRPA1, TRPV1, both channels (TRPA1/TRPV1), or neither channel (double neg). **A:** Percentage of basophil granulocytes expressing TRP channels. **B:** One representative dot plot out of n=20 showing TRP channel expression in basophil granulocytes from NA donors. **C:** One exemplary dot plot out of n=8 of basophil granulocytes from AD patients demonstrating the TRP channel distribution. Statistical analysis was performed using a two-way ANOVA mixed-effects analysis followed by Šídák's post-hoc test. Data are presented as mean ± SEM.

3.2.2 TRPA1/TRPV1 co-expression is modulated by IL-33 and NGFβ

After establishing that both channels are expressed on basophil granulocytes, the next step was to investigate whether their surface expression could be modulated. As described in Chapters 2.2.7 and 3.1.5, isolated human peripheral blood basophil granulocytes were stimulated with IL-3, Th2 cytokines, and neurotrophins (Figure 20), and the amount of

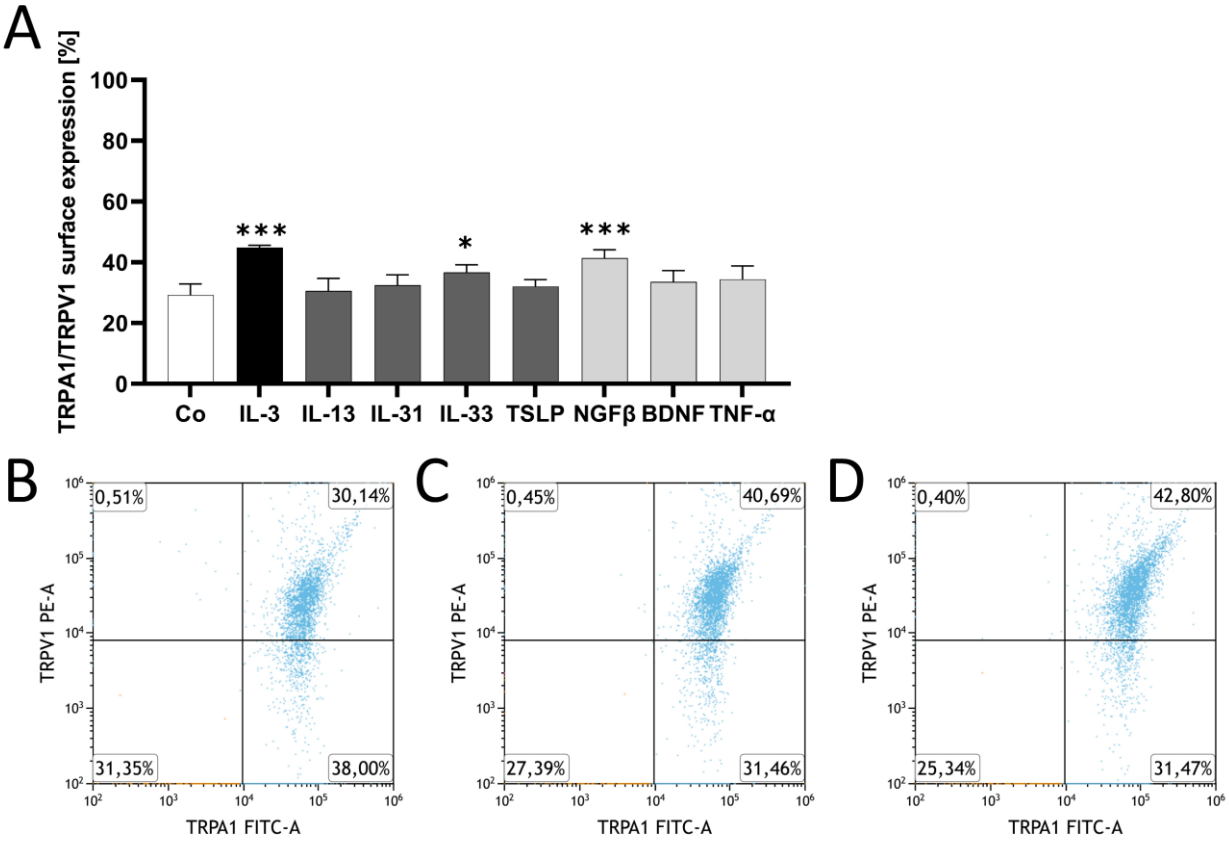

Figure 20: Effect of inflammatory mediators on TRPA1/TRPV1 surface protein co-expression on human basophil granulocytes. Basophil granulocytes from NA donors were stimulated for 4 hours at 37°C at 5% CO_2 with RPMI complete medium (Co), interleukin (IL)-3, IL-31, IL-33, thymic stromal lymphopoietin (TSLP), nerve growth factor-beta (NGFβ), tumor necrosis factor alpha (TNF-α) (10 ng/mL), IL-13, and brain-derived neurotrophic factor (BDNF) (50 ng/mL). TRPA1/TRPV1 co-expression was analyzed by flow cytometry (n=3). **A:** Percentage of basophil granulocytes co-expressing TRPA1/TRPV1 after incubation with various stimuli. **B:** One representative dot plot out of n=3 of basophil granulocytes incubated with RPMI complete medium as control showing TRPA1/TRPV1 co-expression. **C:** One representative dot plot out of n=3 of TRPA1/TRPV1 co-expressing basophil granulocytes stimulated with IL-33. **D:** One representative dot plot out of n=3 of basophil granulocytes incubated with NGFβ showing TRPA1/TRPV1 co-expression. Statistical analysis was performed using a one-way ANOVA followed by Dunnett's post-hoc test. A p-value < 0.05 was considered significant. * < 0.05, *** < 0.001. Data are presented as mean ± SEM.

basophil granulocytes expressing both TRP channels was analyzed by flow cytometry. Consistent with the results shown in Figure 11, the addition of IL-3 ($p=<0.0001$) and NGFβ ($p=0.0002$) significantly increased the co-expression of TRPA1/TRPV1 (Figure 20A, C, D) compared to the control (Figure 20B). Moreover, incubation with IL-33 also enhanced the presence of both cation channels ($p=0.0167$) (Figure 20A, Supplementary Table 24). These findings suggest a similar upregulation pattern for TRPV1 as observed for TRPA1, since the same mediators induced their expression. Notably, IL-33 appears to play a role in the co-expression of TRPVA1/TRPV1, as it significantly enhanced the co-expression of both channels compared to its effect on the expression of TRPA1 alone (Figure 11).

3.2.3 Modulation of TRPA1/TRPV1 co-expression by pH

Finally, human peripheral blood basophil granulocytes were incubated in medium with acidic pH or at an increased temperature (see Chapter 2.2.7), as these are common aspects of inflammation. A mildly decreased pH of 6.5 did not affect the co-expression of both TRP channels on basophil granulocytes, compared to the control at pH 7. However, strong acidification at pH 5.0 led to a significant increase of TRPA/TRPV1 ($p=0.0015$) (Figure 21A, Supplementary Table 25). In contrast, elevated temperature, another important factor in inflammation, had no effect on the percentage of human peripheral blood basophil granulocytes expressing both ion channels (Figure 21B, Supplementary Table 26). These results are consistent with the findings for single expression of TRPA1 (Figure 12) and confirm that a strongly acidic pH milieu promotes the upregulation of the TRP channel surface expression, while elevated temperature does not affect it.

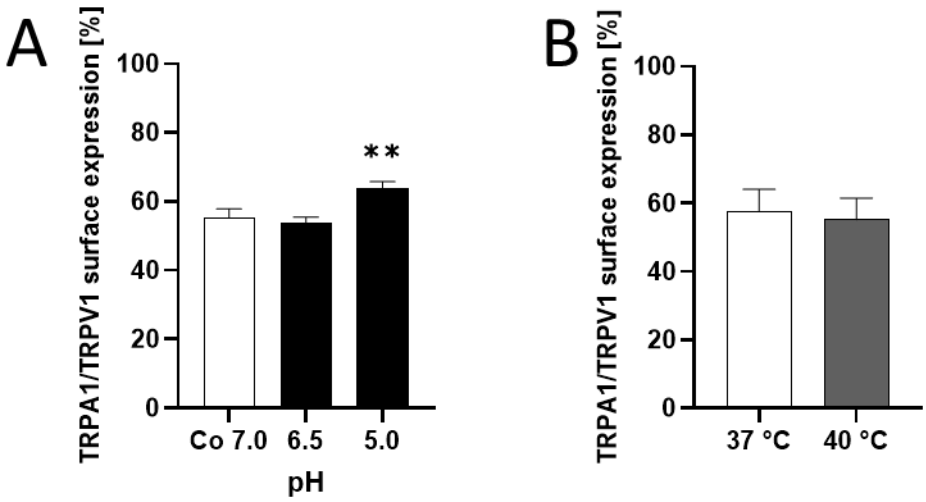

Figure 21: Co-expression of TRPA1 and TRPV1. Isolated basophil granulocytes from NA donors were incubated for 4 hours at 37°C and 5% CO_2 in acidified RPMI complete medium or at elevated temperatures. TRPA1/TRPV1 co-expression was analyzed by flow cytometry. **A:** Basophil granulocytes were exposed to acidified medium at pH 6.5 and 5.0. RPMI complete medium (Co) at pH 7.0 was used as a control (n=4). **B:** Basophil granulocytes were incubated at 37°C and 40°C (n=3). Statistical analysis was performed using a one-way ANOVA followed by Dunnett's post-hoc test (A) or a paired Student's t-test (B). A p-value < 0.05 was considered significant. ** < 0.01. Data are presented as mean ± SEM.

To summarize, TRPA1 is expressed in human peripheral basophil granulocytes and functions as a calcium-permeable cation channel, activated in a dose-dependent manner. Its expression is modulated by the pruritogen IL-31, growth factor NGFβ, and strongly acidified pH. TRPA1 activation does not affect basophil granulocyte viability. In addition to the expression of TRPA1, the co-expression of TRPV1 is also confirmed by these findings. The modulation of the TRP channel complex is expanded to the Th2 cytokine IL-33, which is known to have a priming effect on [157] and enhances the IL-4 production in basophil granulocytes [157]. Thus, the basophil-TRPA1 channel linkage identified in this study may be a novel therapeutic target for pruritic and inflammatory skin diseases, such as AD.

4 Discussion

Atopic dermatitis is a debilitating pruritic skin disease, which severely affects the quality of life in patients [38]. Itching is the main symptom and proves difficult to treat, as antihistamines are often ineffective [61]. However, new therapies, including monoclonal antibodies, have shown promise in improving symptoms [63–66]. The pathogenesis of AD remains to be elucidated; therefore, the key players involved in the disease need to be identified. Basophil granulocytes have been found in the skin of AD patients, furthering the occurring inflammation [48–50]. They have been observed to be located closely to neurons in the skin, indicating neuro-immune interactions [16]. In this regard, TRP channels are commonly expressed in neurons and immune cells. The TRPV1 channel has been confirmed in $CD4^+$ T cells [158], eosinophils [126], and basophils [127], as has the TRPA1 channel in mast cells, macrophages [159], and T cells [99, 102]. However, the expression of TRPA1 in basophil granulocytes has not previously been investigated. This doctoral thesis examined the expression of the TRPA1 channel, as well as its co-expression with TRPV1, in basophil granulocytes to further advance the understanding of the disease.

Basophil granulocytes are known to express TRPV1 [127]. Since 30% of TRPV1-positive neurons also express TRPA1 [94], the presence of TRPA1 in basophil granulocytes was considered to be likely. Analysis by qPCR and flow cytometry confirmed the expression of TRPA1 in basophil granulocytes in skin healthy NA donors and in those with skin inflammation such as AD patients. This is in accordance with a previous study, where the TRPV1 channel was found to be expressed in basophils and similarly upregulated during AD [127]. Interestingly, Weihrauch *et al.* [126] verified the expression of TRPV1 in human peripheral blood eosinophils, another type of granulocytes. However, in contrast to the findings of this thesis, TRPV1 expression in eosinophils did not differ between NA donors and patients with AD [126], indicating different expression patterns in individual subtypes of granulocytes.

Next, the functionality of the TRPA1 channel in human peripheral blood basophil granulocytes was confirmed by calcium flux imaging. Activation of the channel resulted in

a slow and dose-dependent increase in intracellular calcium over time in isolated peripheral blood basophils. In contrast, Matsubara *et al.* [160] and Szabó *et al.* [161] reported a faster and slightly stronger reaction of the TRPA1 channel to the selective agonist JT010 in TRPA1 expressing HEK cells, as well as in mouse peritoneal cells and thymocytes, respectively. However, the concentrations they used were 10-40 times higher than the highest concentration used in this thesis. The concentrations used in this thesis are based on the study published by Takaya *et al.* [105], which described the discovery of JT010. There they applied the agonist in concentrations ranging from 1 to 1000 nM to TRPA1-transfected HEK293 cells [105]. Nonetheless, activation of TRPA1 had no effect on the expression or externalization of the basophil granulocyte activation markers CD203c and CD63, respectively. A similar effect has been observed in eosinophil granulocytes concerning the TRPV1 channel, where its activation also did not cause an upregulation of activation markers [126]. Interestingly, when T cells were stimulated with TRPA1 agonists, inhibition of TRPA1 with the specific antagonist A-967079 resulted in reduced T cell activation [102]. Expression levels of the T cell activation markers CD25 and CD69 were found to be significantly decreased, indicating that TRPA1 and the induced calcium flux are necessary for the activation of T cells [102], but not of basophil granulocytes.

In AD a variety of cytokines and neurotrophins are involved in the pathogenesis of the disease. Therefore, TRPA1 expression was analyzed after stimulation with IL-3, IL-13, IL-31, IL-33, TSLP, NGFβ, BDNF, and TNF-α. TRPA1 expression in basophil granulocytes was found to be modulated by the cytokines IL-3 and IL-31, as well as the neurotrophin NGFβ. IL-3 is secreted by basophil granulocytes and affects the cells in an autocrine manner by exhibiting priming actions [26]. In the present study, there was an increase of TRPA1 expression after stimulation with IL-3. Furthermore, stimulation with IL-3 leads to the release of IL-13 [162], which exacerbates the itching sensation that patients experience [163]. The neurotrophin NGF is increased in keratinocytes in early AD lesions [164] and has been found to be elevated in plasma, and its presence correlating with disease severity [165]. In this thesis, stimulation with NGFβ caused a significant increase of TRPA1 expression in basophil granulocytes, showing that the neurotrophin can modulate the channels

expression. TRPA1 expression was significantly increased after stimulation with IL-31. IL-31 is known to induce pruritus by binding to its receptor, IL-31RA, which is expressed on TRPA1/TRPV1-positive sensory nerves [51]. Moreover, IL-31 is increased in lesional skin of patients with AD [51]. When administered or overexpressed in mice, this pruritic cytokine leads to a phenotype similar to AD [166]. In AD patients, overexpression of IL-31 has been observed in both lesional and non-lesional skin [167]. Furthermore, in AD patients, IL-31 serum levels are significantly higher than in healthy donors and correlate with disease severity [139]. A Student's t-test analysis revealed that TRPA1 modulation by IL-31 was increased in human basophil granulocytes of AD patients compared to the stimulation with culture medium only. Analysis of TRPA1 modulation with other inflammatory mediators, analyzed by ANOVA, showed no significant increase of TRPA1 expression in basophil granulocytes. This difference may be due to the sample size and the nature of the statistical tests. A limiting circumstance in this regard may be the different sample sizes ranging from n=3 up to n=5. However, this is also due to the fact that the amount of basophil granulocytes and the status of baseline activation may vary between patients, which complicates sample collection. In addition, the tests differ slightly in their methodology. The Student's t-test examines the differences between two groups directly, while the ANOVA evaluates whether at least one mean value deviates from the others. This means that a small difference may not be significant. Therefore, basophil granulocytes from two more NA donors are needed to achieve the same number of tested subjects and statistical power.

Although the remaining cytokines and neurotrophins did not affect TRPA1 expression, they are all involved in the AD disease. The pruritogenic cytokine IL-13 is increased in the lesional skin of patients with AD [163]. It increases TRPA1 expression in mast cells [98] and recruits T cells and eosinophils to sites of inflammation [163]. Additionally, the cytokine IL-13 decreases the expression of epidermal barrier proteins and is part of the itch transmission [163], all of which contribute to the inflammatory and pruritic nature of AD. IL-33 is upregulated in lesional skin of AD patients. Mechanical trauma, such as scratching, increases IL-33 expression [168]. The cytokine is known to selectively activate TRPA1 on enterochromaffin cells [169]. TSLP initiates a cascade of AD development [170] by acting as

a pruritogen and leading to TRPA1 activation [171]. BDNF has been observed to be increased in serum and plasma of AD patients [172] and enhances TRPA1 activity in rat DRG neurons [173]. However, the neurotrophin BDNF had no effect on TRPA1 expression in human basophil granulocytes. TNF-α, a pro-inflammatory cytokine [174], is also increased in patients with AD [175]. It leads to translocation of TRPA1 to the cell surface in sensory neurons [176]. Furthermore, it increases the TSLP gene expression in human keratinocytes [177], promoting inflammation. It is interesting that although all these cytokines and neurotrophins play a role in the pathogenesis of AD, they do not directly affect TRPA1 expression.

As an inflammatory disease, AD is also characterized by an acidic milieu and increased temperature. Although there is no current literature regarding the exact pH of inflamed skin, it is known that acidification occurs through the production of lactate [152]. As TRPA1 is activated at a pH between 5.0 and 5.5 [154], pH 5.0 was chosen as the lowest pH in the experiment. This milieu caused a significant increase in the expression of TRPA1 in basophil granulocytes. Similar increases in receptor expression at pH 5.0 were observed in eosinophil and basophil granulocytes and the TRPV1 channel [126, 127]. Elevated temperature, however, did not have any effect on TRPA1 expression. May *et al.* demonstrated that TRPA1 expression can increase due to heat, which was observed in HEK293T17 cells expressing human TRPA1 that were incubated for 10 minutes at 49°C, resulting in a significant elevation [115]. However, this temperature far exceeds the physiological (37°C) and febrile (41.1°C) temperatures [178] and was therefore not applied to basophil granulocytes. These results are consistent with previous studies describing TRPA1 as a cold sensor [108, 109]; however, this effect in humans remains controversial.

Furthermore, the effect of TRPA1 activation on basophil granulocyte viability was investigated. Stimulation with JT010 did not affect basophil granulocyte viability when compared to the control, regardless of the health status of the blood donor or stimulation period. This is supported by other studies, as sole activation of the TRPA1 channel has neither pro- nor anti-apoptotic effects [179, 180]. Nevertheless, this might be dependent on which types of cells express TRPA1, as activation of TRPA1 in metastatic colorectal

carcinoma cells has been observed to reduce cell viability [179]. In contrast, non-neoplastic cells from adjacent tissue are not affected [179]. Viability of human lung myofibroblast cells is also reduced after activation of TRPA1 [181]. Moreover, activation of TRPA1 might represent another step in the apoptotic pathway, as stimulation of synovial fibroblasts with TNF sensitizes the TRPA1 channel, increases calcium flux, and results in a pro-apoptotic reaction [182]. Basophil granulocytes from NA donors demonstrated overall higher viability when incubated for 4 hours, compared to 24 hours. As basophil granulocytes have a short life span of approximately 60 hours [2, 6, 10, 11], some may have died due to the incubation period, regardless of other factors. Basophil granulocytes from AD patients showed lower viability after stimulation with staurosporine compared to basophil granulocytes from NA donors. Although no definitive explanation was found in literature, this might be due to basophil granulocytes being in a heightened state of activity in AD [183], leaving them more vulnerable to apoptosis-inducing factors.

Basophil granulocytes were found in lesional skin of AD patients; however, none were observed in skin of NA donors. This has been confirmed by other studies, where basophil granulocytes were present in AD skin [49, 50, 148], while they were absent in healthy skin [7].

Co-expression of TRPA1/TRPV1 has been observed in peripheral blood basophil granulocytes from both NA donors and AD patients. Previously, this co-expression had also been found in murine and rat neurons [51, 94, 184, 185] and other cells, such as cardiac muscle cells [186] and keratinocytes [187]. Preliminary data from the group of Raap *et al.* confirms the co-expression in human eosinophil granulocytes (data not shown), which indicates that other immune cells might also possess similar co-expression patterns.

As TRPA1/TRPV1 co-expression has been confirmed in basophil granulocytes, it would be interesting to analyze if TRPA1 and TRPV1 heterotetramers also exist in basophils (TRPA1-TRPV1). The possibility of TRP channel heterotetramer formation from the same or different TRP subfamily has previously been investigated. The combinations of TRPP2-TRPC1 [188, 189], TRPP2-TRPV4 [190], TRPC3-TRPC4 [191], TRPM6-TRPM7 [192], TRPC1-TRPC3 [193], and TRPC1-TRPC5 [194] are only a few to be named. Interestingly, TRPP2 did not form

heterotetramers with TRPM8 or TRPA1 [190], which indicates limitations in the formation of heterotetramers. A synthetically produced TRPA1-TRPV1 heterotetramer is possible, as demonstrated by Fischer *et al.* [195], and can be activated by heat, capsaicin, acidic pH of 5.5, and ethanol, similar to the TRPV1 homotetramer. However, it has fewer binding sites for capsaicin, which results in a lower total current that this channel is able to conduct [195], indicating that this limitation is introduced by the TRPA1 channel. Furthermore, stimulation with the TRPA1 agonists AITC, carvacrol, or hydrogen peroxide did not result in activation of the heterotetramer [195], suggesting a dominance of the TRPV1 channel regarding the heterotetramer's functional properties. Further experiments are necessary to confirm if a TRPA1-TRPV1 heterotetramer channel exists in basophil granulocytes.

Co-expression of TRPA1/TRPV1 was observed to be modulated similarly to the expression of TRPA1 alone, namely by IL-3 and NGFβ, but also by IL-33. IL-33 is known to induce a Ca^{2+} response in DRGs; however, the addition of specific agonists for TRPA1 and TRPV1 has been observed to decrease this effect [196]. This demonstrates the importance of both TRP channels for the development of itch, also in the context of AD. The percentage of basophil granulocytes that expressed both channels was visibly lower than the amount of basophil granulocytes that expressed TRPA1 alone. This is in accordance with the findings of Story *et al.* [94], who reported that only approximately 30% of TRPV1-positive neurons also express TRPA1.

Modulation of TRPA1/TRPV1 co-expression by pH or temperature was also similar to the modulation of TRPA1 alone. However, the percentage of TRPA1/TRPV1-positive basophil granulocytes was about 20% lower than the number of cells that expressed solely TRPA1. This result again confirms the findings of Story *et al*. [94] that only approximately a third of TRPV1-expressing neurons are also TRPA1-positive.

Working with basophil granulocytes presents a variety of limitations. Due to their scarcity in the human body, as basophil granulocytes comprise less than 1% of all leukocytes [1], experiments are limited by the number of conditions that can be analyzed. Moreover, the number of basophil granulocytes varies from donor to donor [197, 198], which increases the number of required donors. Although a basophil granulocyte cell line was recently

established by Celprogen, the use of basophil granulocytes from NA donors and patients with AD remains necessary [14], as only in this way differences between diseased and healthy skin can be accurately analyzed. Furthermore, utilizing concentrated buffy coat blood from blood donations is also not ideal, as the medical history of the donors is not provided, making it impossible to differentiate between NA donors and AD patients. Moreover, due to the collection process, the freshness of buffy coat blood is not guaranteed and might affect basophil granulocytes' ability to respond to stimuli in experimental settings. Taken together, this shows the limitations of working with basophil granulocytes in experimental settings and emphasizes the need for more reliable models in future studies.

In conclusion, basophil granulocytes express the TRPA1 and the TRPV1 channels. TRPA1 channel expression is significantly increased in patients with AD, highlighting its role in the disease. The channel is functional, but its activation does not cause an elevation in the presence of the basophil granulocyte activation markers CD63 and CD203c or the cells viability. TRPA1 expression can be modulated by IL-3, NGFβ, and, in the case of co-expression with TRPV1, by IL-33. Acidic pH also increases the expression of TRPA1, alone and in combination with TRPV1, but temperature has no effect. Basophil granulocytes that express TRPA1 are also found in lesional skin of AD patients. All these results underscore the importance of basophil granulocytes and TRP channels in AD, hopefully contributing to elucidating part of the disease's pathogenesis.

5 Outlook

The results in this doctoral thesis show the importance of the TRPA1 channel in human basophil granulocytes of AD patients and aim to expand the understanding of the disease. However, more research is necessary.

In future experiments, the presence of TRPA1-TRPV1 heterotetramers in human basophil granulocytes could be analyzed. This could be done in cooperation with Dr. Jochen Behrends from the Research Center Borstel, as they have a FACSDiscover S8 with CellView Image Technology, which enables the capture of high-resolution images of cells. With respective antibodies, visualization of TRPA1-TRPV1 heterotetramers may be possible.

Another potential experiment could involve co-culturing human peripheral blood basophil granulocytes with *Staphylococcus aureus*, a Gram-positive bacterium. It is known to colonize the skin of AD patients [52] and releases protein A, which activates basophil granulocytes [55]. Analyzing TRPA1 expression after co-culture with *Staphylococcus aureus*, as well as examining the contents of the supernatant, may elucidate further aspects of AD pathogenesis.

In cooperation with the team of Prof. Dr. Anja Bräuer from the Department of Anatomy, basophil granulocytes could be co-cultured with neurons or neuronal supernatants. The supernatant itself and TRPA1 expression of basophil granulocytes after co-cultivation could both be examined. Due to the close spatial proximity of basophil granulocytes and neurons in the skin of AD patients [16], this experiment could give important insight into the development of the disease, especially regarding itch development and transmission.

All these experiments could broaden the understanding of AD and contribute to the development of new treatments. One possible treatment approach could be a topical cream containing a TRPA1 antagonist to reduce itch in lesional skin. Treatment of mice and rats with the TRPA1 antagonist HC-030031 has already shown promising results [112, 199], attenuating both itch and pain in the respective animal models.

In summary, further investigation of basophil granulocytes and TRPA1 could elucidate the pathogenesis of AD, as well as create new therapies, improving patient outcomes and quality of life.

References

1. Ehrlich P (1879) Beiträge zur Kenntnis der granulirten Bindegewebszellen und der eosinophilen Leukocythen. Archiv für Anatomie und Physiologie: Physiologische Abteilung, 3-166.
2. Siracusa MC, Comeau MR, Artis D (2011) New insights into basophil biology: initiators, regulators, and effectors of type 2 inflammation. Annals of the New York Academy of Sciences 1217, 166–177. 10.1111/j.1749-6632.2010.05918.x.
3. Valent P, Schmidt G, Besemer J, Mayer P, Zenke G, Liehl E, Hinterberger W, Lechner K, Maurer D, Bettelheim P (1989) Interleukin-3 is a differentiation factor for human basophils. Blood 73(7), 1763–1769. 10.1182/blood.V73.7.1763.1763.
4. Valent P, Schmidt G, Besemer J, Mayer P, Zenke G, Liehl E, Hinterberger W, Lechner K, Maurer D, Bettelheim P (1989) Interleukin-3 is a differentiation factor for human basophils. Blood 73(7), 1763–1769.
5. Whetstone CE, Amer R, Maqbool S, Javed T, Gauvreau GM (2025) Pathobiology and Regulation of Eosinophils, Mast Cells, and Basophils in Allergic Asthma. Immunological reviews 331(1), e70018. 10.1111/imr.70018.
6. Miyake K, Karasuyama H (2017) Emerging roles of basophils in allergic inflammation. Allergology international official journal of the Japanese Society of Allergology 66(3), 382–391. 10.1016/j.alit.2017.04.007.
7. Shibuya R, Kim BS (2022) Skin-homing basophils and beyond. Frontiers in immunology 13, 1059098. 10.3389/fimmu.2022.1059098.
8. Sokol CL, Medzhitov R (2010) Emerging functions of basophils in protective and allergic immune responses. Mucosal immunology 3(2), 129–137. 10.1038/mi.2009.137.
9. Galli SJ (2000) Mast cells and basophils. Current opinion in hematology 7(1), 32–39. 10.1097/00062752-200001000-00007.
10. Ohnmacht C, Voehringer D (2009) Basophil effector function and homeostasis during helminth infection. Blood 113(12), 2816–2825. 10.1182/blood-2008-05-154773.

11. Karasuyama H, Mukai K, Obata K, Tsujimura Y, Wada T (2011) Nonredundant roles of basophils in immunity. Annual review of immunology 29, 45–69. 10.1146/annurev-immunol-031210-101257.
12. Arock M, Schneider E, Boissan M, Tricottet V, Dy M (2002) Differentiation of human basophils: an overview of recent advances and pending questions. Journal of leukocyte biology 71(4), 557–564. 10.1189/jlb.71.4.557.
13. Knol EF, Olszewski M (2011) Basophils and mast cells: Underdog in immune regulation? Immunology letters 138(1), 28–31. 10.1016/j.imlet.2011.02.012.
14. Gray N, Wiebe D, Weihrauch T, Raap U, Limberg MM (2024) Density Gradient Centrifugation-Independent Purification of Human Basophils. Current protocols 4(2), e991. 10.1002/cpz1.991.
15. Peng J, Siracusa MC (2021) Basophils in antihelminth immunity. Seminars in immunology 53, 101529. 10.1016/j.smim.2021.101529.
16. Wiebe D, Limberg MM, Gray N, Raap U (2023) Basophils in pruritic skin diseases. Frontiers in immunology 14, 1213138. 10.3389/fimmu.2023.1213138.
17. Zhao S, Tang Y, Hong L, Xu M, Pan S, Zhen K, Tang R, Zhai X, Shi Z, Wang H (2020) Interleukin 2 regulates the activation of human basophils. Cytokine 127, 154934. 10.1016/j.cyto.2019.154934.
18. Raap U, Gehring M, Kleiner S, Rüdrich U, Eiz-Vesper B, Haas H, Kapp A, Gibbs BF (2017) Human basophils are a source of - and are differentially activated by - IL-31. Clinical and experimental allergy journal of the British Society for Allergy and Clinical Immunology 47(4), 499–508. 10.1111/cea.12875.
19. Sokol CL, Barton GM, Farr AG, Medzhitov R (2008) A mechanism for the initiation of allergen-induced T helper type 2 responses. Nature immunology 9(3), 310–318. 10.1038/ni1558.
20. Wang P, Su Z, Sun C, Yao W-H, Zeng Y-P (2025) The Role of Basophils in Atopic Dermatitis, from Pathogenesis to Therapeutic Perspectives. Journal of asthma and allergy 18, 675–682. 10.2147/JAA.S522343.

21. Nakashima C, Ishida Y, Kitoh A, Otsuka A, Kabashima K (2019) Interaction of peripheral nerves and mast cells, eosinophils, and basophils in the development of pruritus. Experimental dermatology 28(12), 1405–1411. 10.1111/exd.14014.
22. Ishizaka K, Tomioka H, Ishizaka T (1970) Mechanisms of passive sensitization. I. Presence of IgE and IgG molecules on human leukocytes. Journal of immunology (Baltimore, Md. 1950) 105(6), 1459–1467.
23. Miyake K, Shibata S, Yoshikawa S, Karasuyama H (2021) Basophils and their effector molecules in allergic disorders. Allergy 76(6), 1693–1706. 10.1111/all.14662.
24. Kurimoto Y, Weck AL de, Dahinden CA (1989) Interleukin 3-dependent mediator release in basophils triggered by C5a. The Journal of experimental medicine 170(2), 467–479. 10.1084/jem.170.2.467.
25. Schleimer RP, Derse CP, Friedman B, Gillis S, Plaut M, Lichtenstein LM, MacGlashan DW (1989) Regulation of human basophil mediator release by cytokines. I. Interaction with antiinflammatory steroids. The Journal of Immunology 143(4), 1310–1317. 10.4049/jimmunol.143.4.1310.
26. Schroeder JT, Chichester KL, Bieneman AP (2009) Human basophils secrete IL-3: evidence of autocrine priming for phenotypic and functional responses in allergic disease. Journal of immunology (Baltimore, Md. 1950) 182(4), 2432–2438. 10.4049/jimmunol.0801782.
27. Bischoff SC, Dahinden CA (1992) Effect of nerve growth factor on the release of inflammatory mediators by mature human basophils. Blood 79(10), 2662–2669.
28. Bischoff SC, Brunner T, Weck AL de, Dahinden CA (1990) Interleukin 5 modifies histamine release and leukotriene generation by human basophils in response to diverse agonists. The Journal of experimental medicine 172(6), 1577–1582. 10.1084/jem.172.6.1577.
29. Chirumbolo S, Vella A, Ortolani R, Gironcoli M de, Solero P, Tridente G, Bellavite P (2008) Differential response of human basophil activation markers: a multi-parameter flow cytometry approach. Clinical and molecular allergy CMA 6, 12. 10.1186/1476-7961-6-12.

30. Yoshimura C, Yamaguchi M, Iikura M, Izumi S, Kudo K, Nagase H, Ishii A, Walls AF, Ra C, Iwata T, Igarashi T, Yamamoto K, Hirai K (2002) Activation markers of human basophils: CD69 expression is strongly and preferentially induced by IL-3. The Journal of allergy and clinical immunology 109(5), 817–823. 10.1067/mai.2002.123532.
31. Steiner M, Huber S, Harrer A, Himly M (2016) The Evolution of Human Basophil Biology from Neglect towards Understanding of Their Immune Functions. BioMed research international 2016, 8232830. 10.1155/2016/8232830.
32. Bühring H-J, Streble A, Valent P (2004) The basophil-specific ectoenzyme E-NPP3 (CD203c) as a marker for cell activation and allergy diagnosis. International archives of allergy and immunology 133(4), 317–329. 10.1159/000077351.
33. Boumiza R, Debard A-L, Monneret G (2005) The basophil activation test by flow cytometry: recent developments in clinical studies, standardization and emerging perspectives. Clinical and molecular allergy CMA 3, 9. 10.1186/1476-7961-3-9.
34. Crivellato E, Nico B, Mallardi F, Beltrami CA, Ribatti D (2003) Piecemeal degranulation as a general secretory mechanism? The anatomical record. Part A, Discoveries in molecular, cellular, and evolutionary biology 274(1), 778–784. 10.1002/ar.a.10095.
35. Kolb L, Ferrer-Bruker SJ (2025) StatPearls: Atopic Dermatitis. Treasure Island (FL).
36. Williams H, Robertson C, Stewart A, Aït-Khaled N, Anabwani G, Anderson R, Asher I, Beasley R, Björkstén B, Burr M, Clayton T, Crane J, Ellwood P, Keil U, Lai C, Mallol J, Martinez F, Mitchell E, Montefort S, Pearce N, Shah J, Sibbald B, Strachan D, Mutius E von, Weiland SK (1999) Worldwide variations in the prevalence of symptoms of atopic eczema in the international study of asthma and allergies in childhood. Journal of Allergy and Clinical Immunology 103(1), 125–138. 10.1016/S0091-6749(99)70536-1.
37. Schmitt J, Bauer A, Meurer M (2008) Atopisches Ekzem im Erwachsenenalter. Der Hautarzt; Zeitschrift fur Dermatologie, Venerologie, und verwandte Gebiete 59(10), 841-50; quiz 851. 10.1007/s00105-008-1503-5.
38. Vicho-de-la-Fuente N, Martinez-Santos A-E, Rodríguez-González R, Florez Á, Sheaf G, Coyne I (2024) Impact of Atopic Dermatitis on Adolescents and Families: A Mixed-Method Systematic Review. Journal of advanced nursing. 10.1111/jan.16652.

39. Spergel JM, Paller AS (2003) Atopic dermatitis and the atopic march. Journal of Allergy and Clinical Immunology 112(6 Suppl), S118-27. 10.1016/j.jaci.2003.09.033.
40. Leung DY (2000) Atopic dermatitis: new insights and opportunities for therapeutic intervention. Journal of Allergy and Clinical Immunology 105(5), 860–876. 10.1067/mai.2000.106484.
41. Facheris P, Jeffery J, Del Duca E, Guttman-Yassky E (2023) The translational revolution in atopic dermatitis: the paradigm shift from pathogenesis to treatment. Cellular & molecular immunology 20(5), 448–474. 10.1038/s41423-023-00992-4.
42. Weidinger S, Beck LA, Bieber T, Kabashima K, Irvine AD (2018) Atopic dermatitis. Nature reviews. Disease primers 4(1), 1. 10.1038/s41572-018-0001-z.
43. Boguniewicz M, Leung DYM (2011) Atopic dermatitis: a disease of altered skin barrier and immune dysregulation. Immunological reviews 242(1), 233–246. 10.1111/j.1600-065X.2011.01027.x.
44. Patrick GJ, Archer NK, Miller LS (2021) Which Way Do We Go? Complex Interactions in Atopic Dermatitis Pathogenesis. The Journal of investigative dermatology 141(2), 274–284. 10.1016/j.jid.2020.07.006.
45. Tsuji G, Yamamura K, Kawamura K, Kido-Nakahara M, Ito T, Nakahara T (2023) Novel Therapeutic Targets for the Treatment of Atopic Dermatitis. Biomedicines 11(5). 10.3390/biomedicines11051303.
46. Lopez AF, Sanderson CJ, Gamble JR, Campbell HD, Young IG, Vadas MA (1988) Recombinant human interleukin 5 is a selective activator of human eosinophil function. The Journal of experimental medicine 167(1), 219–224. 10.1084/jem.167.1.219.
47. Bieber T (2022) Atopic dermatitis: an expanding therapeutic pipeline for a complex disease. Nature reviews. Drug discovery 21(1), 21–40. 10.1038/s41573-021-00266-6.
48. Borriello F, Granata F, Marone G (2014) Basophils and skin disorders. The Journal of investigative dermatology 134(5), 1202–1210. 10.1038/jid.2014.16.
49. Ito Y, Satoh T, Takayama K, Miyagishi C, Walls AF, Yokozeki H (2011) Basophil recruitment and activation in inflammatory skin diseases. Allergy 66(8), 1107–1113. 10.1111/j.1398-9995.2011.02570.x.

50. Miyake K, Ito J, Karasuyama H (2022) Role of Basophils in a Broad Spectrum of Disorders. Frontiers in immunology 13, 902494. 10.3389/fimmu.2022.902494.
51. Cevikbas F, Wang X, Akiyama T, Kempkes C, Savinko T, Antal A, Kukova G, Buhl T, Ikoma A, Buddenkotte J, Soumelis V, Feld M, Alenius H, Dillon SR, Carstens E, Homey B, Basbaum A, Steinhoff M (2014) A sensory neuron-expressed IL-31 receptor mediates T helper cell-dependent itch: Involvement of TRPV1 and TRPA1. The Journal of allergy and clinical immunology 133(2), 448–460. 10.1016/j.jaci.2013.10.048.
52. Geoghegan JA, Irvine AD, Foster TJ (2018) Staphylococcus aureus and Atopic Dermatitis: A Complex and Evolving Relationship. Trends in microbiology 26(6), 484–497. 10.1016/j.tim.2017.11.008.
53. Totté JEE, van der Feltz WT, Hennekam M, van Belkum A, van Zuuren EJ, Pasmans SGMA (2016) Prevalence and odds of Staphylococcus aureus carriage in atopic dermatitis: a systematic review and meta-analysis. The British journal of dermatology 175(4), 687–695. 10.1111/bjd.14566.
54. Kong HH, Oh J, Deming C, Conlan S, Grice EA, Beatson MA, Nomicos E, Polley EC, Komarow HD, Murray PR, Turner ML, Segre JA (2012) Temporal shifts in the skin microbiome associated with disease flares and treatment in children with atopic dermatitis. Genome research 22(5), 850–859. 10.1101/gr.131029.111.
55. Marone G, Tamburini M, Giudizi MG, Biagiotti R, Almerigogna F, Romagnani S (1987) Mechanism of activation of human basophils by Staphylococcus aureus Cowan 1. Infection and immunity 55(3), 803–809. 10.1128/iai.55.3.803-809.1987.
56. Guseva D, Rüdrich U, Kotnik N, Gehring M, Patsinakidis N, Agelopoulos K, Ständer S, Homey B, Kapp A, Gibbs BF, Ponimaskin E, Raap U (2020) Neuronal branching of sensory neurons is associated with BDNF-positive eosinophils in atopic dermatitis. Clinical and experimental allergy journal of the British Society for Allergy and Clinical Immunology 50(5), 577–584. 10.1111/cea.13560.
57. Nagashima N, Ugajin T, Miyake K, Walls AF, Namiki T, Yokozeki H, Karasuyama H, Okiyama N (2024) Cutaneous basophil infiltration in atopic dermatitis is associated with abundant epidermal infiltration of helper T cells: A preliminary retrospective study. The Journal of dermatology 51(1), 130–134. 10.1111/1346-8138.16987.

58. Kim BS, Wang K, Siracusa MC, Saenz SA, Brestoff JR, Monticelli LA, Noti M, Tait Wojno ED, Fung TC, Kubo M, Artis D (2014) Basophils promote innate lymphoid cell responses in inflamed skin. The Journal of Immunology 193(7), 3717–3725. 10.4049/jimmunol.1401307.
59. Cheng LE, Sullivan BM, Retana LE, Allen CDC, Liang H-E, Locksley RM (2015) IgE-activated basophils regulate eosinophil tissue entry by modulating endothelial function. The Journal of experimental medicine 212(4), 513–524. 10.1084/jem.20141671.
60. Pan Y, Wang Y, Xu M, Zhong M, Peng X, Zeng K, Huang X (2024) The Roles of Innate Immune Cells in Atopic Dermatitis. Journal of innate immunity 16(1), 385–396. 10.1159/000539534.
61. Sidbury R, Davis DM, Cohen DE, Cordoro KM, Berger TG, Bergman JN, Chamlin SL, Cooper KD, Feldman SR, Hanifin JM, Krol A, Margolis DJ, Paller AS, Schwarzenberger K, Silverman RA, Simpson EL, Tom WL, Williams HC, Elmets CA, Block J, Harrod CG, Begolka WS, Eichenfield LF (2014) Guidelines of care for the management of atopic dermatitis: section 3. Management and treatment with phototherapy and systemic agents. Journal of the American Academy of Dermatology 71(2), 327–349. 10.1016/j.jaad.2014.03.030.
62. He A, Feldman SR, Fleischer AB (2018) An assessment of the use of antihistamines in the management of atopic dermatitis. Journal of the American Academy of Dermatology 79(1), 92–96. 10.1016/j.jaad.2017.12.077.
63. Beck LA, Deleuran M, Bissonnette R, Bruin-Weller M de, Galus R, Nakahara T, Seo SJ, Khokhar FA, Vakil J, Xiao J, Marco AR, Levit NA, O'Malley JT, Shabbir A (2022) Dupilumab Provides Acceptable Safety and Sustained Efficacy for up to 4 Years in an Open-Label Study of Adults with Moderate-to-Severe Atopic Dermatitis. American journal of clinical dermatology 23(3), 393–408. 10.1007/s40257-022-00685-0.
64. Wollenberg A, Blauvelt A, Guttman-Yassky E, Worm M, Lynde C, Lacour J-P, Spelman L, Katoh N, Saeki H, Poulin Y, Lesiak A, Kircik L, Cho SH, Herranz P, Cork MJ, Peris K, Steffensen LA, Bang B, Kuznetsova A, Jensen TN, Østerdal ML, Simpson EL (2021) Tralokinumab for moderate-to-severe atopic dermatitis: results from two 52-week,

randomized, double-blind, multicentre, placebo-controlled phase III trials (ECZTRA 1 and ECZTRA 2). The British journal of dermatology 184(3), 437–449. 10.1111/bjd.19574.

65. Silverberg JI, Guttman-Yassky E, Thaçi D, Irvine AD, Stein Gold L, Blauvelt A, Simpson EL, Chu C-Y, Liu Z, Gontijo Lima R, Pillai SG, Seneschal J (2023) Two Phase 3 Trials of Lebrikizumab for Moderate-to-Severe Atopic Dermatitis. The New England journal of medicine 388(12), 1080–1091. 10.1056/NEJMoa2206714.
66. Kabashima K, Furue M, Hanifin JM, Pulka G, Wollenberg A, Galus R, Etoh T, Mihara R, Nakano M, Ruzicka T (2018) Nemolizumab in patients with moderate-to-severe atopic dermatitis: Randomized, phase II, long-term extension study. The Journal of allergy and clinical immunology 142(4), 1121-1130.e7. 10.1016/j.jaci.2018.03.018.
67. Bonnekoh H, Butze M, Metz M (2022) Characterization of the effects on pruritus by novel treatments for atopic dermatitis. Journal der Deutschen Dermatologischen Gesellschaft = Journal of the German Society of Dermatology JDDG 20(2), 150–156. 10.1111/ddg.14678.
68. Siracusa MC, Kim BS, Spergel JM, Artis D (2013) Basophils and allergic inflammation. The Journal of allergy and clinical immunology 132(4), 789-801; quiz 788. 10.1016/j.jaci.2013.07.046.
69. Kwatra SG, Misery L, Clibborn C, Steinhoff M (2022) Molecular and cellular mechanisms of itch and pain in atopic dermatitis and implications for novel therapeutics. Clinical & translational immunology 11(5), e1390. 10.1002/cti2.1390.
70. Steinhoff M, Ahmad F, Pandey A, Datsi A, AlHammadi A, Al-Khawaga S, Al-Malki A, Meng J, Alam M, Buddenkotte J (2022) Neuroimmune communication regulating pruritus in atopic dermatitis. The Journal of allergy and clinical immunology 149(6), 1875–1898. 10.1016/j.jaci.2022.03.010.
71. Cosens DJ, Manning A (1969) Abnormal electroretinogram from a Drosophila mutant. Nature 224(5216), 285–287. 10.1038/224285a0.
72. Minke B, Wu C, Pak WL (1975) Induction of photoreceptor voltage noise in the dark in Drosophila mutant. Nature 258(5530), 84–87. 10.1038/258084a0.
73. Montell C, Birnbaumer L, Flockerzi V, Bindels RJ, Bruford EA, Caterina MJ, Clapham DE, Harteneck C, Heller S, Julius D, Kojima I, Mori Y, Penner R, Prawitt D, Scharenberg

AM, Schultz G, Shimizu N, Zhu MX (2002) A unified nomenclature for the superfamily of TRP cation channels. Molecular cell 9(2), 229–231. 10.1016/S1097-2765(02)00448-3.

74. Clapham DE, Montell C, Schultz G, Julius D (2003) International Union of Pharmacology. XLIII. Compendium of voltage-gated ion channels: transient receptor potential channels. Pharmacological reviews 55(4), 591–596. 10.1124/pr.55.4.6.
75. Haberberger RV, Barry C, Dominguez N, Matusica D (2019) Human Dorsal Root Ganglia. Frontiers in cellular neuroscience 13, 271. 10.3389/fncel.2019.00271.
76. Held K, Tóth BI (2021) TRPM3 in Brain (Patho)Physiology. Frontiers in cell and developmental biology 9, 635659. 10.3389/fcell.2021.635659.
77. Khalil M, Alliger K, Weidinger C, Yerinde C, Wirtz S, Becker C, Engel MA (2018) Functional Role of Transient Receptor Potential Channels in Immune Cells and Epithelia. Frontiers in immunology 9, 174. 10.3389/fimmu.2018.00174.
78. Bertin S, Raz E (2016) Transient Receptor Potential (TRP) channels in T cells. Seminars in immunopathology 38(3), 309–319. 10.1007/s00281-015-0535-z.
79. Sawamura S, Shirakawa H, Nakagawa T, Mori Y, Kaneko S (2017) Neurobiology of TRP Channels: TRP Channels in the Brain: What Are They There For? Boca Raton (FL).
80. Mahmoud O, Soares GB, Yosipovitch G (2022) Transient Receptor Potential Channels and Itch. International journal of molecular sciences 24(1). 10.3390/ijms24010420.
81. Pan Z, Yang H, Reinach PS (2011) Transient receptor potential (TRP) gene superfamily encoding cation channels. Hum Genomics 5(2), 108–116. 10.1186/1479-7364-5-2-108.
82. Nilius B, Owsianik G, Voets T, Peters JA (2007) Transient receptor potential cation channels in disease. Physiological reviews 87(1), 165–217. 10.1152/physrev.00021.2006.
83. Zhang M, Ma Y, Ye X, Zhang N, Pan L, Wang B (2023) TRP (transient receptor potential) ion channel family: structures, biological functions and therapeutic interventions for diseases. Signal transduction and targeted therapy 8(1), 261. 10.1038/s41392-023-01464-x.
84. Damann N, Voets T, Nilius B (2008) TRPs in our senses. Current biology CB 18(18), R880-9. 10.1016/j.cub.2008.07.063.
85. Yue L, Xu H (2021) TRP channels in health and disease at a glance. Journal of cell science 134(13). 10.1242/jcs.258372.

86. Meseguer V, Alpizar YA, Luis E, Tajada S, Denlinger B, Fajardo O, Manenschijn J-A, Fernández-Peña C, Talavera A, Kichko T, Navia B, Sánchez A, Señarís R, Reeh P, Pérez-García MT, López-López JR, Voets T, Belmonte C, Talavera K, Viana F (2014) TRPA1 channels mediate acute neurogenic inflammation and pain produced by bacterial endotoxins. Nature communications 5, 3125. 10.1038/ncomms4125.
87. Tsuji F, Aono H (2012) Role of transient receptor potential vanilloid 1 in inflammation and autoimmune diseases. Pharmaceuticals (Basel, Switzerland) 5(8), 837–852. 10.3390/ph5080837.
88. Bujak JK, Kosmala D, Szopa IM, Majchrzak K, Bednarczyk P (2019) Inflammation, Cancer and Immunity-Implication of TRPV1 Channel. Frontiers in oncology 9, 1087. 10.3389/fonc.2019.01087.
89. Papoiu ADP, Yosipovitch G (2010) Topical capsaicin. The fire of a 'hot' medicine is reignited. Expert opinion on pharmacotherapy 11(8), 1359–1371. 10.1517/14656566.2010.481670.
90. Fallah HP, Ahuja E, Lin H, Qi J, He Q, Gao S, An H, Zhang J, Xie Y, Liang D (2022) A Review on the Role of TRP Channels and Their Potential as Drug Targets_An Insight Into the TRP Channel Drug Discovery Methodologies. Frontiers in pharmacology 13, 914499. 10.3389/fphar.2022.914499.
91. Wilson SR, Gerhold KA, Bifolck-Fisher A, Liu Q, Patel KN, Dong X, Bautista DM (2011) TRPA1 is required for histamine-independent, Mas-related G protein-coupled receptor-mediated itch. Nature neuroscience 14(5), 595–602. 10.1038/nn.2789.
92. Nattkemper LA, Tey HL, Valdes-Rodriguez R, Lee H, Mollanazar NK, Albornoz C, Sanders KM, Yosipovitch G (2018) The Genetics of Chronic Itch: Gene Expression in the Skin of Patients with Atopic Dermatitis and Psoriasis with Severe Itch. The Journal of investigative dermatology 138(6), 1311–1317. 10.1016/j.jid.2017.12.029.
93. Jaquemar D, Schenker T, Trueb B (1999) An ankyrin-like protein with transmembrane domains is specifically lost after oncogenic transformation of human fibroblasts. The Journal of biological chemistry 274(11), 7325–7333. 10.1074/jbc.274.11.7325.
94. Story GM, Peier AM, Reeve AJ, Eid SR, Mosbacher J, Hricik TR, Earley TJ, Hergarden AC, Andersson DA, Hwang SW, McIntyre P, Jegla T, Bevan S, Patapoutian A (2003)

ANKTM1, a TRP-like channel expressed in nociceptive neurons, is activated by cold temperatures. Cell 112(6), 819–829. 10.1016/S0092-8674(03)00158-2.

95. Talavera K, Startek JB, Alvarez-Collazo J, Boonen B, Alpizar YA, Sanchez A, Naert R, Nilius B (2020) Mammalian Transient Receptor Potential TRPA1 Channels: From Structure to Disease. Physiological reviews 100(2), 725–803. 10.1152/physrev.00005.2019.
96. Atoyan R, Shander D, Botchkareva NV (2009) Non-neuronal expression of transient receptor potential type A1 (TRPA1) in human skin. The Journal of investigative dermatology 129(9), 2312–2315. 10.1038/jid.2009.58.
97. Valdes-Rodriguez R, Kaushik SB, Yosipovitch G (2013) Transient receptor potential channels and dermatological disorders. Current topics in medicinal chemistry 13(3), 335–343. 10.2174/15680266112129990090.
98. Oh M-H, Oh SY, Lu J, Lou H, Myers AC, Zhu Z, Zheng T (2013) TRPA1-dependent pruritus in IL-13-induced chronic atopic dermatitis. Journal of immunology (Baltimore, Md. 1950) 191(11), 5371–5382. 10.4049/jimmunol.1300300.
99. Naert R, López-Requena A, Talavera K (2021) TRPA1 Expression and Pathophysiology in Immune Cells. International journal of molecular sciences 22(21). 10.3390/ijms222111460.
100. Stokes A, Wakano C, Koblan-Huberson M, Adra CN, Fleig A, Turner H (2006) TRPA1 is a substrate for de-ubiquitination by the tumor suppressor CYLD. Cellular signalling 18(10), 1584–1594. 10.1016/j.cellsig.2005.12.009.
101. Bandell M, Story GM, Hwang SW, Viswanath V, Eid SR, Petrus MJ, Earley TJ, Patapoutian A (2004) Noxious cold ion channel TRPA1 is activated by pungent compounds and bradykinin. Neuron 41(6), 849–857. 10.1016/S0896-6273(04)00150-3.
102. Sahoo SS, Majhi RK, Tiwari A, Acharya T, Kumar PS, Saha S, Kumar A, Goswami C, Chattopadhyay S (2019) Transient receptor potential ankyrin1 channel is endogenously expressed in T cells and is involved in immune functions. Bioscience reports 39(9). 10.1042/BSR20191437.
103. Bautista DM, Movahed P, Hinman A, Axelsson HE, Sterner O, Högestätt ED, Julius D, Jordt S-E, Zygmunt PM (2005) Pungent products from garlic activate the sensory ion

channel TRPA1. Proceedings of the National Academy of Sciences of the United States of America 102(34), 12248–12252. 10.1073/pnas.0505356102.

104. Meents JE, Fischer MJM, McNaughton PA (2016) Agonist-induced sensitisation of the irritant receptor ion channel TRPA1. The Journal of physiology 594(22), 6643–6660. 10.1113/JP272237.

105. Takaya J, Mio K, Shiraishi T, Kurokawa T, Otsuka S, Mori Y, Uesugi M (2015) A Potent and Site-Selective Agonist of TRPA1. Journal of the American Chemical Society 137(50), 15859–15864. 10.1021/jacs.5b10162.

106. Moparthi L, Kichko TI, Eberhardt M, Högestätt ED, Kjellbom P, Johanson U, Reeh PW, Leffler A, Filipovic MR, Zygmunt PM (2016) Human TRPA1 is a heat sensor displaying intrinsic U-shaped thermosensitivity. Scientific reports 6, 28763. 10.1038/srep28763.

107. Sawada Y, Hosokawa H, Hori A, Matsumura K, Kobayashi S (2007) Cold sensitivity of recombinant TRPA1 channels. Brain research 1160, 39–46. 10.1016/j.brainres.2007.05.047.

108. Chen J, Kang D, Xu J, Lake M, Hogan JO, Sun C, Walter K, Yao B, Kim D (2013) Species differences and molecular determinant of TRPA1 cold sensitivity. Nature communications 4, 2501. 10.1038/ncomms3501.

109. Moparthi L, Survery S, Kreir M, Simonsen C, Kjellbom P, Högestätt ED, Johanson U, Zygmunt PM (2014) Human TRPA1 is intrinsically cold- and chemosensitive with and without its N-terminal ankyrin repeat domain. Proceedings of the National Academy of Sciences of the United States of America 111(47), 16901–16906. 10.1073/pnas.1412689111.

110. Chen J, Joshi SK, DiDomenico S, Perner RJ, Mikusa JP, Gauvin DM, Segreti JA, Han P, Zhang X-F, Niforatos W, Bianchi BR, Baker SJ, Zhong C, Simler GH, McDonald HA, Schmidt RG, McGaraughty SP, Chu KL, Faltynek CR, Kort ME, Reilly RM, Kym PR (2011) Selective blockade of TRPA1 channel attenuates pathological pain without altering noxious cold sensation or body temperature regulation. Pain 152(5), 1165–1172. 10.1016/j.pain.2011.01.049.

111. Petrus M, Peier AM, Bandell M, Hwang SW, Huynh T, Olney N, Jegla T, Patapoutian A (2007) A role of TRPA1 in mechanical hyperalgesia is revealed by pharmacological inhibition. Molecular pain 3, 40. 10.1186/1744-8069-3-40.

112. Eid SR, Crown ED, Moore EL, Liang HA, Choong K-C, Dima S, Henze DA, Kane SA, Urban MO (2008) HC-030031, a TRPA1 selective antagonist, attenuates inflammatory- and neuropathy-induced mechanical hypersensitivity. Molecular pain 4, 48. 10.1186/1744-8069-4-48.

113. Shang S, Zhu F, Liu B, Chai Z, Wu Q, Hu M, Wang Y, Huang R, Zhang X, Wu X, Sun L, Wang Y, Wang L, Xu H, Teng S, Liu B, Zheng L, Zhang C, Zhang F, Feng X, Zhu D, Wang C, Liu T, Zhu MX, Zhou Z (2016) Intracellular TRPA1 mediates Ca2+ release from lysosomes in dorsal root ganglion neurons. The Journal of cell biology 215(3), 369–381. 10.1083/jcb.201603081.

114. Schmidt M, Dubin AE, Petrus MJ, Earley TJ, Patapoutian A (2009) Nociceptive signals induce trafficking of TRPA1 to the plasma membrane. Neuron 64(4), 498–509. 10.1016/j.neuron.2009.09.030.

115. May D, Baastrup J, Nientit MR, Binder A, Schünke M, Baron R, Cascorbi I (2012) Differential expression and functionality of TRPA1 protein genetic variants in conditions of thermal stimulation. The Journal of biological chemistry 287(32), 27087–27094. 10.1074/jbc.M112.341776.

116. Yang D (2024) TRPA1-Related Diseases and Applications of Nanotherapy. International journal of molecular sciences 25(17). 10.3390/ijms25179234.

117. Liu B, Escalera J, Balakrishna S, Fan L, Caceres AI, Robinson E, Sui A, McKay MC, McAlexander MA, Herrick CA, Jordt SE (2013) TRPA1 controls inflammation and pruritogen responses in allergic contact dermatitis. FASEB journal official publication of the Federation of American Societies for Experimental Biology 27(9), 3549–3563. 10.1096/fj.13-229948.

118. Namer B, Seifert F, Handwerker HO, Maihöfner C (2005) TRPA1 and TRPM8 activation in humans: effects of cinnamaldehyde and menthol. Neuroreport 16(9), 955–959. 10.1097/00001756-200506210-00015.

119. Sun S, Dong X (2016) Trp channels and itch. Seminars in immunopathology 38(3), 293–307. 10.1007/s00281-015-0530-4.

120. Soga F, Katoh N, Inoue T, Kishimoto S (2007) Serotonin activates human monocytes and prevents apoptosis. The Journal of investigative dermatology 127(8), 1947–1955. 10.1038/sj.jid.5700824.

121. Morita T, McClain SP, Batia LM, Pellegrino M, Wilson SR, Kienzler MA, Lyman K, Olsen ASB, Wong JF, Stucky CL, Brem RB, Bautista DM (2015) HTR7 Mediates Serotonergic Acute and Chronic Itch. Neuron 87(1), 124–138. 10.1016/j.neuron.2015.05.044.

122. Caterina MJ, Schumacher MA, Tominaga M, Rosen TA, Levine JD, Julius D (1997) The capsaicin receptor: a heat-activated ion channel in the pain pathway. Nature 389(6653), 816–824. 10.1038/39807.

123. Caterina MJ, Leffler A, Malmberg AB, Martin WJ, Trafton J, Petersen-Zeitz KR, Koltzenburg M, Basbaum AI, Julius D (2000) Impaired nociception and pain sensation in mice lacking the capsaicin receptor. Science (New York, N.Y.) 288(5464), 306–313. 10.1126/science.288.5464.306.

124. Quartu M, Serra MP, Boi M, Poddighe L, Picci C, Demontis R, Del Fiacco M (2016) TRPV1 receptor in the human trigeminal ganglion and spinal nucleus: immunohistochemical localization and comparison with the neuropeptides CGRP and SP. Journal of anatomy 229(6), 755–767. 10.1111/joa.12529.

125. Omari SA, Adams MJ, Geraghty DP (2017) TRPV1 Channels in Immune Cells and Hematological Malignancies. Advances in pharmacology (San Diego, Calif.) 79, 173–198. 10.1016/bs.apha.2017.01.002.

126. Weihrauch T, Gray N, Wiebe D, Schmelz M, Limberg MM, Raap U (2024) TRPV1 Channel in Human Eosinophils: Functional Expression and Inflammatory Modulation. International journal of molecular sciences 25(3). 10.3390/ijms25031922.

127. Limberg MM, Wiebe D, Gray N, Weihrauch T, Bräuer AU, Kremer AE, Homey B, Raap U (2024) Functional expression of TRPV1 in human peripheral blood basophils and its regulation in atopic dermatitis. Allergy 79(1), 225–228. 10.1111/all.15802.

128. Gao N, Li M, Wang W, Liu Z, Guo Y (2024) The dual role of TRPV1 in peripheral neuropathic pain: pain switches caused by its sensitization or desensitization. Frontiers in molecular neuroscience 17, 1400118. 10.3389/fnmol.2024.1400118.

129. Willis WD (2009) The role of TRPV1 receptors in pain evoked by noxious thermal and chemical stimuli. Experimental brain research 196(1), 5–11. 10.1007/s00221-009-1760-2.

130. Qu Y, Fu Y, Liu Y, Liu C, Xu B, Zhang Q, Jiang P (2023) The role of TRPV1 in RA pathogenesis: worthy of attention. Frontiers in immunology 14, 1232013. 10.3389/fimmu.2023.1232013.

131. Csekő K, Beckers B, Keszthelyi D, Helyes Z (2019) Role of TRPV1 and TRPA1 Ion Channels in Inflammatory Bowel Diseases: Potential Therapeutic Targets? Pharmaceuticals (Basel, Switzerland) 12(2). 10.3390/ph12020048.

132. Yu G, Yang N, Li F, Chen M, Guo CJ, Wang C, Hu D, Yang Y, Zhu C, Wang Z, Shi H, Gegen T, Tang M, He Q, Liu Q, Tang Z (2016) Enhanced itch elicited by capsaicin in a chronic itch model. Molecular pain 12. 10.1177/1744806916645349.

133. Shim W-S, Tak M-H, Lee M-H, Kim M, Kim M, Koo J-Y, Lee C-H, Kim M, Oh U (2007) TRPV1 mediates histamine-induced itching via the activation of phospholipase A2 and 12-lipoxygenase. The Journal of neuroscience the official journal of the Society for Neuroscience 27(9), 2331–2337. 10.1523/JNEUROSCI.4643-06.2007.

134. Lee S, Lim NY, Kang MS, Jeong Y, Ahn J-O, Choi JH, Chung J-Y (2023) IL-31RA and TRPV1 Expression in Atopic Dermatitis Induced with Trinitrochlorobenzene in Nc/Nga Mice. International journal of molecular sciences 24(17). 10.3390/ijms241713521.

135. Park CW, Kim BJ, Lee YW, Won C, Park CO, Chung BY, Lee DH, Jung K, Nam H-J, Choi G, Park Y-H, Kim KH, Park M (2022) Asivatrep, a TRPV1 antagonist, for the topical treatment of atopic dermatitis: Phase 3, randomized, vehicle-controlled study (CAPTAIN-AD). The Journal of allergy and clinical immunology 149(4), 1340-1347.e4. 10.1016/j.jaci.2021.09.024.

136. Yun J-W, Seo JA, Jeong YS, Bae I-H, Jang W-H, Lee J, Kim S-Y, Shin S-S, Woo B-Y, Lee K-W, Lim K-M, Park Y-H (2011) TRPV1 antagonist can suppress the atopic dermatitis-like symptoms by accelerating skin barrier recovery. Journal of dermatological science 62(1), 8–15. 10.1016/j.jdermsci.2010.10.014.

137. Alsabbagh M, Ismaeel A (2022) The role of cytokines in atopic dermatitis: a breakthrough in immunopathogenesis and treatment. Acta Dermatovenerologica Alpina Pannonica et Adriatica 31(1). 10.15570/actaapa.2022.3.

138. Raap U, Weißmantel S, Gehring M, Eisenberg AM, Kapp A, Fölster-Holst R (2012) IL-31 significantly correlates with disease activity and Th2 cytokine levels in children with atopic dermatitis. Pediatric allergy and immunology official publication of the European Society of Pediatric Allergy and Immunology 23(3), 285–288. 10.1111/j.1399-3038.2011.01241.x.

139. Raap U, Wichmann K, Bruder M, Ständer S, Wedi B, Kapp A, Werfel T (2008) Correlation of IL-31 serum levels with severity of atopic dermatitis. The Journal of allergy and clinical immunology 122(2), 421–423. 10.1016/j.jaci.2008.05.047.

140. Luo J, Zhu Z, Zhai Y, Zeng J, Li L, Di Wang, Deng F, Chang B, Zhou J, Sun L (2023) The Role of TSLP in Atopic Dermatitis: From Pathogenetic Molecule to Therapeutical Target. Mediators of inflammation 2023, 7697699. 10.1155/2023/7697699.

141. Hodeib A, El-Samad ZA, Hanafy H, El-Latief AA, El-Bendary A, Abu-Raya A (2010) Nerve growth factor, neuropeptides and cutaneous nerves in atopic dermatitis. Indian journal of dermatology 55(2), 135–139. 10.4103/0019-5154.62735.

142. Fölster-Holst R, Papakonstantinou E, Rüdrich U, Buchner M, Pite H, Gehring M, Kapp A, Weidinger S, Raap U (2016) Childhood atopic dermatitis-Brain-derived neurotrophic factor correlates with serum eosinophil cationic protein and disease severity. Allergy 71(7), 1062–1065. 10.1111/all.12916.

143. Nicholls C, Li H, Liu J-P (2012) GAPDH: a common enzyme with uncommon functions. Clinical and experimental pharmacology & physiology 39(8), 674–679. 10.1111/j.1440-1681.2011.05599.x.

144. Gee KR, Brown KA, Chen WN, Bishop-Stewart J, Gray D, Johnson I (2000) Chemical and physiological characterization of fluo-4 Ca(2+)-indicator dyes. Cell calcium 27(2), 97–106. 10.1054/ceca.1999.0095.

145. Lautens M, Colucci JT, Hiebert S, Smith ND, Bouchain G (2002) Total synthesis of ionomycin using ring-opening strategies. Organic letters 4(11), 1879–1882. 10.1021/ol025872f.

146. Lakshmanan I, Batra SK (2013) Protocol for Apoptosis Assay by Flow Cytometry Using Annexin V Staining Method. Bio-protocol 3(6). 10.21769/bioprotoc.374.

147. Riccardi C, Nicoletti I (2006) Analysis of apoptosis by propidium iodide staining and flow cytometry. Nature protocols 1(3), 1458–1461. 10.1038/nprot.2006.238.

148. Gray N, Limberg MM, Wiebe D, Weihrauch T, Langner A, Brandt N, Bräuer AU, Raap U (2022) Differential Upregulation and Functional Activity of S1PR1 in Human Peripheral Blood Basophils of Atopic Patients. International journal of molecular sciences 23(24). 10.3390/ijms232416117.

149. Lang G (2006) Histotechnik: Praxislehrbuch für die Biomedizinische Analytik, 1st edn. Vienna: Springer-Verlag; Imprint: Springer.

150. Kao JPY, Li G, Auston DA (2010) Practical aspects of measuring intracellular calcium signals with fluorescent indicators. Methods in cell biology 99, 113–152. 10.1016/B978-0-12-374841-6.00005-0.

151. Knol EF, Mul FP, Jansen H, Calafat J, Roos D (1991) Monitoring human basophil activation via CD63 monoclonal antibody 435. Journal of Allergy and Clinical Immunology 88(3 Pt 1), 328–338. 10.1016/0091-6749(91)90094-5.

152. Manosalva C, Quiroga J, Hidalgo AI, Alarcón P, Anseoleaga N, Hidalgo MA, Burgos RA (2021) Role of Lactate in Inflammatory Processes: Friend or Foe. Frontiers in immunology 12, 808799. 10.3389/fimmu.2021.808799.

153. Chanmugam A, Langemo D, Thomason K, Haan J, Altenburger EA, Tippett A, Henderson L, Zortman TA (2017) Relative Temperature Maximum in Wound Infection and Inflammation as Compared with a Control Subject Using Long-Wave Infrared Thermography. Advances in skin & wound care 30(9), 406–414. 10.1097/01.ASW.0000522161.13573.62.

154. Wang YY, Chang RB, Liman ER (2010) TRPA1 is a component of the nociceptive response to CO2. The Journal of neuroscience the official journal of the Society for Neuroscience 30(39), 12958–12963. 10.1523/JNEUROSCI.2715-10.2010.

155. Sarkar R, Choudhury SM, Kanneganti T-D (2024) Classical apoptotic stimulus, staurosporine, induces lytic inflammatory cell death, PANoptosis. The Journal of biological chemistry 300(9), 107676. 10.1016/j.jbc.2024.107676.

156. Wedi B, Raap U, Lewrick H, Kapp A (1997) Delayed eosinophil programmed cell death in vitro: a common feature of inhalant allergy and extrinsic and intrinsic atopic dermatitis. Journal of Allergy and Clinical Immunology 100(4), 536–543. 10.1016/S0091-6749(97)70147-7.

157. Afferni C, Buccione C, Andreone S, Galdiero MR, Varricchi G, Marone G, Mattei F, Schiavoni G (2018) The Pleiotropic Immunomodulatory Functions of IL-33 and Its Implications in Tumor Immunity. Frontiers in immunology 9, 2601. 10.3389/fimmu.2018.02601.

158. Bertin S, Aoki-Nonaka Y, Jong PR de, Nohara LL, Xu H, Stanwood SR, Srikanth S, Lee J, To K, Abramson L, Yu T, Han T, Touma R, Li X, González-Navajas JM, Herdman S, Corr M, Fu G, Dong H, Gwack Y, Franco A, Jefferies WA, Raz E (2014) The ion channel TRPV1 regulates the activation and proinflammatory properties of $CD4^+$ T cells. Nature immunology 15(11), 1055–1063. 10.1038/ni.3009.

159. Tóth E, Tornóczky T, Kneif J, Perkecz A, Katona K, Piski Z, Kemény Á, Gerlinger I, Szolcsányi J, Kun J, Pintér E (2018) Upregulation of extraneuronal TRPV1 expression in chronic rhinosinusitis with nasal polyps. Rhinology 56(3), 245–254. 10.4193/Rhin17.108.

160. Matsubara M, Muraki Y, Hatano N, Suzuki H, Muraki K (2022) Potent Activation of Human but Not Mouse TRPA1 by JT010. International journal of molecular sciences 23(22). 10.3390/ijms232214297.

161. Szabó K, Makkai G, Konkoly J, Kormos V, Gaszner B, Berki T, Pintér E (2024) TRPA1 Covalent Ligand JT010 Modifies T Lymphocyte Activation. Biomolecules 14(6). 10.3390/biom14060632.

162. Redrup AC, Howard BP, MacGlashan DW, Kagey-Sobotka A, Lichtenstein LM, Schroeder JT (1998) Differential regulation of IL-4 and IL-13 secretion by human basophils: their relationship to histamine release in mixed leukocyte cultures. Journal of immunology (Baltimore, Md. 1950) 160(4), 1957–1964.

163. Napolitano M, Di Vico F, Ruggiero A, Fabbrocini G, Patruno C (2023) The hidden sentinel of the skin: An overview on the role of interleukin-13 in atopic dermatitis. Frontiers in medicine 10, 1165098. 10.3389/fmed.2023.1165098.

164. Dou Y-C, Hagströmer L, Emtestam L, Johansson O (2006) Increased nerve growth factor and its receptors in atopic dermatitis: an immunohistochemical study. Archives of dermatological research 298(1), 31–37. 10.1007/s00403-006-0657-1.

165. Toyoda M, Nakamura M, Makino T, Hino T, Kagoura M, Morohashi M (2002) Nerve growth factor and substance P are useful plasma markers of disease activity in atopic dermatitis. The British journal of dermatology 147(1), 71–79. 10.1046/j.1365-2133.2002.04803.x.

166. Dillon SR, Sprecher C, Hammond A, Bilsborough J, Rosenfeld-Franklin M, Presnell SR, Haugen HS, Maurer M, Harder B, Johnston J, Bort S, Mudri S, Kuijper JL, Bukowski T, Shea P, Dong DL, Dasovich M, Grant FJ, Lockwood L, Levin SD, LeCiel C, Waggie K, Day H, Topouzis S, Kramer J, Kuestner R, Chen Z, Foster D, Parrish-Novak J, Gross JA (2004) Interleukin 31, a cytokine produced by activated T cells, induces dermatitis in mice. Nature immunology 5(7), 752–760. 10.1038/ni1084.

167. Sonkoly E, Muller A, Lauerma AI, Pivarcsi A, Soto H, Kemeny L, Alenius H, Dieu-Nosjean M-C, Meller S, Rieker J, Steinhoff M, Hoffmann TK, Ruzicka T, Zlotnik A, Homey B (2006) IL-31: a new link between T cells and pruritus in atopic skin inflammation. Journal of Allergy and Clinical Immunology 117(2), 411–417. 10.1016/j.jaci.2005.10.033.

168. Savinko T, Matikainen S, Saarialho-Kere U, Lehto M, Wang G, Lehtimäki S, Karisola P, Reunala T, Wolff H, Lauerma A, Alenius H (2012) IL-33 and ST2 in atopic dermatitis: expression profiles and modulation by triggering factors. The Journal of investigative dermatology 132(5), 1392–1400. 10.1038/jid.2011.446.

169. Chen Z, Luo J, Li J, Kim G, Stewart A, Urban JF, Huang Y, Chen S, Wu L-G, Chesler A, Trinchieri G, Li W, Wu C (2021) Interleukin-33 Promotes Serotonin Release from Enterochromaffin Cells for Intestinal Homeostasis. Immunity 54(1), 151-163.e6. 10.1016/j.immuni.2020.10.014.

170. Jariwala SP, Abrams E, Benson A, Fodeman J, Zheng T (2011) The role of thymic stromal lymphopoietin in the immunopathogenesis of atopic dermatitis. Clinical and experimental allergy journal of the British Society for Allergy and Clinical Immunology 41(11), 1515–1520. 10.1111/j.1365-2222.2011.03797.x.

171. Wilson SR, Thé L, Batia LM, Beattie K, Katibah GE, McClain SP, Pellegrino M, Estandian DM, Bautista DM (2013) The epithelial cell-derived atopic dermatitis cytokine TSLP activates neurons to induce itch. Cell 155(2), 285–295. 10.1016/j.cell.2013.08.057.

172. Raap U, Goltz C, Deneka N, Bruder M, Renz H, Kapp A, Wedi B (2005) Brain-derived neurotrophic factor is increased in atopic dermatitis and modulates eosinophil functions compared with that seen in nonatopic subjects. Journal of Allergy and Clinical Immunology 115(6), 1268–1275. 10.1016/j.jaci.2005.02.007.

173. Ciobanu C, Reid G, Babes A (2009) Acute and chronic effects of neurotrophic factors BDNF and GDNF on responses mediated by thermo-sensitive TRP channels in cultured rat dorsal root ganglion neurons. Brain research 1284, 54–67. 10.1016/j.brainres.2009.06.014.

174. Jang D-I, Lee A-H, Shin H-Y, Song H-R, Park J-H, Kang T-B, Lee S-R, Yang S-H (2021) The Role of Tumor Necrosis Factor Alpha (TNF-α) in Autoimmune Disease and Current TNF-α Inhibitors in Therapeutics. International journal of molecular sciences 22(5). 10.3390/ijms22052719.

175. Junghans V, Gutgesell C, Jung T, Neumann C (1998) Epidermal cytokines IL-1beta, TNF-alpha, and IL-12 in patients with atopic dermatitis: response to application of house dust mite antigens. The Journal of investigative dermatology 111(6), 1184–1188. 10.1046/j.1523-1747.1998.00409.x.

176. Meng J, Wang J, Steinhoff M, Dolly JO (2016) TNFα induces co-trafficking of TRPV1/TRPA1 in VAMP1-containing vesicles to the plasmalemma via Munc18-1/syntaxin1/SNAP-25 mediated fusion. Scientific reports 6, 21226. 10.1038/srep21226.

177. Xie Y, Takai T, Chen X, Okumura K, Ogawa H (2012) Long TSLP transcript expression and release of TSLP induced by TLR ligands and cytokines in human keratinocytes. Journal of dermatological science 66(3), 233–237. 10.1016/j.jdermsci.2012.03.007.

178. Del Bene VE (1990) Clinical Methods: The History, Physical, and Laboratory Examinations: Temperature, 3rd edn. Boston.

179. Faris P, Rumolo A, Pellavio G, Tanzi M, Vismara M, Berra-Romani R, Gerbino A, Corallo S, Pedrazzoli P, Laforenza U, Montagna D, Moccia F (2023) Transient receptor

potential ankyrin 1 (TRPA1) mediates reactive oxygen species-induced Ca2+ entry, mitochondrial dysfunction, and caspase-3/7 activation in primary cultures of metastatic colorectal carcinoma cells. Cell death discovery 9(1), 213. 10.1038/s41420-023-01530-x.

180. Stueber T, Eberhardt MJ, Caspi Y, Lev S, Binshtok A, Leffler A (2017) Differential cytotoxicity and intracellular calcium-signalling following activation of the calcium-permeable ion channels TRPV1 and TRPA1. Cell calcium 68, 34–44. 10.1016/j.ceca.2017.10.003.

181. Virk HS, Biddle MS, Smallwood DT, Weston CA, Castells E, Bowman VW, McCarthy J, Amrani Y, Duffy SM, Bradding P, Roach KM (2021) TGFβ1 induces resistance of human lung myofibroblasts to cell death via down-regulation of TRPA1 channels. British journal of pharmacology 178(15), 2948–2962. 10.1111/bph.15467.

182. Lowin T, Bleck J, Schneider M, Pongratz G (2018) Selective killing of proinflammatory synovial fibroblasts via activation of transient receptor potential ankyrin (TRPA1). Biochemical pharmacology 154, 293–302. 10.1016/j.bcp.2018.05.015.

183. James JM, Kagey-Sobotka A, Sampson HA (1993) Patients with severe atopic dermatitis have activated circulating basophils. Journal of Allergy and Clinical Immunology 91(6), 1155–1162. 10.1016/0091-6749(93)90318-a.

184. Kobayashi K, Fukuoka T, Obata K, Yamanaka H, Dai Y, Tokunaga A, Noguchi K (2005) Distinct expression of TRPM8, TRPA1, and TRPV1 mRNAs in rat primary afferent neurons with adelta/c-fibers and colocalization with trk receptors. The Journal of comparative neurology 493(4), 596–606. 10.1002/cne.20794.

185. Diogenes A, Akopian AN, Hargreaves KM (2007) NGF up-regulates TRPA1: implications for orofacial pain. Journal of dental research 86(6), 550–555. 10.1177/154405910708600612.

186. Andrei SR, Sinharoy P, Bratz IN, Damron DS (2016) TRPA1 is functionally co-expressed with TRPV1 in cardiac muscle: Co-localization at z-discs, costameres and intercalated discs. Channels (Austin, Tex.) 10(5), 395–409. 10.1080/19336950.2016.1185579.

187. Fernandes ES, Fernandes MA, Keeble JE (2012) The functions of TRPA1 and TRPV1: moving away from sensory nerves. British journal of pharmacology 166(2), 510–521. 10.1111/j.1476-5381.2012.01851.x.

188. Zhang P, Luo Y, Chasan B, González-Perrett S, Montalbetti N, Timpanaro GA, Del Cantero MR, Ramos AJ, Goldmann WH, Zhou J, Cantiello HF (2009) The multimeric structure of polycystin-2 (TRPP2): structural-functional correlates of homo- and hetero-multimers with TRPC1. Human molecular genetics 18(7), 1238–1251. 10.1093/hmg/ddp024.

189. Kobori T, Smith GD, Sandford R, Edwardson JM (2009) The transient receptor potential channels TRPP2 and TRPC1 form a heterotetramer with a 2:2 stoichiometry and an alternating subunit arrangement. The Journal of biological chemistry 284(51), 35507–35513. 10.1074/jbc.M109.060228.

190. Stewart AP, Smith GD, Sandford RN, Edwardson JM (2010) Atomic force microscopy reveals the alternating subunit arrangement of the TRPP2-TRPV4 heterotetramer. Biophysical journal 99(3), 790–797. 10.1016/j.bpj.2010.05.012.

191. Poteser M, Graziani A, Rosker C, Eder P, Derler I, Kahr H, Zhu MX, Romanin C, Groschner K (2006) TRPC3 and TRPC4 associate to form a redox-sensitive cation channel. Evidence for expression of native TRPC3-TRPC4 heteromeric channels in endothelial cells. The Journal of biological chemistry 281(19), 13588–13595. 10.1074/jbc.M512205200.

192. Li M, Jiang J, Yue L (2006) Functional characterization of homo- and heteromeric channel kinases TRPM6 and TRPM7. The Journal of general physiology 127(5), 525–537. 10.1085/jgp.200609502.

193. Liu X, Bandyopadhyay BC, Singh BB, Groschner K, Ambudkar IS (2005) Molecular analysis of a store-operated and 2-acetyl-sn-glycerol-sensitive non-selective cation channel. Heteromeric assembly of TRPC1-TRPC3. The Journal of biological chemistry 280(22), 21600–21606. 10.1074/jbc.C400492200.

194. Strübing C, Krapivinsky G, Krapivinsky L, Clapham DE (2001) TRPC1 and TRPC5 form a novel cation channel in mammalian brain. Neuron 29(3), 645–655. 10.1016/S0896-6273(01)00240-9.

195. Fischer MJM, Balasuriya D, Jeggle P, Goetze TA, McNaughton PA, Reeh PW, Edwardson JM (2014) Direct evidence for functional TRPV1/TRPA1 heteromers. Pflugers Archiv European journal of physiology 466(12), 2229–2241. 10.1007/s00424-014-1497-z.

196. Liu B, Tai Y, Achanta S, Kaelberer MM, Caceres AI, Shao X, Fang J, Jordt S-E (2016) IL-33/ST2 signaling excites sensory neurons and mediates itch response in a mouse model of poison ivy contact allergy. Proceedings of the National Academy of Sciences of the United States of America 113(47), E7572-E7579. 10.1073/pnas.1606608113.

197. Sticco KL, Pandya NK, Zubair M, Lynch DT (2025) StatPearls: Basophilia. Treasure Island (FL).

198. Schroeder JT, Bieneman AP (2016) Isolation of Human Basophils. Current protocols in immunology 112, 7.24.1-7.24.8. 10.1002/0471142735.im0724s112.

199. Liu T, Ji R-R (2012) Oxidative stress induces itch via activation of transient receptor potential subtype ankyrin 1 in mice. Neuroscience bulletin 28(2), 145–154. 10.1007/s12264-012-1207-9.

Appendix

Supplementary Tables

Supplementary Table 1: Summary of unpaired Student's t-test results for the data shown in **Figure 7A**.

Unpaired Student's t-test	Number of samples [n]	Summary	p-values
NA vs. AD	NA: 4, AD: 6	*	0.0347

Supplementary Table 2: Summary of unpaired Student's t-test results for the data shown in **Figure 7C**.

Unpaired Student's t-test	Number of samples [n]	Summary	p-values
NA vs. AD	NA: 8, AD: 7	**	0.0073

Supplementary Table 3: Summary of unpaired Student's t-test results for the data shown in **Figure 7D**. n.s.: not significant

Unpaired Student's t-test	Number of samples [n]	Summary	p-values
NA vs. AD	NA: 8, AD: 7	n.s.	0.1643

Supplementary Table 4: Summary of one-way ANOVA followed by Dunnett's post-hoc test for the data shown in **Figure 8E**. n.s.: not significant

One-way ANOVA	Number of samples [n]	Summary	p-values
Co vs. 10 nM JT010	4	n.s.	0.1791
Co vs. 100 nM JT010	4	*	0.0128
Co vs. 1000 nM JT010	4	***	0.0003

Supplementary Table 5: Summary of one-way ANOVA followed by Dunnett's post-hoc test for the data shown in **Figure 9A**. n.s.: not significant

One-way ANOVA	Number of samples [n]	Summary	p-values
Co vs. fMLP	4	n.s.	0.09
Co vs. a-IgE	4	***	<0.001
Co vs. 10 nM JT010	4	n.s.	>0.99
Co vs. 100 nM JT010	4	n.s.	>0.99
Co vs. 1000 nM JT010	4	n.s.	>0.99

Supplementary Table 6: Summary of one-way ANOVA followed by Dunnett's post-hoc test for the data shown in **Figure 9B**. n.s.: not significant

One-way ANOVA	Number of samples [n]	Summary	p-values
Co vs. fMLP	4	***	<0.001
Co vs. a-IgE	4	***	<0.001
Co vs. 10 nM JT010	4	n.s.	0.74
Co vs. 100 nM JT010	4	n.s.	0.68
Co vs. 1000 nM JT010	4	n.s.	0.70

Supplementary Table 7: Summary of paired Student's t-test results for the data shown in **Figure 10A**.

Paired Student's t-test	Number of samples [n]	Summary	p-values
Co vs. IL-31	4	*	0.0147

Supplementary Table 8: Summary of paired Student's t-test results for the data shown in **Figure 10B**.

Paired Student's t-test	Number of samples [n]	Summary	p-values
Co vs. IL-31	5	*	0.0329

Supplementary Table 9: Summary of paired Student's t-test results for the data shown in **Figure 10C**. n.s.: not significant

Paired Student's t-test	Number of samples [n]	Summary	p-values
Co vs. IL-31	5	n.s.	0.93

Supplementary Table 10: Summary of one-way ANOVA followed by Dunnett's post-hoc test for the data shown in **Figure 11A**. n.s.: not significant

One-way ANOVA	Number of samples [n]	Summary	p-values
Co vs. IL-3	3	***	<0.0001
Co vs. IL-13	3	n.s.	>0.9999
Co vs. IL-31	3	n.s.	0.9974
Co vs. IL-33	3	n.s.	0.4193
Co vs. TSLP	3	n.s.	0.9970
Co vs. NGFβ	3	**	0.0061
Co vs. BDNF	3	n.s.	0.9998
Co vs. TNF-α	3	n.s.	0.9994

Supplementary Table 11: Summary of one-way ANOVA followed by Dunnett's post-hoc test for the data shown in **Figure 11B**. n.s.: not significant

One-way ANOVA	Number of samples [n]	Summary	p-values
Co vs. IL-3	3	***	<0.0001
Co vs. IL-13	3	n.s.	0.9996
Co vs. IL-31	3	n.s.	0.9686
Co vs. IL-33	3	n.s.	0.9446
Co vs. TSLP	3	n.s.	0.9781
Co vs. NGFβ	3	n.s.	0.1055
Co vs. BDNF	3	n.s.	0.5139
Co vs. TNF-α	3	n.s.	0.8185

Supplementary Table 12: Summary of one-way ANOVA followed by Dunnett's post-hoc test for the data shown in **Figure 12A, left**. n.s.: not significant

One-way ANOVA	Number of samples [n]	Summary	p-values
Co 7.0 vs. 6.5	4	n.s.	0.0967
Co 7.0 vs. 5.0	4	**	0.0011

Supplementary Table 13: Summary of one-way ANOVA followed by Dunnett's post-hoc test for the data shown in **Figure 12A, right**. n.s.: not significant

One-way ANOVA	Number of samples [n]	Summary	p-values
Co 7.0 vs. 6.5	4	n.s.	0.3294
Co 7.0 vs. 5.0	4	*	0.0129

Supplementary Table 14: Summary of paired Student's t-test results for the data shown in **Figure 12B, left**. n.s.: not significant

Paired Student's t-test	Number of samples [n]	Summary	p-values
37°C vs. 40°C	3	n.s.	0.4382

Supplementary Table 15: Summary of paired Student's t-test results for the data shown in **Figure 12B, right**.

Paired Student's t-test	Number of samples [n]	Summary	p-values
37°C vs. 40°C	3	*	0.0263

Supplementary Table 16: Summary of one-way ANOVA followed by Dunnett's post-hoc test for the data shown in **Figure 13B**. n.s.: not significant

One-way ANOVA	Number of samples [n]	Summary	p-values
Co vs. Stauro	3	*	0.0362
Co vs. 10 nM JT010	3	n.s.	>0.9999
Co vs. 100 nM JT010	3	n.s.	0.9999
Co vs. 1000 nM JT010	3	n.s.	>0.9999

Supplementary Table 17: Summary of one-way ANOVA followed by Dunnett's post-hoc test for the data shown in **Figure 13C**. n.s.: not significant

One-way ANOVA	Number of samples [n]	Summary	p-values
Co vs. Stauro	3	*	0.0366
Co vs. 10 nM JT010	3	n.s.	>0.9999
Co vs. 100 nM JT010	3	n.s.	>0.9999
Co vs. 1000 nM JT010	3	n.s.	>0.9999

Supplementary Table 18: Summary of one-way ANOVA followed by Dunnett's post-hoc test for the data shown in **Figure 14B**. n.s.: not significant

One-way ANOVA	Number of samples [n]	Summary	p-values
Co vs. Stauro	4	***	0.0006
Co vs. 10 nM JT010	4	n.s.	0.6765
Co vs. 100 nM JT010	4	n.s.	0.9901
Co vs. 1000 nM JT010	4	n.s.	0.9764

Supplementary Table 19: Summary of one-way ANOVA followed by Dunnett's post-hoc test for the data shown in **Figure 14C**. n.s.: not significant

One-way ANOVA	Number of samples [n]	Summary	p-values
Co vs. Stauro	4	***	<0.0001
Co vs. 10 nM JT010	4	n.s.	>0.9999
Co vs. 100 nM JT010	4	n.s.	0.9144
Co vs. 1000 nM JT010	4	n.s.	0.8633

Supplementary Table 20: Summary of one-way ANOVA followed by Dunnett's post-hoc test for the data shown in **Figure 15B**. n.s.: not significant

One-way ANOVA	Number of samples [n]	Summary	p-values
Co vs. Stauro	3	***	0.0003
Co vs. 10 nM JT010	3	n.s.	0.9374
Co vs. 100 nM JT010	3	n.s.	0.6605
Co vs. 1000 nM JT010	3	n.s.	0.9004

Supplementary Table 21: Summary of one-way ANOVA followed by Dunnett's post-hoc test for the data shown in **Figure 15C**. n.s.: not significant

One-way ANOVA	Number of samples [n]	Summary	p-values
Co vs. Stauro	3	***	0.0005
Co vs. 10 nM JT010	3	n.s.	0.9801
Co vs. 100 nM JT010	3	n.s.	0.7868
Co vs. 1000 nM JT010	3	n.s.	0.9698

Supplementary Table 22: Summary of unpaired Student's t-test results for the data shown in **Figure 18C**. n.s.: not significant

Unpaired Student's t-test	Number of samples [n]	Summary	p-values
NA vs. AD	NA: 20, AD: 8	n.s.	0.3131

Supplementary Table 23: Summary of two-way ANOVA mixed-effects analysis followed by Šídák's post-hoc test for the data shown in **Figure 19A**. n.s.: not significant

Two-way ANOVA mixed-effects analysis	**Number of samples [n]**	**Summary**	**p-values**
TRPV1	NA: 20, AD: 8	n.s.	>0.9999
TRPA1	NA: 20, AD: 8	n.s.	0.9528
TRPA1/TRPV1	NA: 20, AD: 8	n.s.	0.5798
Double neg	NA: 20, AD: 8	n.s.	0.9182

Supplementary Table 24: Summary of one-way ANOVA followed by Dunnett's post-hoc test for the data shown in **Figure 20A**. n.s.: not significant

One-way ANOVA	**Number of samples [n]**	**Summary**	**p-values**
Co vs. IL-3	3	***	<0.0001
Co vs. IL-13	3	n.s.	0.9877
Co vs. IL-31	3	n.s.	0.5314
Co vs. IL-33	3	*	0.0167
Co vs. TSLP	3	n.s.	0.6618
Co vs. NGFβ	3	***	0.0002
Co vs. BDNF	3	n.s.	0.2537
Co vs. TNF-α	3	n.s.	0.1301

Supplementary Table 25: Summary of one-way ANOVA followed by Dunnett's post-hoc test for the data shown in **Figure 21A**. n.s.: not significant

One-way ANOVA	**Number of samples [n]**	**Summary**	**p-values**
Co 7.0 vs. 6.5	4	n.s.	0.4487
Co 7.0 vs. 5.0	4	**	0.0015

Supplementary Table 26: Summary of paired Student's t-test results for the data shown in **Figure 21B**. n.s.: not significant

Paired Student's t-test	Number of samples [n]	Summary	p-values
37°C vs. 40°C	3	n.s.	0.2520

Eigenständigkeitserklärung

Hiermit versichere ich, dass ich die vorgelegte Dissertation selbst und ohne unerlaubte Hilfe angefertigt, alle in Anspruch genommenen Quellen und Hilfsmittel in der Dissertation angegeben habe und die Dissertation nicht bereits anderweitig als Prüfungsarbeit vorgelegen hat.

Künstliche Intelligenz in Form von ChatGPT, Perplexity, DeepL und QuillBot wurde verwendet, um die Grammatik zu korrigieren, die Gliederung der Einleitung zu erstellen, Literatur zu recherchieren, bei Übersetzungen zu unterstützen und die Arbeit auf Plagiate zu überprüfen.

Die Dissertation wurde weder in Teilen noch insgesamt bereits veröffentlicht oder bei einer anderen Hochschule zur Begutachtung in einem Promotionsverfahren vorgelegt. Die Leitlinien guter wissenschaftlicher Praxis der Carl von Ossietzky Universität Oldenburg sind befolgt worden.

Im Zusammenhang mit dem Promotionsverfahren sind keine kommerziellen Vermittlungs- oder Beratungsdienste (Promotionsberatung) in Anspruch genommen worden.

Oldenburg, …… …….

(Unterschrift)

Curriculum Vitae

Daniela Wiebe

Date of birth: 29th May 1992 E-Mail: daniela.wiebe@uni-oldenburg.de

Education

- Since 2021: Division of Experimental Allergy and Immunodermatology, Carl von Ossietzky University Oldenburg, Oldenburg, Germany – PhD Student
    - Prof: Univ.-Prof. Dr. med. habil. Ulrike Raap
- 2018 – 2021: Goethe University Frankfurt, Germany – Master degree
    - Thesis title: Relevance of STAT3 for the epithelial intestinal barrier in ACLF cell culture model
- 2011 – 2018: University Bielefeld – Bachelor degree
    - Thesis title: Coproduction of carotenoids and amino acids with metabolically engineered *Corynebacterium glutamicum*

Conferences, seminars and poster presentations

- DFG Research group meeting September, Münster (2024)
- 12th World Congress on Itch, Miami, USA (2023)
- DFG Research group meeting September, Münster (2023)
- DFG Research group meeting March, online (2022)
- DFG Research group meeting September, Münster (2022)
- Research Day University of Oldenburg – Poster presentation (2022)

Membership

- Young Scientists FOR 2690 PruSearch DFG

Coachings

- MOMENTUM Women's Leadership Journey – DFG (2023)
- Female awareness – Effectively counter misogynous behavioral patterns – Martina Schmidt-Tanger (2022)
- Introduction to leadership communication – Martina Schmidt-Tanger (2021)

Grant

- IFSI Travel Grant for the World Congress on Itch in Miami (2023)

Publications

- Weihrauch T, Gray N, **Wiebe D**, Schmelz M, Limberg MM, Raap U (2024) TRPV1 Channel in Human Eosinophils: Functional Expression and Inflammatory Modulation. International journal of molecular sciences 25(3). 10.3390/ijms25031922.

- Gray N, **Wiebe D**, Weihrauch T, Raap U, Limberg MM (2024) Density Gradient Centrifugation-Independent Purification of Human Basophils. Current protocols 4(2), e991. 10.1002/cpz1.991.

- Limberg MM, **Wiebe D**, Gray N, Weihrauch T, Bräuer AU, Kremer AE, Homey B, Raap U (2023) Functional expression of TRPV1 in human peripheral blood basophils and its regulation in atopic dermatitis. Allergy. 10.1111/all.15802.

- **Wiebe D**, Limberg MM, Gray N, Raap U (2023) Basophils in pruritic skin diseases. Front. Immunol. 14. 10.3389/fimmu.2023.1213138

- Gray N, Limberg MM, **Wiebe D**, Weihrauch T, Langner A, Brandt N, Bräuer AU, Raap U (2022) Differential Upregulation and Functional Activity of S1PR1 in Human Peripheral Blood Basophils of Atopic Patients. International journal of molecular sciences 23(24). 10.3390/ijms232416117.

- Henke NA, **Wiebe D**, Pérez-García F, Peters-Wendisch P, Wendisch VF (2018) Coproduction of cell-bound and secreted value-added compounds: Simultaneous production of carotenoids and amino acids by *Corynebacterium glutamicum*. Bioresource technology 247, 744–752. 10.1016/j.biortech.2017.09.167.

Danksagung

An dieser Stelle möchte ich mich herzlich bei allen bedanken, die mich während der Entstehung dieser Dissertation unterstützt haben.

Mein besonderer Dank gilt meiner Erstbetreuerin, Prof. Dr. Ulrike Raap, die mich in dieser Zeit mit großem Engagement begleitet und stets unterstützt hat. Ihre fachliche Expertise, ihre motivierenden Worte und ihr Vertrauen in meine Arbeit haben maßgeblich zum Gelingen dieser Dissertation beigetragen.

Ebenso danke ich meiner Zweitbetreuerin, Prof. Dr. Anja Bräuer, für ihre Unterstützung. Ich schätze die konstruktiven Diskussionen und die hilfreichen Besprechungen der Ergebnisse während der Promotionskomitee Meetings, die mir neue Impulse gegeben haben.

Ein weiterer Dank gilt dem Forschungspool der Universität Oldenburg, der diese Arbeit durch finanzielle Förderung unterstützt hat. Die bereitgestellten Mittel haben einen wichtigen Beitrag zur Realisierung des Projekts geleistet und die Durchführung der Forschungsarbeiten maßgeblich ermöglicht.

Ein großes Dankeschön gilt auch meinen Kolleg:innen, Alexandra Marten, Natalie Gray und Tobias Weihrauch. Ich bin sehr dankbar für die fachlichen Diskussionen, die hilfreiche Unterstützung bei der Auswertung der Ergebnisse und dafür, dass sie mir besonders in schwierigen Zeiten Rückhalt gegeben haben. Ohne euch hätte ich diese Arbeit nicht bewältigen können. Vielen Dank an Silvia Ellinghaus, für ihre überragende Organisation, wodurch sie einiges ermöglicht und auch erleichtert hat, und auch für die Gespräche zwischendurch, die die Situation immer wieder aufgelockert haben.

Ein besonderer Dank gilt auch dem Team aus dem Klinikum, das mit großem Einsatz und Engagement die Proben gesammelt hat. Durch eure Arbeit habt ihr einen wesentlichen Beitrag zum Gelingen dieser Dissertation geleistet. Ohne eure Unterstützung wäre die Durchführung der Doktorarbeit in dieser Form nicht möglich gewesen.

Nicht zuletzt möchte ich meiner Familie von Herzen danken, für ihre beständige Unterstützung, ihr Verständnis und ihre Geduld während der gesamten Zeit. Ihr Rückhalt hat mir die Kraft gegeben, dieses Projekt zu Ende zu bringen.